**THOMAZ MARTINO TESSLER**

# WEATHER DOWNTIME ANALYSIS FOR CUTTER SUCTION DREDGERS

**São Paulo**

**2016**

**THOMAZ MARTINO TESSLER**

# WEATHER DOWNTIME ANALYSIS FOR CUTTER SUCTION DREDGERS

**Dissertação apresentada a Escola Politécnica da Universidade de São Paulo para obtenção do título de Mestre em Ciências**

Área de concentração:
**Engenharia Naval e Oceânica**

Tutor:
**Prof. Dr. Alexandre Nicolaos Simos**

**São Paulo**

**2016**

Este exemplar foi revisado e alterado em relação à versão original, sob responsabilidade única do autor e com a anuência de seu orientador.

São Paulo, 07 de Dezembro de 2016

Assinatura do autor: _____

Assinatura do orientador: _____

Catalogação-na-publicação

Tessler, Thomaz
Weather Downtime Analysis for Cutter Suction Dredgers / T. Tessler – versão corr. São Paulo, 2016.
91 p.

Dissertação (Mestrado) – Escola Politécnica da Universidade de São Paulo. Departamento de Engenharia Naval e Oceânica.

1. Operação de Dragagem 2. Downtime Meteoceanográfico 3. Draga de Sucção e Recalque I. Universidade de São Paulo. Escola Politécnica. Departamento de Engenharia Naval e Oceânica II.t.

# RESUMO

A atividade de dragagem no mundo é cada vez mais significativa em função do aumento dos navios que operam em portos, estes que possuem maior calado e requerem, consequentemente, canais de navegação mais profundos. Alguns projetos de dragagem utilizam dragas de sucção e recalque em mar aberto, dada a capacidade destes equipamentos de remover sedimento compactado e rochas, ainda mantendo uma boa produtividade. Estes fatos motivaram a criação de um programa de previsão de downtime gerado por condições ambientais de dragas de sucção e recalque baseado em modelos matemáticos simplificados. Os movimentos causados por ondas, e as forças e momentos causados na draga por ventos, ondas e correntezas foram analisados de forma a se obter a influência da magnitude e direção de cada um destes parâmetros no comportamento da embarcação. Os principais sistemas da draga influenciados por estas condições foram determinados com base em uma revisão bibliográficas como sendo a potência requerida nos guinchos de varredura, a interação do cortador com o solo e a resistência do sistema de ancoragem, sendo este a tensão de flexão dinâmica na trave do *spud* ou as tensões de ancoragem pelo sistema de árvore de natal. Três modelos matemáticos foram desenvolvidos para representar estes sistemas. Considerando a não linearidade da interação entre a draga e o solo, este processo foi representado por uma força de reação definida pelo usuário e pela velocidade horizontal do cortador. A eficiência destes modelos foi testada ao aplicá-los em um estudo de caso da dragagem do porto de Açu, na costa brasileira pela draga Taurus II. Valores simultâneos de ondas, ventos e correnteza foram utilizadas como entrada nestes modelos, através da criação de um cenário hipotético de série temporal. Os resultados para ambos os casos demonstraram que a operação seria impossibilitada em função de tensões de flexão dinâmicas no *spud* maiores que o limite determinado.

Palavras chave: *Operação de dragagem, downtime meteoceanográfico, draga de sucção e recalque.*

## ABSTRACT

The dredging activity is increasing worldwide due to ships that require bigger drafts, and consequently deeper navigation channels. Some dredging projects requires the operation of cutter suction dredgers on open waters, once these are capable of removing compact sediments and rocks while still maintaining a good productivity. These facts motivated the creation of a weather driven downtime prediction software for this type of operation, based on simplified calculations of the main dredging systems of a CSD. The motions caused by waves, and the forces and moments caused on these dredgers by winds, waves and currents were analyzed in order to evaluate the influence of each parameter magnitude and direction on the behavior of the vessel. The main criteria of the dredger influenced by this conditions were determined by a literature review as being the swing winch required power, the interaction between the cutterhead and the soil, and the anchoring system resistance, this that can be both a spud pole system stress or the Christmas tree cable tension. In this research, only the spud pole system bending stress was considered. Three mathematical models were developed to represent those systems. Since the non-linearity of the relation between the reaction forces of the dredger and the soil was not an object of the study, this process is represented by a constant user defined reaction force and a horizontal cutterhead velocity model. The efficiency of these models were tested by applying them on a case study of the dredging of the Açu port on the Brazilian coast by the Taurus II dredger. Simultaneous wind, wave and current data data were used as input to these models by creating a time series scenario of the operation period. The results for both scenarios showed that the operation would be close to impossible due to wave generated dynamic stress on the spud pole.

Keywords: *Dredging Operation, Weather downtime, Cutter Suction Dredger*.

**CONTENTS**

## LIST OF FIGURES

## LIST OF TABLES

# CHAPTER 1

## Introduction

The dredging activity is re-placing loose or compact sediment present on the bottom of a water body (rivers, lakes, estuaries, open or protected seas). Its objectives are many, such as deepening of access channels and waterways in order to assure safe navigation to larger vessels, underwater mining, decontamination of rivers, and increase of flow capacity of channels. Specially designed equipment, called dredgers, are used in order to remove this material. The development of these equipment features is largely explored in order to increase its productivity and decrease the use of human labor, through systems automation and development of eco-efficient processes and volume capabilities.

Dredging is most commonly measured through volume removed from a certain area, through comparison of bottom surfaces measured before and after dredging. When volume number is considered, the biggest part of the activity is found on port dredging, a share where the largest equipment are found operating. This is easily justified, once deep waterways permits largest vessels to operate on a port, turning the international and domestic trading more efficient and so creating a more suitable environment for economic growth. That is the main reason why

Brazil treated dredging with more concern in the last two decades. Previously operated strictly by governmental companies such as Portobras until the 1990's, the dredging market was opened to international companies in order to successfully achieve the National Dredging Plan (PND), of deepening the accesses and berths of the largest trading ports in the country. Today, dredgers from various national and international contractors operate throughout the entire coast of Brazil, on both governmental and private ports and terminals.

Dredging equipment can operate through hydraulic systems, removing the bottom material via pressure gradients generated by boarded suction pumps, or mechanic system by the use of excavators, jaws and buckets. Mechanical dredgers operates singularly in means of a static condition, fixed and stabilized by rigid poles (or spuds) combined with a peculiar mooring system. Hydraulic dredgers can operate both navigating, such as the trailing suction hopper dredgers (TSHDs), and static, the case of the cutter suction dredgers (CSDs), the last presenting an stabilization system similar to the mechanical dredgers (spud poles). A rotating cutter terminal composes the CSDs, one that allow the removal of consolidated material and marine aggregates (quality also inherent to mechanical dredgers), different from the TSHDs, whose dredging terminal is a rippled head that drags along the bottom and are more suited to the removal of unconsolidated sand and muds. ALFREDINI & ARASAKI (2010) and HERBICH (1998) describe and discuss the detailed characteristics of each type of dredge. In Brazil, the numbers of TSHDs operating is much larger than CSDs, once the sedimentary conditions on a number of ports inherent to shoaling allow these dredgers to be much more productive.

The frequent presence of material with a high degree of compression on the coastal areas and increase of the exploration of marine aggregates results on a bigger demand of the use of mechanical and cutter suction dredgers on unprotected waters. In Brazil, we can observe one typical coastal platform facies, the Barreiras formation (SUGUIO & NOGUEIRA, 1999), a highly compacted sand and gravel deposit. The inevitable interaction between coastal processes and the vessel characterize the natural conditions (waves, winds and currents) as a key factor on the working and non-working periods during dredging operations. The non-working periods, on this case, is referred to as downtime. The indispensable quality of dredging on the materialization of ports and waterways brings importance to the estimation of the downtime ratios, once it helps to decide on a more effective equipment, develop a more reliable planning, and perform solid decisions during the operation, given that costs and time are highly affected

by it. The conclusion is that the interaction between the dredger and the coastal process comes as in important factor for determining the viability of the enterprise investment, and the determination of the most suited equipment in increasing dredging productivity derived from the analysis of this interaction is the main motivation of this research.

VAN DER WAL & DE BOER (2004), WICHERS & CLAESSENS (2000) and WICHERS (1981) presents the usual method for the downtime analysis for cutter suction dredgers, composed by four items. First is the definition of which criteria can be considered as limiting for dredging operations (e.g. tensions on the anchoring cables, movement of the hull). Second is to determine the forces that acts directly on those criteria (waves, currents and winds), followed by the analysis of the interaction between these criteria and forces through equations of forces, moments and tensions. The fourth item is to determine the values of the forces that elevates those criteria to an operational stop so that an analysis of the frequency of occurrence of those cases can be performed for a specific location providing the total weather downtime or prediction.

The definition of the limiting criteria for dredging, as well as the process that act on those can be obtained from the compilation of data from previous projects, interviews with operators, analysis of the equipment and the physical properties of the composing material. These data are incorporated to a force equilibrium model that can be solved both on time or frequency domain. When the interaction between the dredge and the environmental processes is essentially nonlinear, the time domain models are required for representing the system (WICHERS, 1987), while frequency domain models are applied on linear relations and quasi-static approaches. Besides the differences, the application of any of these methods search to formalize the magnitude of the processes that generate the limits of the operational criteria of the equipment. When analyzing the frequency of occurrence of this process for that given magnitude, the downtime rates can be determined. This method of comparing results from dynamic models and time series presents itself as a coherent tool for a generalized analysis for decision making.

Although well described in literature, the analysis method for the characteristics of forces, motions and operational limits of dredging, only a few authors searched to validate the results through observed data. Amongst those, we can quote GRUNDLEHNER ET AL. (2003), which compared the downtime prediction obtained by the DREDSIM software with operational

data obtained during activities on the North Sea. In this case, we assume that the quantity and quality of the information provided by the command and operational team, as well as the downtime records, is proportional to the level of maturity of the analysis in question. It is also important to notice that the academic practice of defining tools for the analysis of operational limits of TSHDs is common, being not so abundant the one related to cutter suction dredgers. Specifically in Brazil, to the author's knowledge, no research was published on the subject, even considering that the quality of the material found on green field port implementation indicates the use of a CSD or a mechanical dredge.

These aspects motivated this research project at the Department of Naval and Ocean Engineering of the Polytechnic School of University of São Paulo, one that aims at analyzing the influence of each stop criteria of cutter suction dredgers on total downtime and develop a software to predict downtime for a dredging operation. This code will allow the user to input a great number of specific parameters for the equipment environmental conditions. The use of simplified models will provide efficiency to the software, given the great number of conditions that can be analyzed. This analysis will be applied for a the Açu port in the Brazilian coast using a hypothetical time series and a frequency domain model composed by a series of forces and moment equilibrium systems, and motion related tensions for a seagoing CSD.

## 1.1 The Cutter Suction Dredge

This section is dedicated to explain the operational layout and system of cutter suction dredgers (CSD), being those self-propelled or not, in order to provide the basis of understanding of the process described during the development of the system models and results. The mean objective of this description is to elucidate what could be the main operational aspects and units that can cause an operational stop due to forces and moments caused by environmental processes (waves, currents and winds), consolidating an effort to determine where on the system we should evaluate critical sea loads. A typical layout of a CSD will be considered by first describing its architectural elements and its means of operation and later analyzing the interaction (processes of force transfer) between its components.

Cutter suction dredgers are barge type vessels composed by a telescopic dredging apparatus at its bow, element that presents at its end a cutting device designed to excavate hard soils (HERBICH, 2000). Generally, at the bow and stern the hull presents a catamaran type conformation, the first in order to allow the cutter ladder to achieve larger dredging depths without compromising the barge stability, and the second to allow the placement of the spud pole and spud carriage. It generally operates at stationary conditions, supported by a spud pole system at the stern and a double, angled mooring system at the bow (VLASBLOOM, 2005). This conformation provides the dredger the ability to move without the help of propellers, as it will be explained further in this section. Figure 1 and Figure 2 shows the main units and conformation of a typical CSD

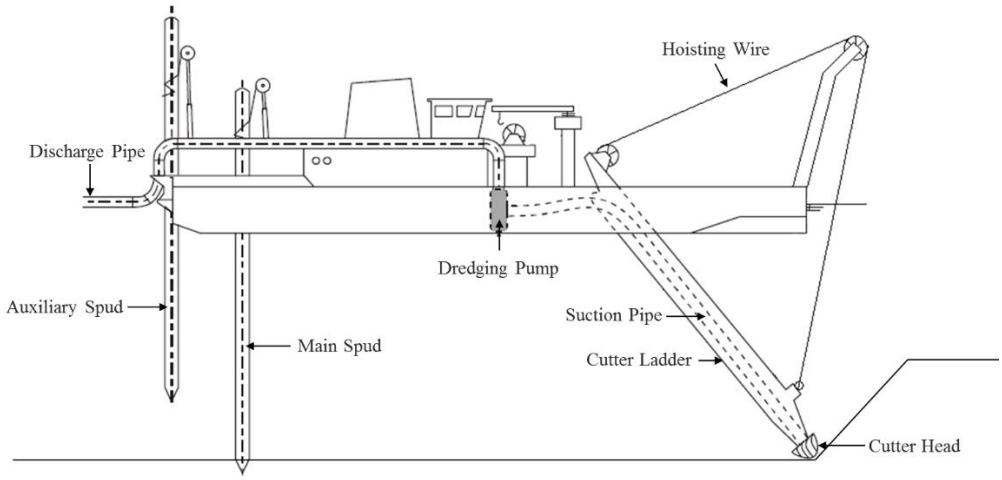


**Figure 1. Profile view of the main units of a cutter suction dredge (modified from Vlasbloom, 2005).**

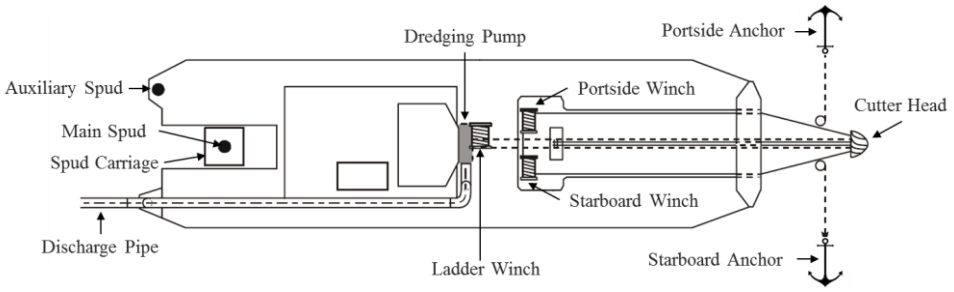


**Figure 2. Top view of the main units of a cutter suction dredge (modified from Vlasbloom, 2005).**

Given its stationary condition, this type of equipment possesses a unique dredging pattern. As an example of its operation, the following is posted: horizontally fixated on the main spud pole, it uses the side winches to gradually tension the portside mooring line and loose the starboard side, to dislocate the whole system continually, together with the cutting ladder and head, to the portside, dredging an arched line along its path. This movement called swing characterizes the CSD dredging technique mainly as a yawing motion. After reaching the limit of the mooring lines (swing) or project geometry, the system needs to dislocate forward (surge). If the equipment possesses a spud carriage, the same is used on de displacement of the barge (and consequently the cutter system). If the equipment does not have a spud carriage system, the displacement is performed with the help of a tugboat. Once the dredge is displaced forward, the winches perform the opposite work, tensioning the once loosed mooring line and losing the other continually to perform other swing movement. Again, in the case of dredgers with spud carriages, this procedure continues until the carriage reaches its length limit, completing one dredging cycle. In the case of dredgers without the spud carriage, the swing is performed one time, and the barge is positioned forward with the use of tugs to perform the next swing. Figure 3 provides the visualization of the schematic view of the dredging pattern.

After completing one dredging cycle, the system advance forward to start dredging a new area. The first procedure is to reallocate the anchors with the assistance of anchor handling support boats. When using a dredge without the spud carriages, this displacement of the dredger is made once more with the help of tugs. When working with spud carriages, the dredger moves forward by itself. From the above stated it could be noticed that the spud carriage piece possesses the artifice of being coupled or not with the barge (BRAY ET AL. 1996), reserving the capacity of both providing stability during dredging or dislocating the barge forward.

Although CSD's are called stationary, the have the ability to gradually move by their own without the use of propellers (in the case of equipment provided with spud carriages), or with the use of propellers. The last case is more common on the so-called "sea going" cutter suction dredgers. This equipment is more robust given the fact that it is designed to operate on open waters with harsher environmental (waves, winds and currents) conditions than a common CSD. This leads to a design where the magnitude of the equipment is larger and the characteristics of its hull resembles a V or U shaped vessel instead of a barge, in order to provide

a less resistant navigation on unsheltered operation areas. For a common barge type CSD, the dislocation and dredging procedure described on this section is represented on Figure 3.

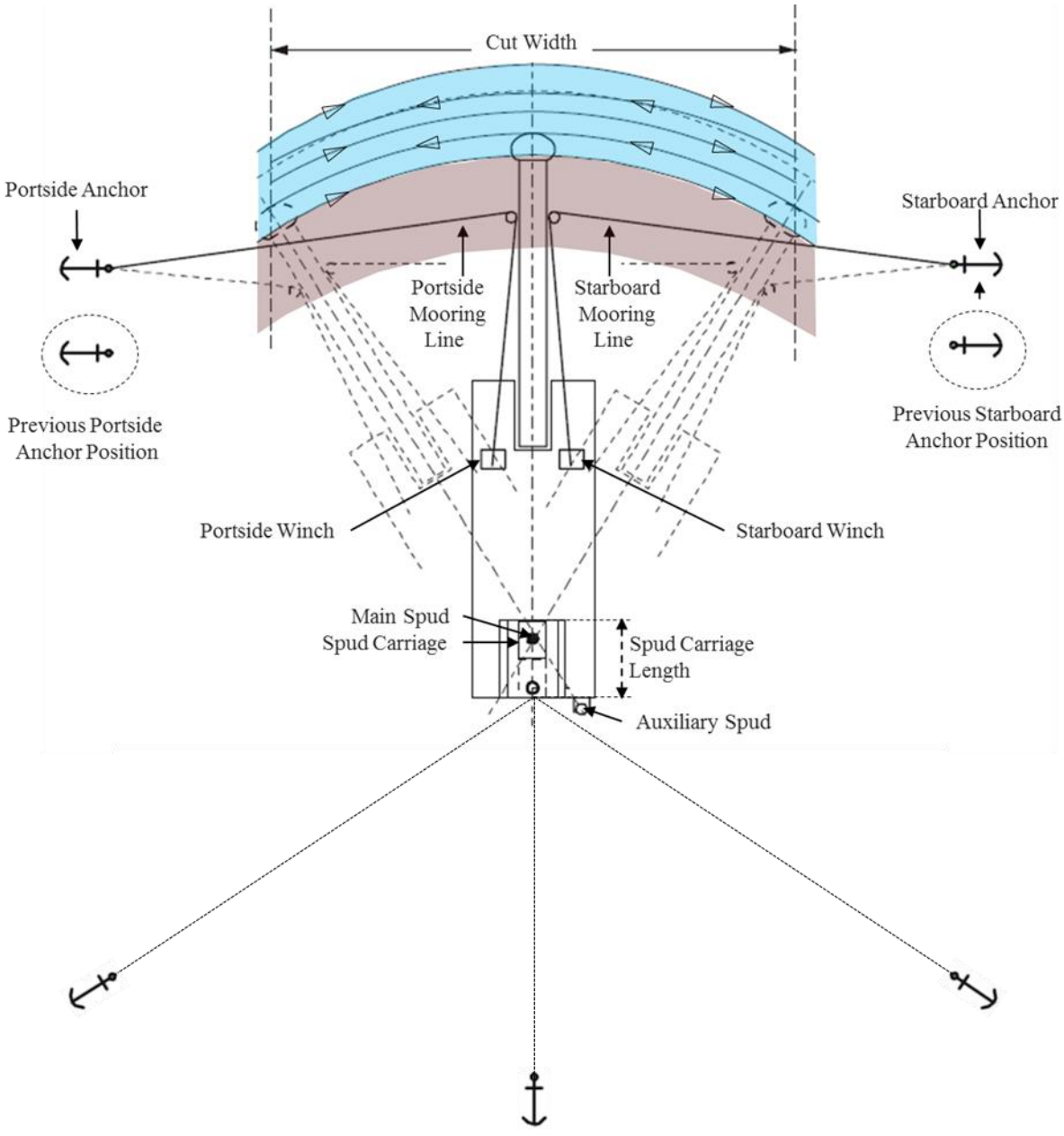


**Figure 3. Operational method of a cutter suction dredger for a four stage spud carriage. The blue area represents the effective dredged area per carriage step, and the red area represents the previously dredged sector. The three anchors positioned at stern represents the setting of the Christmas tree anchoring (modified from Vlasbloom, 2005).**

From the description of the CSD operation we can assume that the main elements of this equipment that are influenced by the motion and forces imposed on the dredge are the spud system, the swing wires and the cutter ladder, as presented by KEUNING & JOURNÉE (1983). This section aims to describe the details of such elements, for a further development of mathematical models of force transfers and operational limits. It is complex to unify the characteristics of those components for every kinds of CSD, once it´s size, shape and swing mechanisms can differ drastically. Those descriptions will be handled for the sea going CSD's typical elements, those that will operate on harsher environmental conditions and will be subjected to downtime caused by environmental processed.

There are a great number of spud systems developed to provide a “walking" mechanism to the dredger. The system described here is composed by two structures: The spud pole and carriage. The spud pole provides stability to the dredging process: the force exercised on the soil in order to perform the cut creates a reaction process that induces a motion on the dredger (either on surge or sway motions). The spud planted on the soil provides resistance to this motion, keeping the dredger at the same point while creating a pivoting point for the purposed induced sway motion (swing). Generally, the pole is a steel cylinder that possesses a sharp end to penetrate the sediment at the bottom. When added the spud carriage, the system provides the dredger the ability to move without the use of propellers or auxiliary boats. On this layout, the work spud is placed on a carriage that with the aid of a hydraulic cylinder or steel cable can travel several meters in longitudinal direction on a well at the opposite side of the cutter ladder. Generally positioned at the center of the hull ($x$ - axis), is supported by four wheels on rails for the vertical forces and by guide rollers or bearing strips for the lateral forces (VLASBLOOM, 2005). Those wheels are positioned on the so-called coupling wheel. Figure 4 provides a general overview of the complete system described.

The spud carriage is generally provided with a winch system that raises the spud pole to travel back to its original position, and releases it to allow it to drive to the ground via gravity. A lifting pulley or sheave is placed at the lower end of the spud pole, allowing the lifting process to be performed through a steel cable. One of the most important components of a CSD is the cutting ladder. It exists to position the cutter head on deeper positions than the static draught, as well as provide reach to shallower areas without compromising the ship stability. The general layout of a cutter ladder and a cutter head are presented on Figure 5.

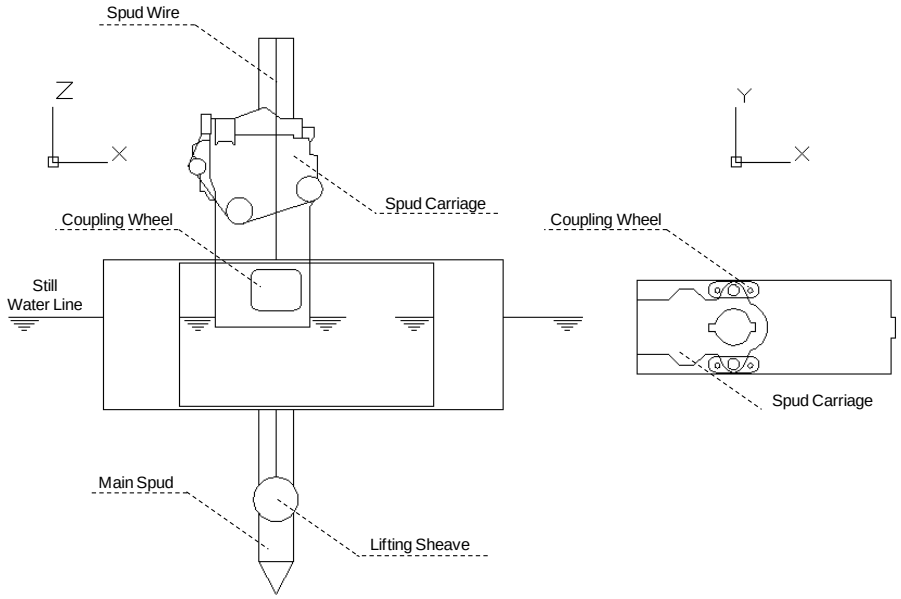


**Figure 4. General Layout of a spud carriage / spud pole system of the Taurus II dredger.**

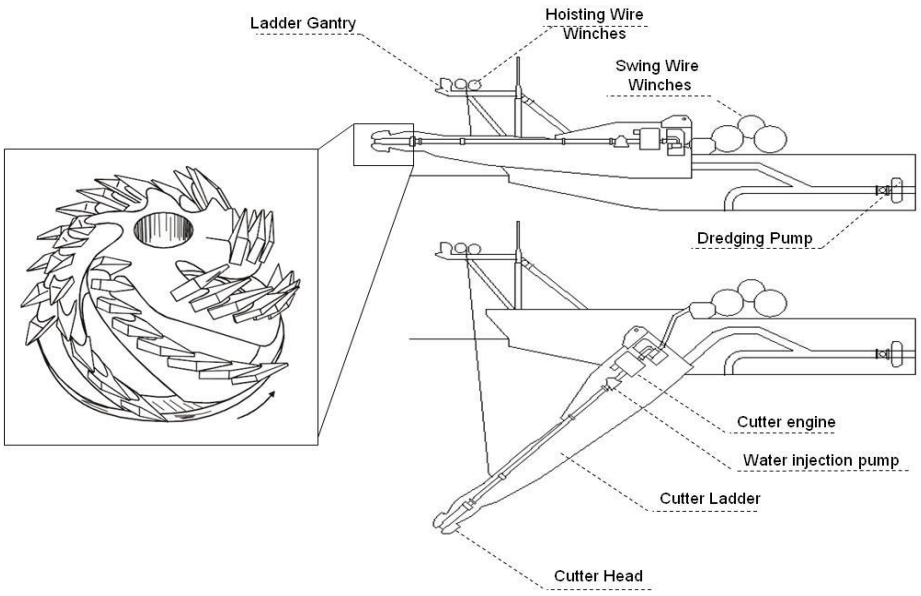


**Figure 5. General components on the cutter ladder system. On the detail, the arrange of a standard cutter head. The upper layout presents a total hoist condition used on navigation, while the lower represent a dredging condition.**

The ladder is fixed on the hull by a hinge axis so that the depth to position the cutter head can be managed by the use of hoisting wires controlled by a winch on an elevated truss or gantry. This aspect denotes that the deeper the dredging depth the smaller the angle formed between the cutter ladder and the hull. Along the ladder a rotating axis is present to power the cutter head motion, and commonly, a water injection system is provided to assist the disaggregation process (EISMA, 2003). The water injection pump, the suction pump and the cutter engine can be positioned both on the cutting ladder (underwater) and in the ships deck. The presence of engines, pumps and axis on the ladder causes its motion to be very undesiring. For sea going CSDs, those that are more subjected to loads from waves, a wave compensation system is placed on the connection between the cutter ladder and the hull (hinge point). The design aspects of those wave compensators are presented by MIEDEMA (1983).

The last significant system of a CSD is the swing system. Two winches located on the deck (portside and starboard), the swing wires and the anchors for each side compose this system. The swing wires, normally a steel cable or linked chain, are connected at one end by the winch and at the other by the anchor. An auxiliary vessel or a boarded crane positions the anchor. The winches develop to create a pre-tension on both wires on the central position, one that provide balanced equilibrium to the system, and gradually loosens and tightens at each side, alternately, in order to create the swing motion.

The point of connection between the anchors and the hull varies. Normally, a pulley is positioned at the end of the cutter ladder to create an optimum angle for the swing in terms of productivity. We should notice that in this case the wire is in contact with the ground from the anchor to the ladder, creating tensions on the horizontal dimension. Oblique winches in relation to the centerline of the hull are common, and when placed on the pontoon’s end provide a good swing coverage. In this case, not only horizontal tensions are present, still vertical force components influences the general equilibrium of the system (HERBICH, 2000). This last configuration is present on CSDs without spuds, when this mooring system is complemented to a triple anchoring scheme at the stern, named the Christmas tree arrangement (Figure 3). This provides a longer swing area in stake of a lower cutting capacity, and it is not a focus of this project. It can, however, be analyzed in future studies.

The cutter suction dredger is the equipment with the best ability to cut and remove hard soil with a good productivity. When we analyze other types of equipment this statement justify

itself, since trailing Suction hopper dredgers are by far the ones that hold the biggest productivity in terms of volume by time, but its suction head cannot be equipped with a cutter device. Once it dredges while navigating, it comprises its ability to remove hard soil. Mechanical dredgers such as clamshells and buckets are competent in removing consolidated material, but the characteristics of its operation provides them with low productivity on wave dominated areas. For that reason, dredging companies started to build the so-called Jumbo cutter suction dredgers, those that withstand the capability to dredge hard soil on open sea environments (OVERHAGEN ET AL., 2004). The design parameters of such equipment are unique to each company, but generalities of basic elements tends to repeat itself. It is important to register that the mean difference from a sea going and a conventional CSD is the size, hull shape and cutter power. On this analysis the sea going CSD Taurus II will be detailed, once it operated on the implementation dredging of the Açu port, located on the southeastern Brazilian coast, the case study that will be used to validate the downtime analysis software. The main plan for this dredger is presented on Figure 6.

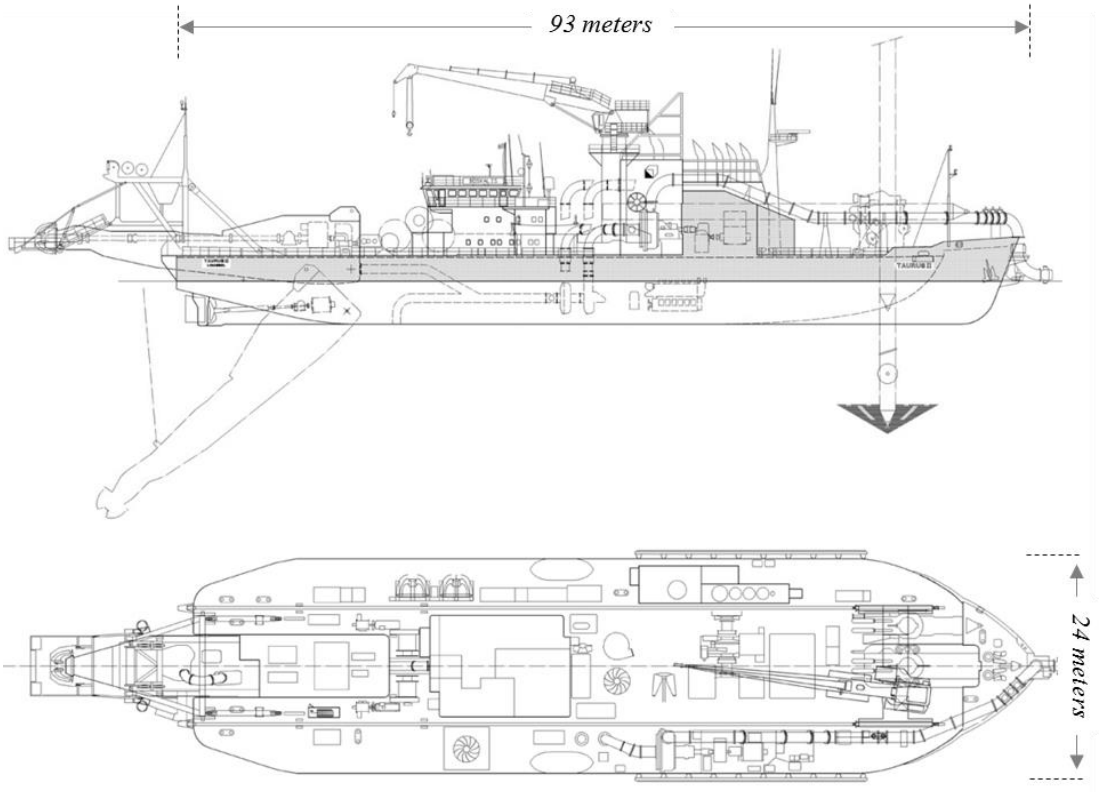


**Figure 6. Plans of the sea going CSD Taurus II (Source: Royal Boskalis Westminster).**

# CHAPTER 2

## Objectives

The main objective of this research is to analyze the operational limits of cutter suction dredgers as a function of waves, winds and currents, and create a software to predict weather downtime. The code must allow the user to define specific values for the dredge parameters (e.g. drift coefficients and equipment dimensions) as well as the possibility to input environmental time series or metocean diagrams, and calculate the total downtime of a future operation. Given the great number of data to be processed by the software, simplified models must rule the same in order to be grant it with efficiency. The following specific steps will be performed in order to achieve this objective:

- Verify the operational stop criteria of cutter suction dredgers from bibliographical review and analysis of the dredger project;
- Obtain the response of the dredger due to waves, winds and currents considering the swing motion performed by the CSD;
- Define force and moment models for the main systems of the dredge involved on operational stops as a function of external forcing;

- Apply a time series and on the system models to determine the downtime rate during an operation through a case study of a real dredging operation on a port on the Brazilian coast.

In order to achieve these objectives, premises and limitations must be considered. The first is that the anchoring system to be detailed and represented as a model is the spud pole system. The Christmas tree system will not be analyzed on this project, being a candidate for future developments. The second is that given the absence of a linear model that represents the interaction of the dredger with the soil or even a series of coefficients that can be used to describe this relation, the reaction force of the cutting process will be represented on the software by a user defined value for ladder push and drag force. A model that calculates the velocity of the cutterhead at the bottom will also represent this interaction as a mean of providing an additional parameter to determine a stop criterion.

One considerably important limitation is that no detailed data of the downtime rate of a real operation was available due to confidentiality of dredging contracts. Real data from the dredger systems, such as spud material, winch generator power and composition of the swing wires were also not available due to the same reason. The partial solution to contour the first limitation was to use the information provided to the author[1] that the Taurus II operation on the Açu port was unsuccessful, almost impossible, while using the spud pole system, and was only efficient when the anchoring system was changed to the Christmas tree solution. The solution for the second limitation was to obtain these data through the observation of market standards from equipment brochures and particulars.

The following content of this dissertation will be presented in order to demonstrate the methods employed for the fulfillment of those objectives and the results obtained from the development of these methods.

[1]This information was provided by a member of the operation during telephonic interview performed on September 21st of 2013. The name of the responsible will remain unsaid due to confidencility reasons.

# CHAPTER 3

## Literature Review

Modeling is no less than a simplification of a natural or mechanical system with the use of equations and assumptions. To determine the forces and moments acting on the components of a dredge, one must assume that a combination of equilibrium systems is capable of representing the main behavior of the loads on the dredge. In order to obtain the influence of the external forces on this equilibrium, we use the wave, wind and current forces and motions as input, as well as aspects inherent to the dredge materials and geometry. On this section, it will be presented how previous authors describe the function mechanisms of a CSD as equations in order to develop simulators and models, as well as how it behaves due to winds, waves and currents forces and motions. At the end, the standard procedure to calculate downtime derived from both process series and metocean statistics will be reviewed.

## 3.1 Operational models for CSDs

The importance of developing dredge simulators for predictions was presented by MIEDEMA (1999), though only a few authors described the operational mechanisms and the behavior of the main systems of a CSD in terms of mathematical formulae, and fewer presented a strictly frequency domain solution for the forces and moments on the systems. The major effort was performed on the Netherlands on the 1980's in order to provide a better production and the correct development of training simulators. WICHERS & CLAESSENS (1981) classified that for cutter suction dredgers, the main items to be considered on estimating downtime due to waves are the forces in the spud pole, either forces in swing wires or holding capacity of the deck winches or the holding capacity of anchors, forces/moments in ladder hinge and the accelerations on the bridge.

According to KEUNING & JOURNEE (1987), the calculation of weather downtime for a cutter suction dredger is the direct sum of the time when the limits of the following aspects are extrapolated:

- Power of the swing wire winches: The winches responsible for retraction, losing and holding the swing wires possesses a nominal and effective power, one that should be capable of sustaining the tensions provided by the wires during a given velocity of swing;
- Forces on the swing wires: The anchor and cable system when subjected to horizontal and vertical forces due to the elongation aspect of the cable, the bottom shear of the cable and the anchor. Knowing that this system will provide a total tension on the wire, this aspect can be translated into power of the swing wire winches;
- Accelerations on the deck and bridge: Generated by first order motions, these accelerations affects the general operation due to dangerous material and equipment escape (such as fuel and heavy elements) and general comfort of the crew;
- Forces on the spud pole: drift forces and moments caused by waves, current and winds, as well as cutting and swing generated forces, are transferred to the spud pole, the structure responsible for maintaining a fix position of the dredger. The sustaining limit of the spud,

determined by a fraction of its breaking loads, when surpassed, characterize an operational stop;

- Forces on the ladder and cutter head: Horizontal and vertical forces on the ladder and cutter head as a result of first order motions, drift forces and moments and the cutting process itself, can generate forces beyond the equipment breaking load;

Once the objective was to analyze the behavior on irregular waves, all the equations were developed on the time domain due to the better representation of this non-linear phenomenon, and are not pertinent to the objective of this project. The hydrodynamic loads on the spud and the cutter ladder were determined by the Morison formulation, approximating the later to a cylindrical conformation. The authors described the loads acting on a spud pole as forces and moments in the spud keeper, the soil reaction forces, hydrodynamic forces, and mass and buoyancy forces. The authors presents the main external forces on the ladder system as the soil reaction forces due to cutting, current forces, hoisting wires forces, the underwater weight of the ladder and forces in the coupling with the barge. As for the mooring lines, important aspects are forces caused by the mass and displacement of the cable, hydrodynamic loads due to cable motions, waves and current and friction forces by the bedding of the cable at the seabed.

Still considering the swing wires system and winch capacity, MIEDEMA (2000) suggested an approach considering the rotation motion around the spud, composing it with the following items:

- The inertial forces of pontoon and ladder
- The water damping on pontoon and ladder
- The spring forces resulting from the swing wires
- The external forces resulting from the current
- The external forces resulting from the cutting process
- The external forces resulting from the swing winches
- The external forces resulting from the pipeline
- The reaction forces on the spud

At the end, the total power required for the winches $P_w$ is sum of the power of the starboard ($P_{sw}$) and portside winches ($P_{pw}$), as a relation of the forces on the swing wires ($F_{sw}$ and $F_{pw}$) and the cable pay and retraction velocity ($v_{sw}$ and $v_{pw}$), as given by the following equation.

$$P_W = P_{pw} + P_{sw} = F_{pw} v_{pw} + F_{sw} v_{sw} \quad \textbf{[Eq. 1]}$$

Where the cable velocity for each board is provided by:

$$v_w = \frac{\dot{\phi}_s L_{ss}}{\sin(\varphi_b - \phi_s)} \quad \textbf{[Eq. 2]}$$

Being $\phi_s$ is the orientation of the dredge when related to its central position, $L_{SS}$ the distance between the spud and the cutter head, and $\varphi_b$ and $\varphi_s$ the swing wire angle in relation to the center axis of the dredge and the angle between the central position and the instant position, respectively. The moment around the spud ($M_{sp}$) is determined as a function of the forces on the starboard ($F_{sw}$) and portside ($F_{pw}$) wires, as given by:

$$M_{sp} = F_{pw}.L_{ss}.\sin(\varphi_{pw} + \phi_s) - F_{sw}.L_{ss}.\sin(\varphi_{sw} - \phi_s) \quad \textbf{[Eq. 3]}$$

In this case, the author is not considering the external moment, which could be added to the right side of the equation. The coordinate system and the general distribution of the parameters are presented at Figure 7.

KEUNING & JOURNEE (1987) listed the loads acting on the spud pole as the forces and moments on the spud keeper, the soil reaction forces, the hydrodynamic and the mass and buoyancy forces. Given its small stiffness ratio, it is stated that the dynamic behavior can be neglected. Although the author points that the reaction forces of the spud pole in relation to the soil is complicated to be determined and therefore not considered, MIEDEMA (1992-1) resolved the spud friction and spud relation to the sea-bottom with assumptions that are not presented on the text. When considering the simplified model, one can assume that the ratio between penetration depth and spud diameter is small, and a clamped situation can be

considered. Finally, MIEDEMA (1999) concludes that the reaction forces on the spud can be determined by the equilibrium equations of forces.

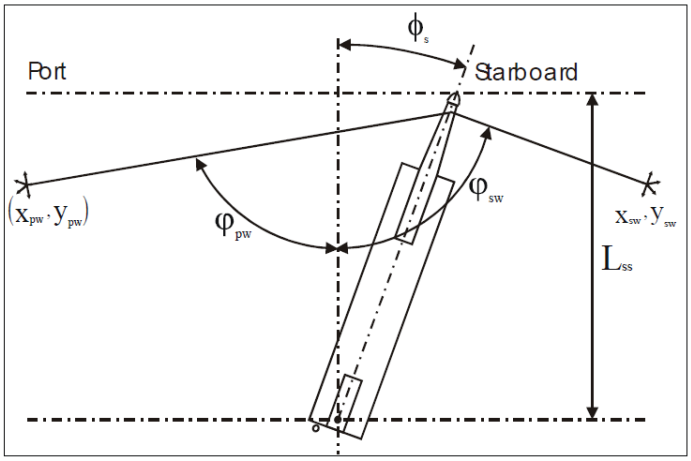


**Figure 7. Local coordinate system for the winch model (Source: MIEDEMA, 2000).**

No references regarding a simple approximation of the ladder response to hydrodynamic loads or its relation to the entire equilibrium system was found. It is discussed that the relation between the ladder and the bottom is nonlinear, and therefore only solvable in a time domain system of equations.

## 3.2 Response of a dredger due to wave, current and wind

Considering the equilibrium system of a CSD, we may consider the hydrodynamic and wind loads as the main external forces responsible for its disruption. The recommended application of these forces are in the form of direction related drift coefficients. In term of waves, the user will need the numerical response of the dredger hull due to regular oscillatory motions caused by gravity waves, in order to create a database of motion response to different frequencies and directions, to enable a complete analysis of the motion the dredger will suffer when working on the environment. Obtaining this relation must be a process that regards linear interactions between the incident waves and the hull. MIEDEMA ET AL. (1983) developed

empirical and mathematical time domain methods for calculating the behavior of dredgers on waves, due to the nonlinear interaction between dredger and soil, while WICHERS (1980) developed a linear formulation by representing the ladder and spud pole as bodies without inertia forces on the barge. Because of the use of the formulation in the frequency domain, any system influencing the behavior of the floating body, such as spud-pole, ladder and mooring system, may only have a linear relation with the displacement, velocity or acceleration of the body.

Nowadays, frequency domain software that calculate the response of the hull due to waves are available, and provides a more robust analysis on the six degrees of freedom that the hull is subjected as a response to income waves: wave motion acting in the longitudinal (surge) direction, wave motion acting in the transversal (sway) direction, wave motion acting in the vertical (heave) direction, wave moment about the longitudinal (roll) axis, wave moment about the transversal (pitch) axis, and wave moment about the vertical (yaw) axis. The one used presently is WAMIT, a radiation / diffraction panel program designed to analyze the linear interaction between surface waves and motions of submerged or semi-submerged bodies, by evaluating the unsteady hydrodynamic pressure, loads and motions on the body, as well as pressure and velocity on the fluid domain (WAMIT, 2012).

The calculation for the velocity potential on the panels on WAMIT can be performed by a simplified solution of a quadrilateral panel for simpler geometries. Once the Hull of sea going cutter suction dredger tends to present a rather complex geometry in order to improve navigation, the high order method of integration is used on WAMIT: instead of using a flat panel, the velocity potentials on the body is represented by a B-spline approximation, where the body surface can be represented by the ensemble of patches continually to obtain the wave drift forces and moment coefficients.

Although it is shown how the program performs the integration of the potential flow along the body patches (or mesh), the important result for the analysis of the response of the body due to waves is the exciting forces, comprised on the form of a transfer function, or response amplitude operator (NEWMAN, 1977). Given this information, what we need to understand is how the program transform this potential flow into the complex amplitude of the body motion in response to an incident wave of unitary amplitude, direction $\beta$ and frequency

ω. It is logical to assume that this transfer function can be calculated if the added mass, exciting, hydrostatic and damping forces are known.

KEUNING & JOURNÉE (1983) suggested the application of current induced drift forces and moments through an equation depending of an empirical coefficient for each angle of attack determined on model tests. For the barge only the current forces in surge, sway and moment in yaw are taken into account, i.e.:

$$F_{1,2}^{c} = \frac{1}{2}\rho v_c^2 T\sqrt{L^2 + B^2}.c_{1,2}(\alpha) \quad \textbf{[Eq. 4]}$$

$$F_{6}^{c} = \frac{3}{5}\rho v_c^2 T(L^2 + B^2).c_{6}(\alpha) \quad \textbf{[Eq. 5]}$$

Where

- $\rho$ – specific weight of water;
- $v_c$ – relative current velocity;
- $T$ – static draught;
- $L$ – Length over all of the hull;
- $B$ – Hull beam;
- $c_{1,2,6}(\alpha)$ – empirical current drift coefficients depending on the angle of attack $\alpha$;

The coefficients were obtained through a scale model of a CSD hull and ladder, and the results are presented on Figure 9.

Wind generated drift is as important as current generated drift when analyzing the forces acting on the dredger by the environment. A different resultant of drift force magnitudes is present on the dredger subjected to different wind directions as a function of its super structure and the hull portion above the water level layout. No specific wind drift coefficient for dredgers is presented in literature. Nevertheless, OWENS & PALO (1982) compiled and developed results from scale model tests from 31 types of vessels of wind drift coefficients. In order to calculate the resulting wind drift force, the following equations are used:

**Figure 8. Profile of the vessel model used by OWENS & PALO (1982) chosen to represent the aerodynamic coefficients of the dredger.**

$$F_1^w = \frac{1}{2}\,\rho_{air}\,v_w^2\,A_x\,c_{w,1}(\alpha)\,f_x(\alpha) \qquad \textbf{[Eq. 6]}$$

$$F_2^w = \frac{1}{2}\,\rho_{air}\,v_w^2\,A_y\,c_{w,2}(\alpha)\,f_y(\alpha) \qquad \textbf{[Eq. 7]}$$

$$F_3^w = \frac{1}{2}\,\rho_{air}\,v_w^2\,A_y L\,c_{w,6}(\alpha) \qquad \textbf{[Eq. 8]}$$

Where:

- $\rho_{air}$ – specific weight of air;
- $v_w$ – relative wind velocity;
- $A_x$ – Projected ship lateral wind area;
- $A_y$ – Projected ship longitudinal wind area;
- $c_{w,1,2,6}(\alpha)$ – empirical wind drift coefficients dependent of the incident wind angle $\alpha$;
- $f_{x,y,n}(\alpha)$ – normalized shape function dependent on incident wind angle $\alpha$.

Through these equations, it is noticeable that the formulation for wind drift force is similar to the ones for current drift force. In this solution, the authors placed a normalization function based on cosines and sines for the empirical wind drift coefficients for longitudinal and lateral winds. These normalization functions are defined by the following equations.

$$f_x(\alpha) = \frac{\sin\gamma - \sin(5\gamma)/10}{1 - 1/10} \quad \textbf{[Eq. 11]}$$

$$f_y(\alpha) = \frac{\sin\alpha - \sin(5\alpha)/20}{1 - 1/20} \quad \textbf{[Eq. 12]}$$

For $\gamma$ determined by,

$$\gamma = \left(\frac{90}{\theta_z}\right)\alpha + 90 \qquad \alpha < \theta_z \quad \textbf{[Eq. 13]}$$

$$\gamma = \left(\frac{90}{180 - \theta_z}\right)\alpha + \left(180 - \frac{90}{180 - \theta_z}\right) \qquad \alpha > \theta_z \quad \textbf{[Eq. 14]}$$

where $\theta_z$ being the zero crossing point for the lateral wind coefficient. From the 31 different typical vessel shapes, the one chosen is the one that is most similar to the TAURUS II superstructure and hull shape. In this layout, where the main superstructure is located just aft of the mid ship line, the zero crossing point is suggested as 100°. The coefficient curves for wind drift are presented together with the current coefficients in Figure 9. Although these coefficients will be used on the study case of this research, in order to provide a more careful analysis the software allows the user to provide its own coefficients for a specific CSD. It can be noticed that wind and current coefficients are not quite similar in terms of shape pattern. For longitudinal coefficients, sine shaped coefficient curves are observed, with peak values near 90º and 270º for both processes forcing. As for longitudinal coefficients, the difference between the shapes of hull and superstructure provides somewhat different patterns for the coefficient curves. Nevertheless, for both processes, the curves presents negative values for stern incidence (180°) and positive values for bow incidence (0°) processes. Yaw moment coefficients are very standard when regarding wind drift, while zero crossing points for current drift coefficients are presented at 0°, 15°, 180°, 345° and 360°. This coefficient will later be used for calculating the wind and current generated drift forces (static forces) generated on the ship. The reference for force application is, on both cases, the ships center of gravity.

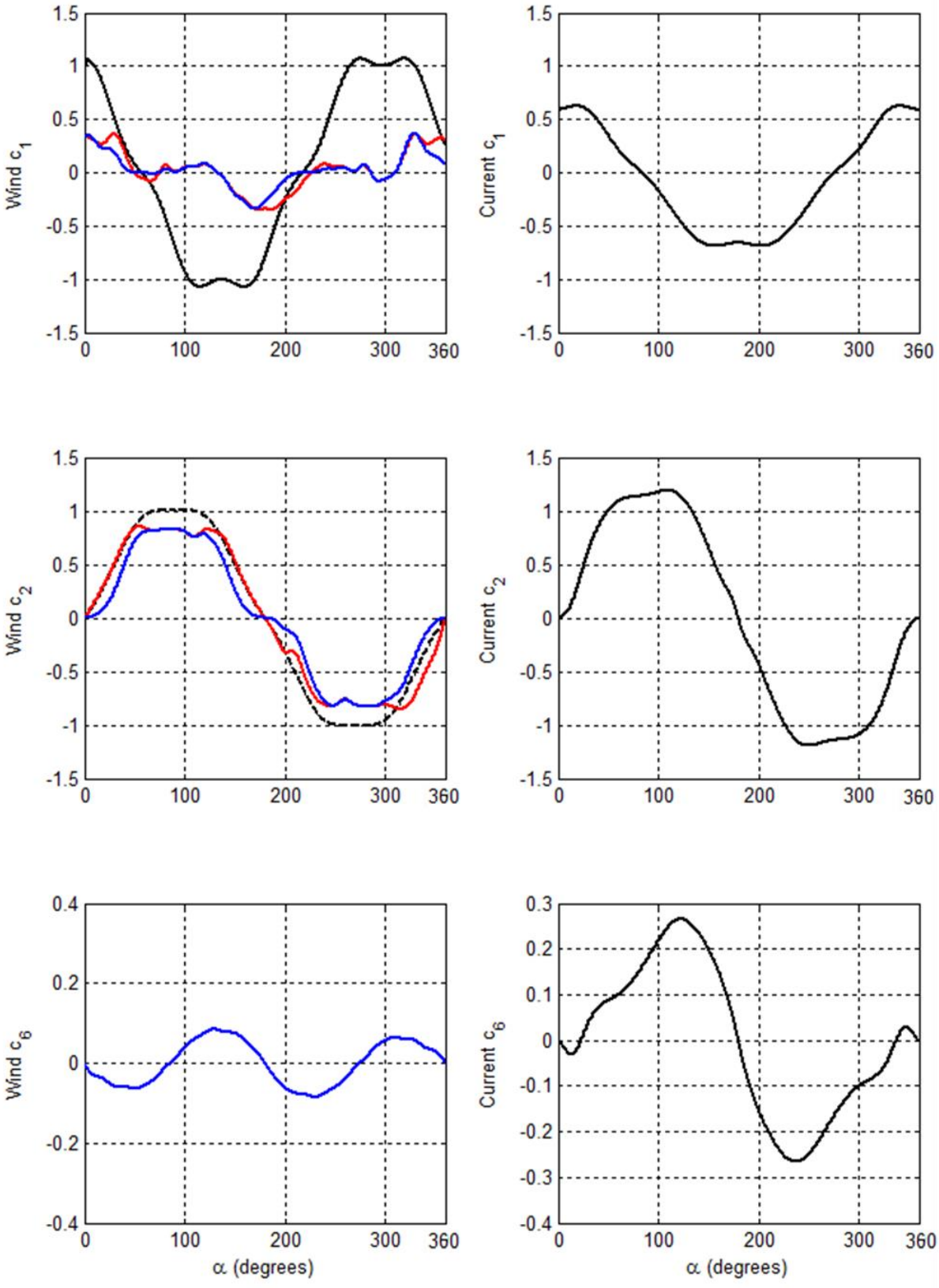


**Figure 9. Typical current and wind drift forces and moment coefficients for a CSD (Source: OWENS & PALO, 1982, and KEUNING & JOURNÉE, 1983)**

## 3.3 Weather downtime calculations

The rate between the working periods and non-working periods of dredging operations is a function of several aspects, being such: maintenance of key elements, crew shift changes, garbage and food transfer from support vessels, fuel and water supply, relocation for a different area on the channel, and weather effects. VAN DER WAL & DE BOER (2004), WICHERS & CLAESSENS (2000) and GRUNDLEHNER ET AL. (2001) describe the downtime induced by the later on dredging operations and its prediction mechanisms. The general consent is that the limits of the equipment due to motions and forces caused by waves, currents and winds, should be the primary analysis input and can be obtained analytically through models, such as the ones described, generating the so called downtime lines or downtime points. If these downtime points or lines are known, the total downtime of a future operation can be estimated by using the scatter method, the job duration scenarios and long-term simulations.

The analysis using wave scatter diagrams consists on the downtime being expressed as a percentage of the time (occurrences) that a certain operation cannot be performed, by combining the known stopping conditions to a joint occurrence diagram. This approach provides the user with the ability to overview the operation condition and choose the most suitable equipment to work in the area.

VAN DER WAL & DE BOER (2004) and GRUNDLEHNER ET AL. (2001) presented the concept on determining the job duration by creating time series scenarios and simulating them on the dredge models. Collected data on the area is combined with the dredge model on a number of scenarios, while the total downtime for the working period is composed later for a larger period of time based on statistics of occurrence. On this case hydrodynamic and wave generation and propagation models are simulated for certain scenarios, while the effects on the operation are analyzed separately and later created a general scenario based on job duration.

WICHERS & CLAESSENS (2000) suggests the same approach but with the use of long-term simulations. With this method, the selection of cases to be simulated, its order and its correlation with other processes can be quite complex and can interfere directly on the final

results, but provides a general overview of the time the dredge won't be able to operate as a function of wind, waves and currents.

When the objective is to predict downtime during the operation, for example, for the next three or four days, the use of wave, currents and winds prediction databases available online is reasonable. However, prediction models have a precise response for offshore areas, where the influence of the bottom and topography on the propagation and circulation patterns of the processes can be neglected. This is such once the resolution and formulation of global generation models is not one that guarantees the correct representation of the processes modification on shallow water (for waves and currents) or land (for winds) of the area of interest. Given that, the availability of reliable prediction data for coastal regions is low, but can be achieved through operational models or determination of propagation coefficients via the use of shallow water models.

The advances on numerical modeling of coastal circulation is such that allows a precise verification of the governing hydrodynamic processes. Operational models for a certain area are constantly fed with offshore global generation models and propagates the processes to shallow waters, providing a reliable prediction. The implementation of such models is extending mainly because of port operations, and once coupled with a vessel dynamic model can also be used to predict the operational downtime for the next days for a given vessel. An example of this process can be observed on DOBROCHINSKI (2003) and HOLTHUIJSEN et al. (1989).

Considering the definition of the critical systems of a CSD that are influenced by external processes, as well as the means of calculating the forces, moments and motions transfers to the floating body and finally the downtime rates, the following chapter will present the methods used to determine these aspects and calculating this interaction.

# CHAPTER 4

# Models development and analysis

## 4.1 Input parameters and conventions

The implementation of three models was performed in order to estimate the dredge downtime due to waves, currents and winds. It was defined, through indication of past studies and the objective and limitations, that the systems and processes that the following systems can be represented by linear models and will be implemented: a winch power, a horizontal cutterhead velocity and a spud stress model. In order to apply those calculations, the user must provide several data related to the dredge, ladder and spud geometry, dredge hydrodynamics, dredge aerodynamics, material resistance and external forcing. The list provided in Table 1 indicates and describes each necessary data. Ladder drag and push force are the representation of the soil interaction with the dredge. The decision to consider the latter as user defined was

based on the complexity of this interaction. A more refined model extrapolates the objective of this research. Spud distance and cutterhead distance from center of gravity must be provided with the x, y and z coordinates.

**Table 1. Input data for the dredge downtime calculations.**

| Category | Variable | Symbol | Unity |
|---|---|---|---|
| **Ships particulars** | Length overall without ladder | $L$ | ***[m]*** |
| | Beam at midship | $B$ | ***[m]*** |
| | Static draft | $T$ | ***[m]*** |
| | Ladder length | $L_{lad}$ | ***[m]*** |
| | Spud distance from stern | $S_{ps}$ | ***[m]*** |
| | Spud distance from center of gravity | $S_{cg}$ | ***[m]*** |
| | Cutterhead distance from center of gravity | $C_{cg}$ | ***[m]*** |
| **Equipment particulars** | Spud length | $S_L$ | ***[m]*** |
| | Spud diameter | $S_D$ | ***[m]*** |
| | Spud thickness | $S_T$ | ***[mm]*** |
| | Spud module of elasticity | $E$ | ***[kg/m2]*** |
| **Anchoring and swing** | Dredge orientation (true north) | $D_{or}$ | ***[º]*** |
| | Maximum swing angle | $S_W$ | ***[º]*** |
| | Swing angle discretization | $S_{WD}$ | ***[º]*** |
| | Time to perform a full swing | $S_{WT}$ | ***[min]*** |
| | Portside anchor position | $A_{CP}$ | ***[m]*** |
| | Starboard anchor position | $A_{CS}$ | ***[m]*** |
| **Environmental** | Significant wave height | $H_s$ | ***[m]*** |
| | Wave period | $T_p$ | ***[s]*** |
| | Wave direction | $Dir$ | ***[º]*** |
| | Number of frequecy classes on spectrum | $f$ | ***[-]*** |
| | Current magnitude | $v_C$ | ***[m/s]*** |
| | Current direction | $C_D$ | ***[º]*** |
| | Wind magnitude | $v_w$ | ***[m/s]*** |
| | Wind direction | $W_D$ | ***[º]*** |
| | Water density | $\rho_w$ | ***[kg/m3]*** |
| | Air density | $\rho_a$ | ***[kg/m3]*** |
| | Acceleration of gravity | $g$ | ***[m/s2]*** |
| | Ladder drag force | $L_{DF}$ | ***[kN]*** |
| | Ladder push force | $L_{PF}$ | ***[kN]*** |
| | Dredging depth | $h$ | ***[m]*** |
| **Limits** | Maximum winch power | $P_{MAX}$ | ***[kW]*** |
| | Maximum Cutterhead velocity at bottom | $V_{CUTT}$ | ***[m/s]*** |
| | Yield tension of spud | $\sigma l_{im}$ | ***[MPA]*** |
| | Yield tension safety coefficient | $\sigma_{SC}$ | ***[-]*** |

The ability of the code to calculate the final results for a pre-determined dredging heading provides the user the ability on analyzing the optimum dredging orientation for agiven situation. All programming, pre and post processing of data was performed in the Matlab programing environment. The angle conventions differs from each input. Three coordinate systems are used in the code and sub-codes that governs the software that performs the calculations. In order to properly transform and process the data through the computation, this aspect is to be carefully managed. The conventions used for data from the ships particular category is the Cartesian convention, while the remaining data must be provided on nautical convention. All results are described considering the nautical convention.

## 4.2 Dredge response due to waves

In order to calculate the forces, moments and motions on the main operation units of the CSD, those that will define the operational stop criteria and later the total environmental downtime for a given period, we must understand how the hull of the dredger behaves (in its six degrees of freedom) when subjected to oscillatory movements of the sea, as well as the drift forces and moments caused by waves, currents and winds. This section is dedicated to present the procedures and results of the analysis used to predict this behavior due to waves. For that, the CSD hull was modelled in WAMIT®, a diffraction radiation code widely used in industry and academy for seakeeping studies (WAMIT, 2012).

The first input of the model is the grid for the submerged part of the Taurus dredger. The grid was created on the software *Rhinoceros 4.0*, considering the geometry of the body as shown on Figure 6, resulting on the model shown on Figure 10. The position of center of gravity and other hydrostatic coefficients were estimated based on the volume distribution, since its actual position and values are unknown. The results are shown on Table 2.

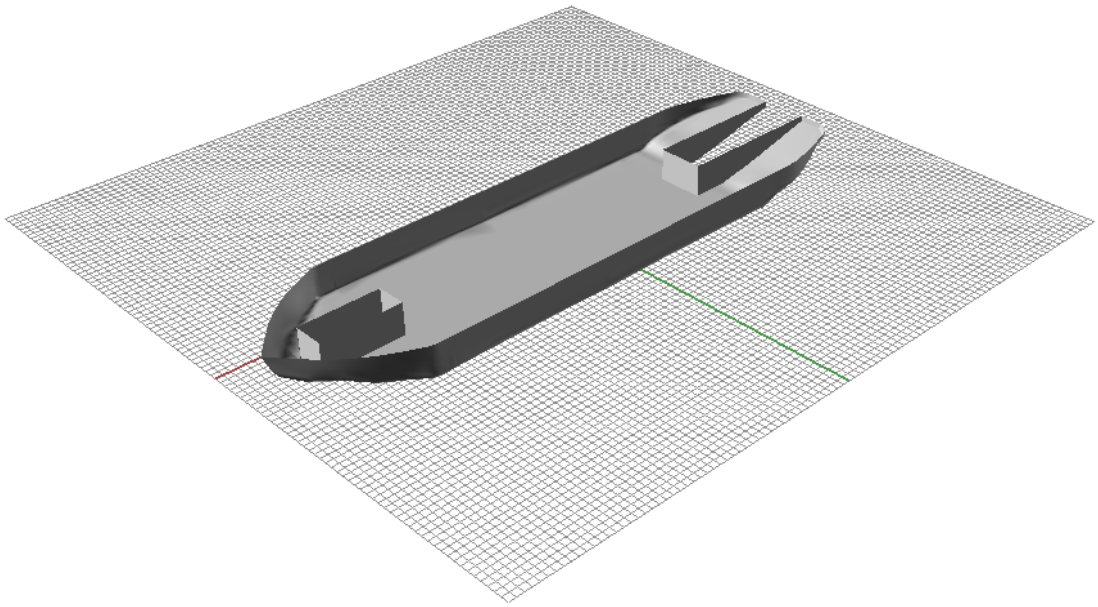

**Figure 10. 3D visualization of the hull structure used on the dynamical model.**

**Table 2. Hydrostatic coefficients for Taurus II**

| Parameter | Value | Dimension |
|---|---|---|
| Length on Water Line | 90.4 | ***[m]*** |
| Maximum Beam on Water Line | 24.11 | ***[m]*** |
| Static draft | 4.68 | ***[m]*** |
| Total Displacement | 7,757.42 | ***[Ton]*** |
| Longitudinal Centre of Gravity from mid ship | 0.42 | ***[m]*** |
| Vertical Centre of Gravity from keel | 2.18 | ***[m]*** |
| Roll Radius of Gyration | 8.43 | ***[m]*** |
| Pitch Radius of Gyration | 6.02 | ***[m]*** |
| Yaw Radius of Gyration | 6.02 | ***[m]*** |

Another input required by the WAMIT model is the body's inertia matrix. This matrix is simplified by adding terms only on the main diagonal, excluding crossed terms between degrees of freedom, as shown on Eq. 13. The elements regarding the moments of translation are represented by the total displacement of the vessel times the density of the fluid (1,025 $kg/m^3$ for seawater). As for the elements related to the moments of rotation, the formulations are described on Eq. 14 to Eq. 16.

$$I = \begin{bmatrix} \rho_w \nabla & 0 & 0 & 0 & 0 & 0 \\ 0 & \rho_w \nabla & 0 & 0 & 0 & 0 \\ 0 & 0 & \rho_w \nabla & 0 & 0 & 0 \\ 0 & 0 & 0 & I_{xx} & 0 & 0 \\ 0 & 0 & 0 & 0 & I_{yy} & 0 \\ 0 & 0 & 0 & 0 & 0 & I_{zz} \end{bmatrix} \quad \textbf{[Eq. 13]}$$

$$I_{xx} = {K_{xx}}^2 \rho_w \nabla \quad \textbf{[Eq. 14]}$$

$$I_{yy} = {K_{yy}}^2 \rho_w \nabla \quad \textbf{[Eq. 15]}$$

$$I_{zz} = {K_{zz}}^2 \rho_w \nabla \quad \textbf{[Eq. 16]}$$

Where $K_{xx}$, $K_{yy}$ and $K_{zz}$ are the radius of gyration on the *x*, *y* and *z*-axis, respectively. These were defined as 8.5, 22.5 and 22.5 meters respectively, as observed in typical rates on LEWIS (1988).

The WAMIT software computed dredge motions in the six degrees of freedom and the wave drift coefficients on horizontal plane for 72 directions of incidence of waves (from 0º to 360º, spaced by a 5º angle), and 62 different periods (from 2 to 4 seconds with a 1 second increment, from 4 to 25 seconds with a 0.5 second increment, and from 25 to 40 seconds with a 1 second increment). In total, the program computed 4,320 cases propagating into the hull. Another important aspect to consider when reaching to predict realistic transfer functions for roll motions is the determination of the viscous damping coefficient. A series of authors searched to create and predict that coefficient for barge type hulls, such as the Taurus II (e.g. HAJIARAB ET AL., 2010, DHAVALIKAR & NEGI, 2009, CHAKRABARTI, 2001), either by creating non-linear models to predict viscous damping due to wave magnitude and slope, or compiling experimental data. Results from the last approach will be used and show that for a unitary wave height, roll motions tends to present a magnitude between 10º and 15º (MAGNUSON, 2010). In order to reach this order of magnitude, a 5% damping coefficient for roll was applied on the final model run. The difference between RAOs with and without the linearized damping is presented on Figure 11.

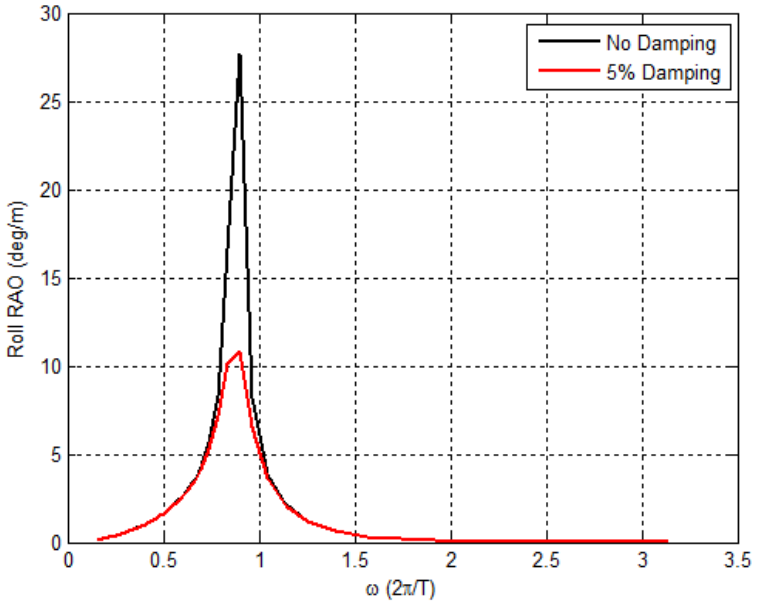


**Figure 11. Results for Roll transfer functions without and with 5% damping coefficient.**

Results for the computation of the response amplitude operators are presented from Figure 12 to Figure 17, already applying the 5% damping coefficient for roll motions.

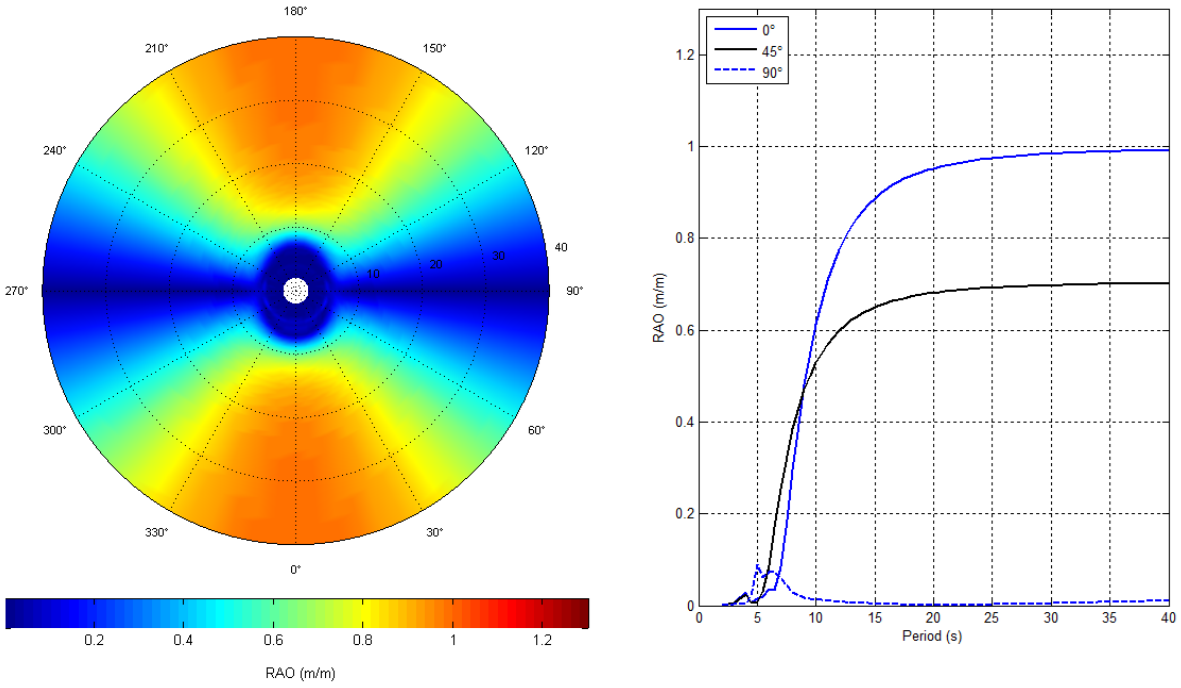


**Figure 12. First order response amplitude operators for surge.**

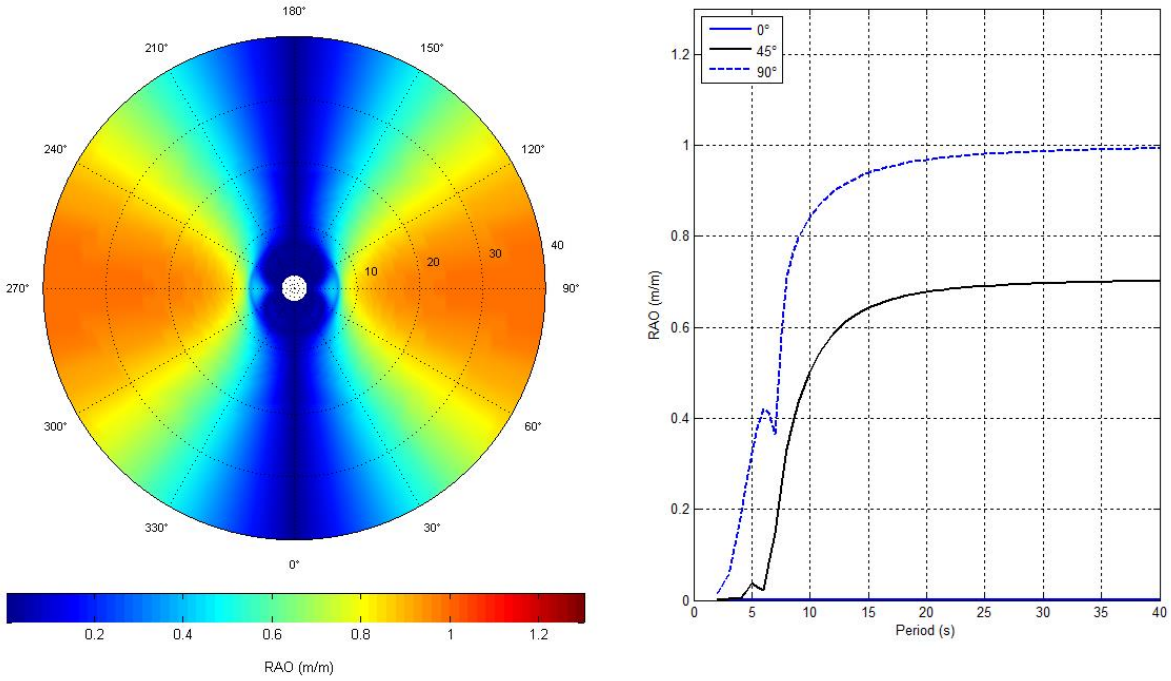


**Figure 13. First order response amplitude operators for sway.**

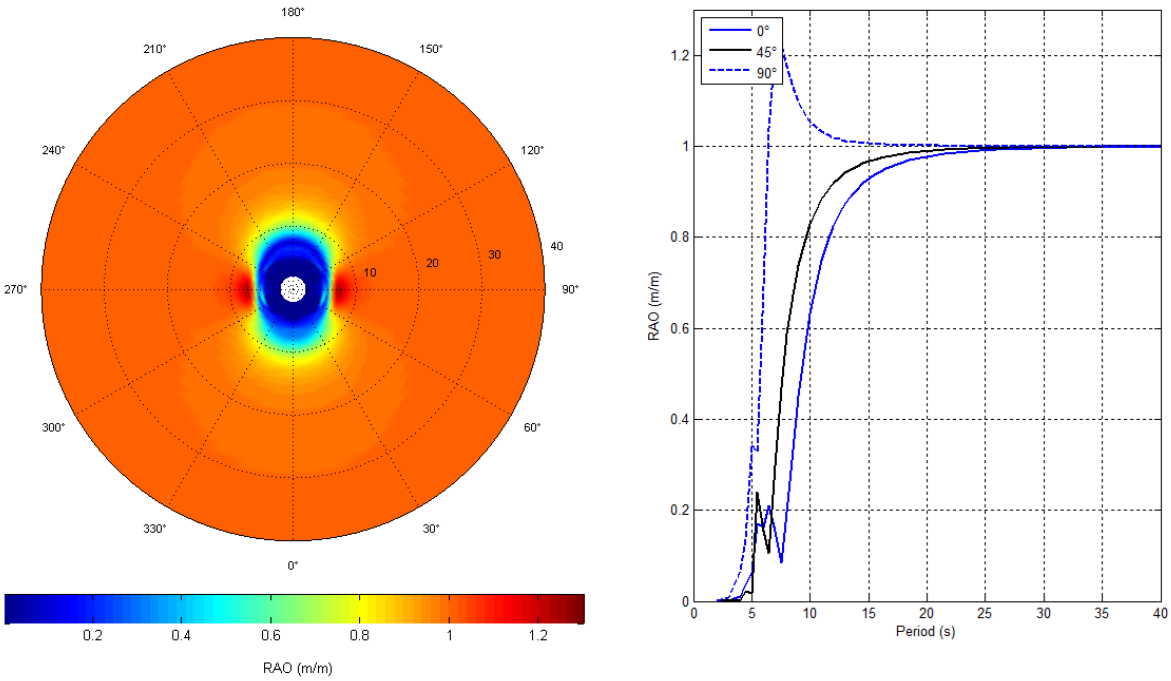


**Figure 14. First order response amplitude operators for heave.**

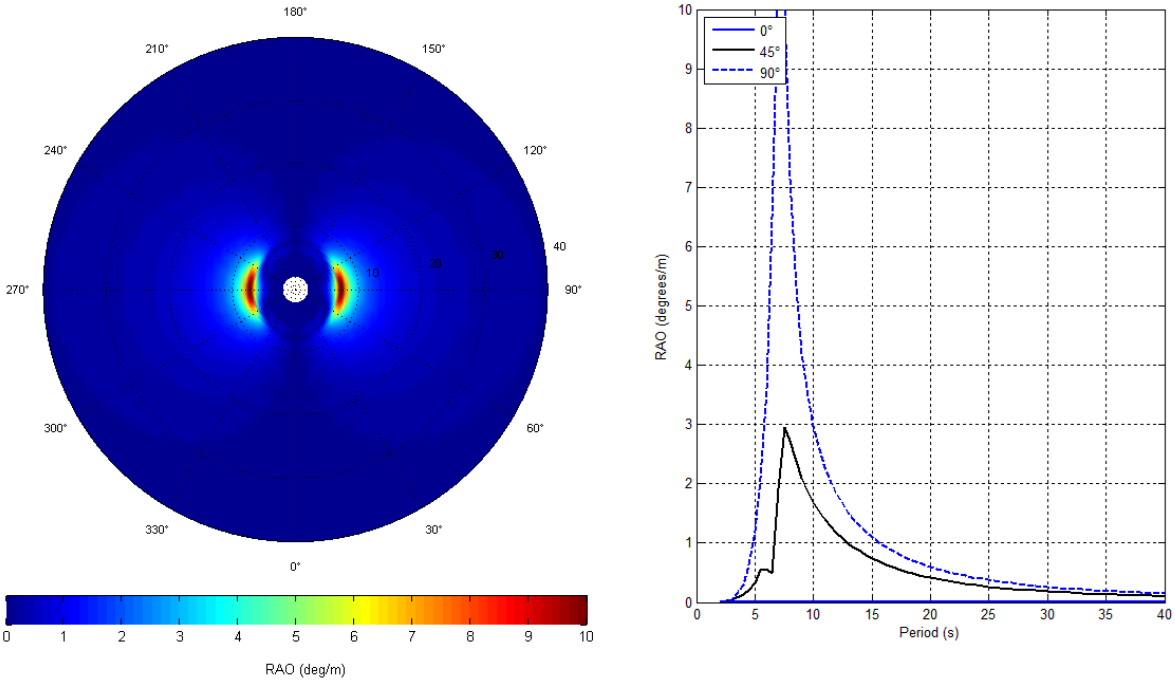


**Figure 15. First order response amplitude operators for roll.**

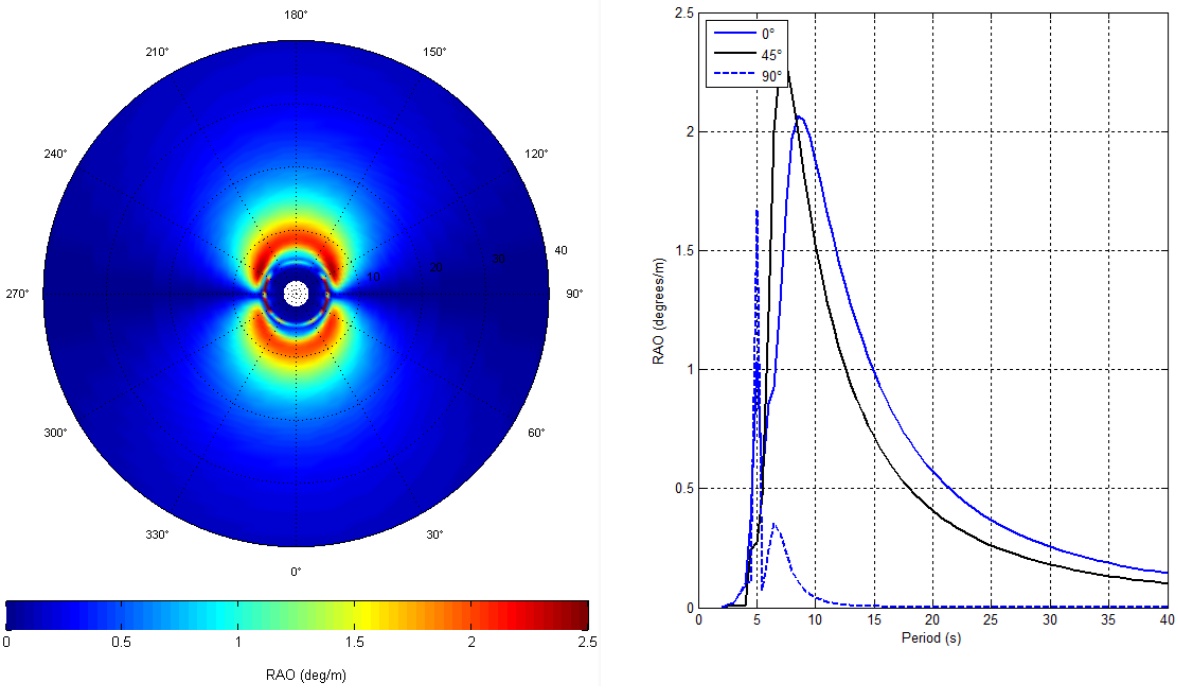


**Figure 16. First order response amplitude operators for pitch.**

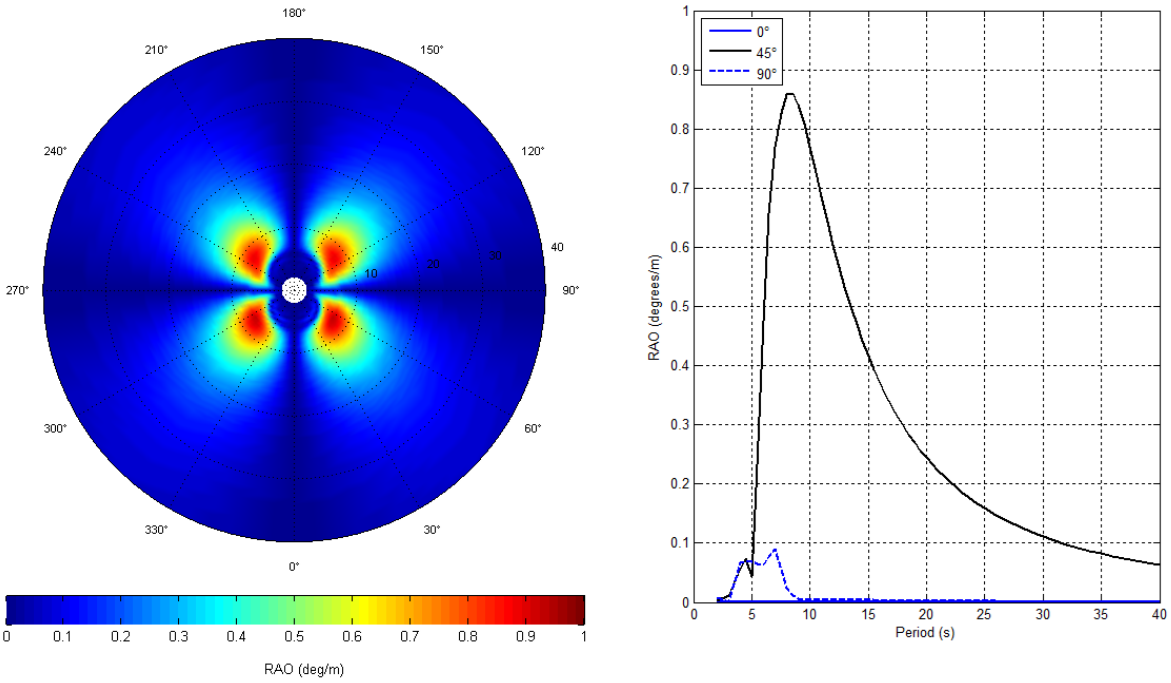


**Figure 17. First order response amplitude operators for yaw.**

Heave responses presented an amplification of the function operator for 90º and 270º incident waves, resulting on values greater than one for 8 seconds waves from those directions, characterizing this period as its resonance period. Peaks are seen on the 8 seconds sway 90º curve and 5 to 10 seconds heave 0º and 45º curves. These are probably a software response to the peculiar hull geometry of the dredge. A peak of 1.7 degrees per wave meter is observed for pitch for a 90º incident wave. This response characterizes the resonance period as 5 seconds. Deviation on curve trends that are not related to resonance periods are observed for pitch and yaw on low periods for practically all directions, which could be a response from the presence of the spud moon pool or well or a numerical noise derived from the model.

Different from response amplitude operators, the coefficients for drift forces and moments presents negative and positive values, depending on the wave incidence direction. The WAMIT software provides the total wave drift forces for the hull. The calculation of this force was performed by the software by integrating total hydrodynamic pressure on the hull. The equation for the representation of this force as an output of the model is:

$$\bar{F}_i = \frac{F_i}{\rho_w g A^2 L_k}$$ **[Eq. 17]**

where A is the wave amplitude, $F_i$ is the mean drift force and $L_k$ is a scale term, in this case, 1. In order to provide dimension for the total drift force, the values provided by the software have to be multiplied by $\rho_w g A^2$. Results for the drift forces for the surge, sway and yaw motions are presented from Figure 18 to Figure 20.

The drift relations of the hull and the waves are given as a value for each wave frequency simulated for a given direction, per the wave height squared. What we search is to obtain the total forces on *x, y* and moments for a given direction of incidence, so the value can be applied on the model. We obtain this single value by crossing the wave spectrum to the drift relation and integrating the resulting vector. The governing formulations for this step are:

$$F_{1,2} = 2\int S(\omega)F(\omega)_{1,2}\, d\omega$$ **[Eq. 18]**

$$M_0 = 2\int S(\omega)M(\omega)_{1,2}\, d\omega$$ **[Eq. 19]**

Where $F_{1,2}$ is the total force for the surge and sway and $M_0$ the total moment, and $S(\omega)$ the wave spectrum density function. In this case the spectrum is created as a standard Jonswap spectrum for a given significant wave height and peak period, and the wave height parameter considered on the calculation is placed between $H_1$ and $H_{10}$, condition that approaches the analysis to the Morrisson formulation approach for the hydrodynamic loads on the hull and ladder. The code developed provides the user the ability to choose the spectrum peekednes value and the number of frequency classes to be generated. In the case of the frequency classes of the wave spectrum and the drift relation differs, the one with the bigger resolution is used to interpolate the lower by using the linear method. The results for the wave generated drift forces and moments are presented from Figure 18 to Figure 20.

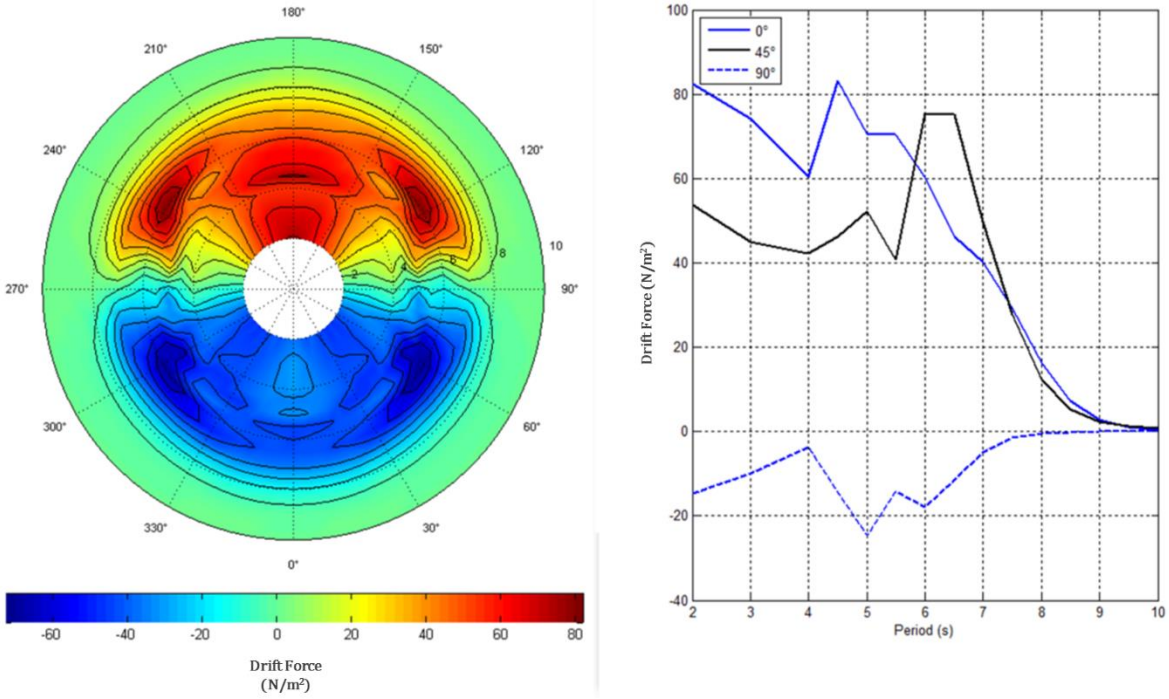


**Figure 18. Surge drift force coefficients.**

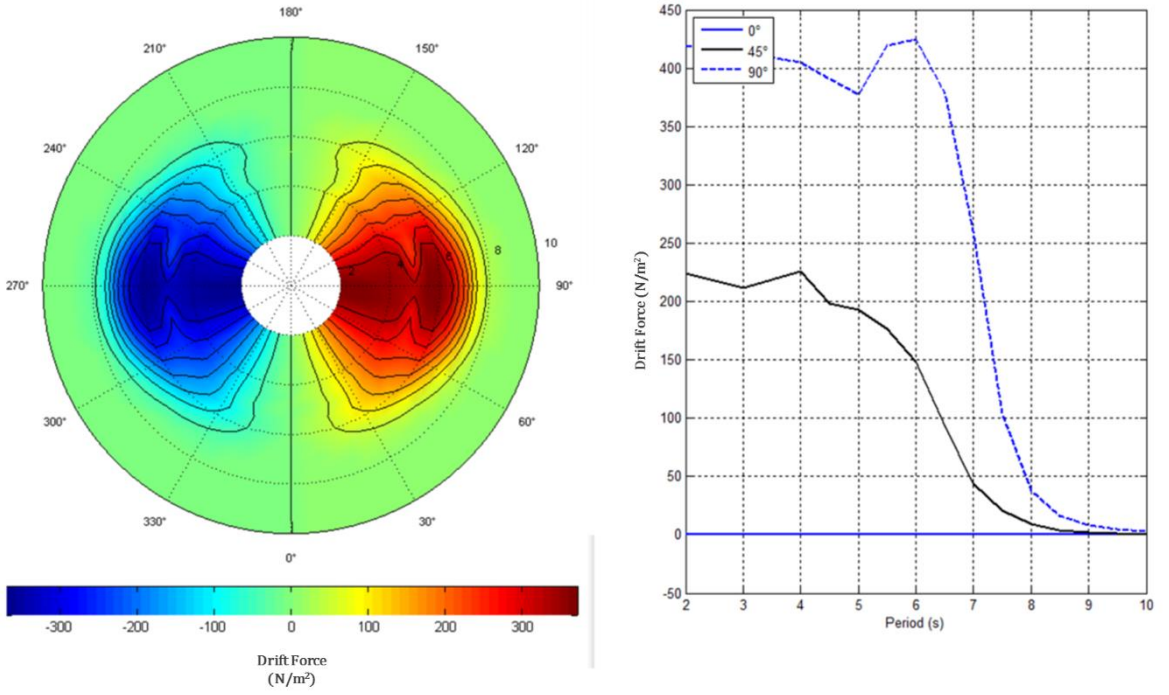


**Figure 19. Sway drift force coefficients.**

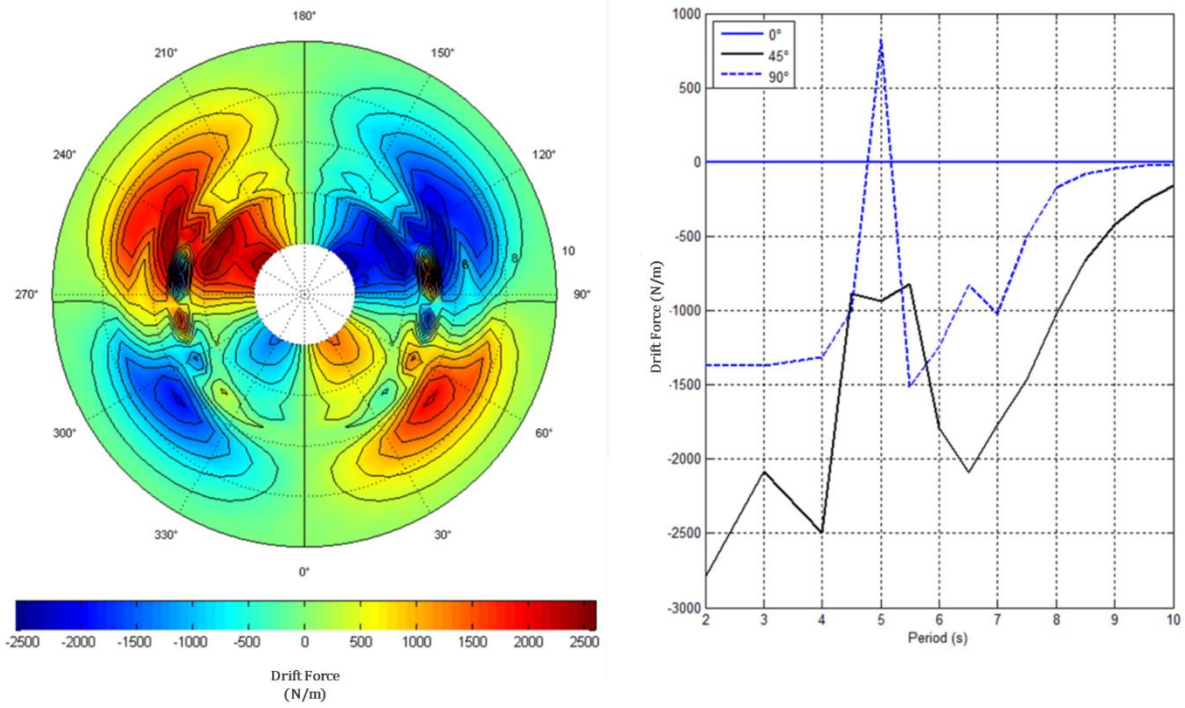


**Figure 20. Yaw drift moment coefficients.**

Drift force coefficients for surge are positive for waves attacking from 270º to 90º, and negative for the two remaining quadrants. Maximum observed values are 80 kN/m, both positive and negative. Surge drift forces can be observed with transversal wave incidence due to hulls asymmetry from bow to stern. This way, a 90º wave generates non-zero coefficients for this motion. Values for sway drift are greater in magnitude than those of surge, since the longitudinal hull area is bigger than the transversal one. The peak values are for 90º and 270º waves, being approximately 430 kN/m. Waves attacking from pure bow and stern directions do not generate any sway drift force. Yaw drift moment coefficients are antisymmetric with respect to the dredger center plane, being zero only for the 0º and 180º incident waves. Values of yaw drift moment peaks at 2,500 kN/m$^2$, for waves coming from 100º and 260º.

Presented the response of the dredger due to waves, on the next section, the response of the dredger to the other two main environmental processes (winds and currents) will be presented in terms of magnitude and trends.

## 4.3 Dredge forces due to winds and currents

Drift forces and moments on the dredge are also generated by winds and currents. If the drift forces and moments generated by waves are smaller than those generated by winds and currents, we should expect that the processes depending on static forces on the dredge will be more affected by winds and currents than waves. This section is dedicated to present the influence of the magnitude and direction of winds and currents on the dredger through the calculation of the drift forces and moments. Both wind and current drift force coefficient are divided into transversal and longitudinal components, as seen on Eq. 6 and Eq. 7, and were obtained from the references presented in the dredge response section on literature review. For each component, incidences of 0°, 45°, 90°, 135° and 90° were analyzed. The same analysis was performed for drift moments. For each angle and component, different magnitudes of wind and current velocity were used in the calculations. Results for current drift forces and moments are presented on Figure 21 and Figure 22, while wind drift forces and moments are presented on Figure 23 and Figure 24, respectively.

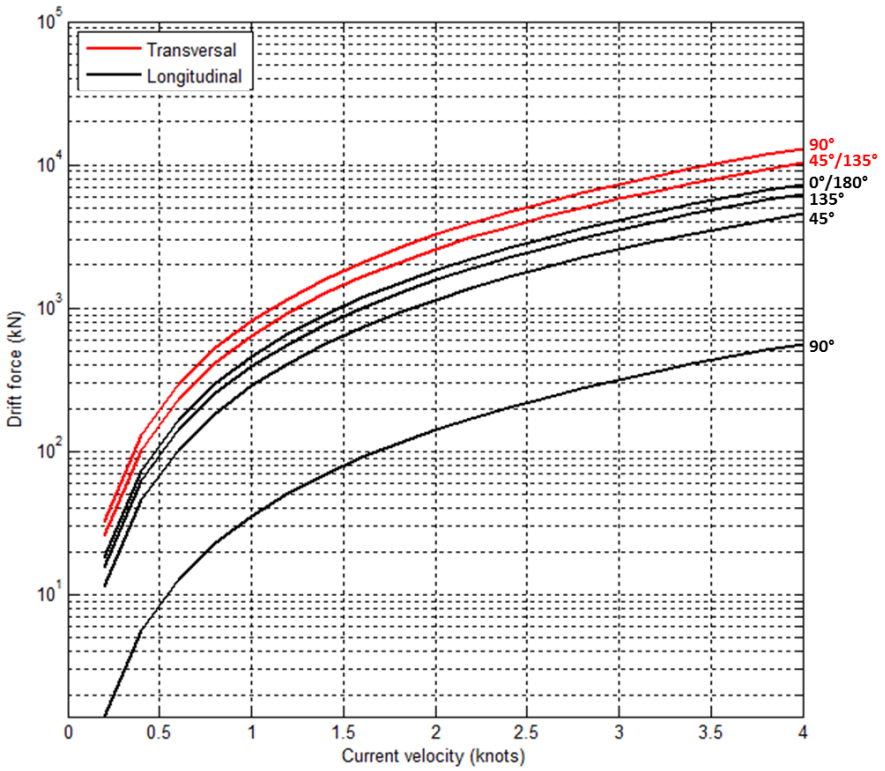


**Figure 21. Drift force module as a function of current magnitude.**

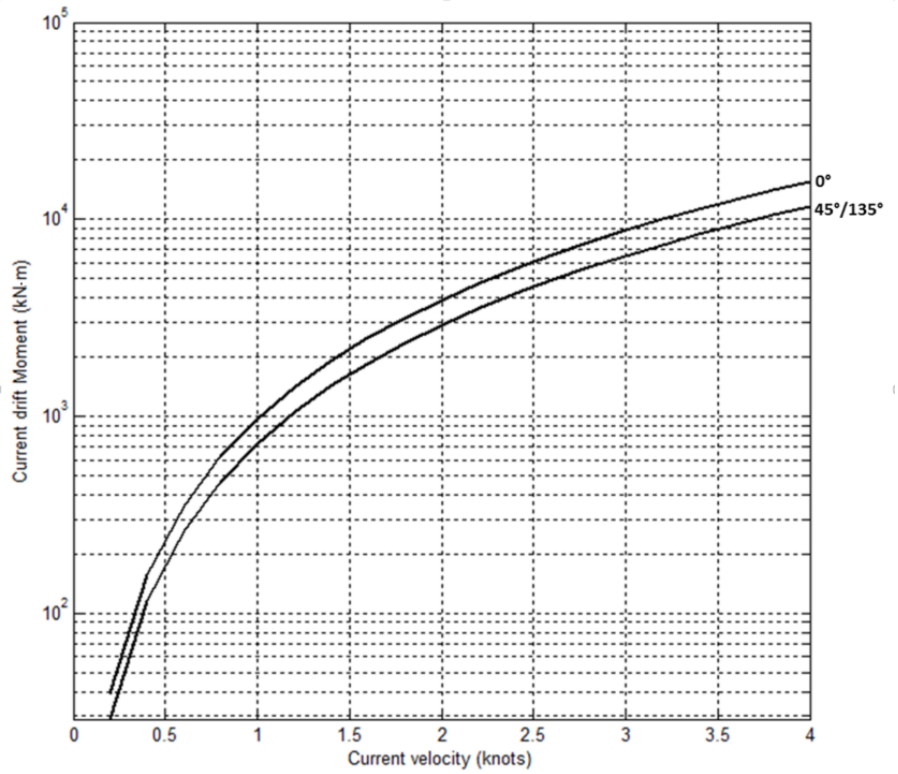


**Figure 22. Drift moment module as a function of current magnitude.**

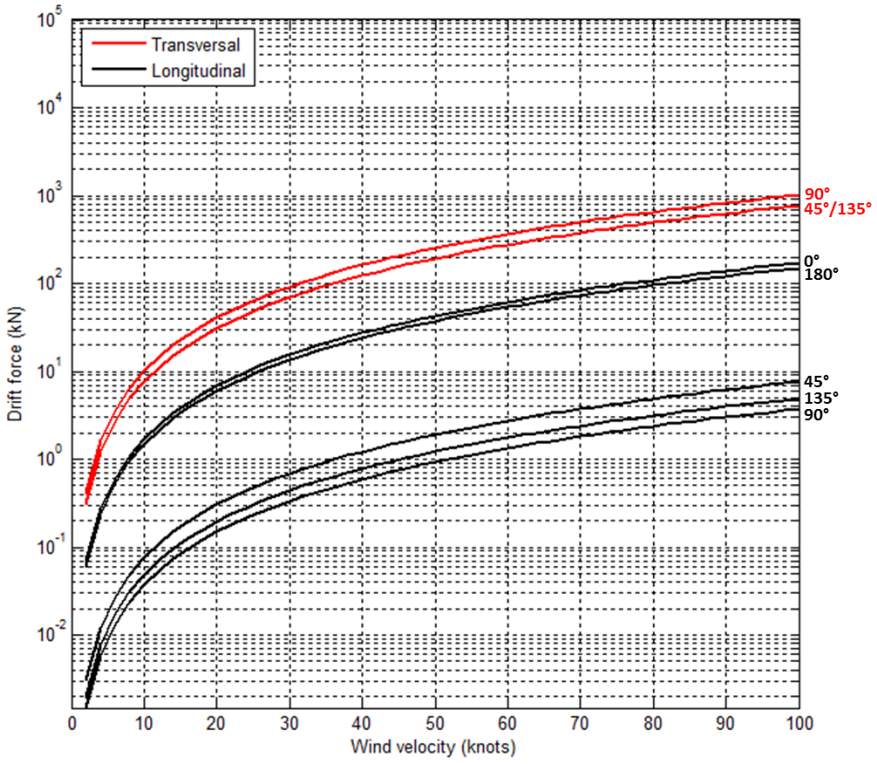


**Figure 23. Drift force module as a function of wind magnitude.**

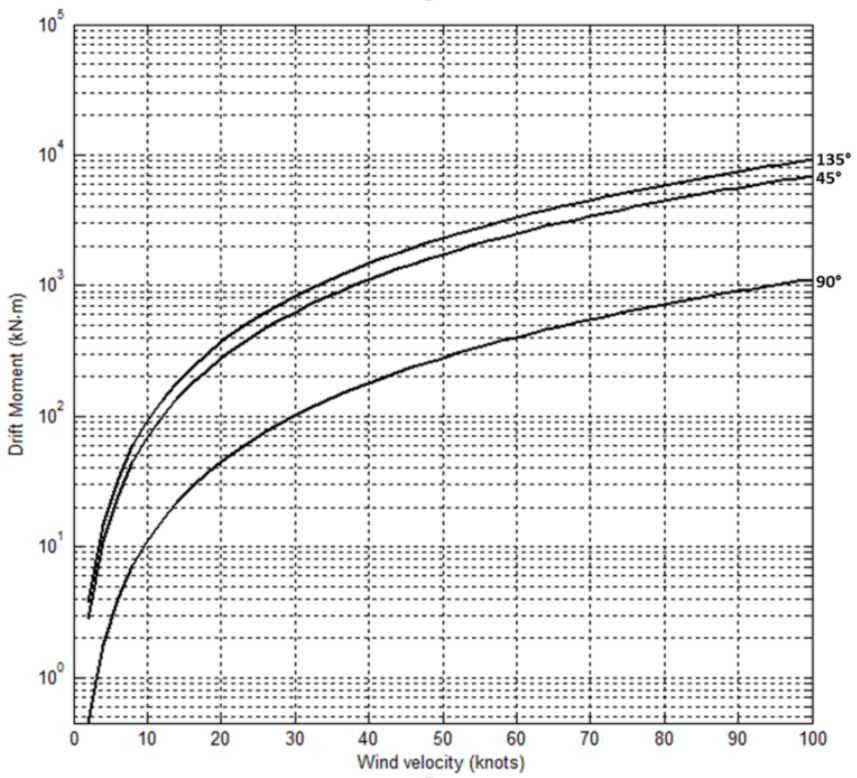


**Figure 24. Drift moment module as a function of wind magnitude.**

The greatest current generated drift forces are transversal to the dredge, at a 90° angle, condition when a 1 knot current generates a $10^2$ kN order force, while the greatest longitudinal forces are from 0° and 180°. The increase on current velocity generates a quadratic growth of drift force, considering the squared component of current velocity on the drift force calculation. The same behavior is observed for current generated drift moment, while its magnitude is of order $10^3$ kN/m when subjected to a 1 knot current.

Quadratic behavior is also observed for wind generated drift, one the direction relation is equal to the current generated drift. Compared to the current loads, the magnitude of $10^2$ kN and $10^3$ kN/m for force and moment respectively, are obtained for a 30 knot wind.

## 4.4 Swing winches model

Effort is being made in order to formulate linearized models to calculate the forces, moments and accelerations on the dredger systems, with the objective of providing the basis of comparison of these values to the operational limits. For that reason, the swing winches power model were developed based on the swing motion around the spud and the geometry of the mooring system, considered as a two-dimensional approximation on the *x*-*y* plane of a force and moment equilibrium system. The main components of the system are the external forces and moments caused by waves, currents and winds, the tensions on the port and starboard wires and the reaction forces of the spud pole. The latter is critical since the main objective of the structure is to keep the vessel on a fixed position, hence the importance of its reaction forces on the total equilibrium of the system. In the end, the combined cable tension and swing velocity provides the required power for a given wave, wind and current case.

In order to generate a coherent model that can be processed in the frequency domain, some assumptions have to be made. The first assumption is that the swing lines are pre-tensioned and forces in *z* are neglected. The pre-tension condition approximates the system to a model similar to a body hold in place by two springs: the total tension of the spring $T$ is the sum of the pre-tension $T_0$ and the tension interval $\Delta_T$, proportional to the dislocation of the body on the plane (Figure 25). $\Delta_T$ will be positive or negative depending on the direction of the dislocation to port or starboard. While assuming this condition, this system generates only one unknown variable, $\Delta_T$. The second assumption is that the swing motion can be represented as a quasi-static process: the position of the dredger during the swing will determine the angles between the wires and the vessel, while the swing velocity (as input) is accounted only for the power calculation on the winches. The third assumption is the equilibrium state of the system. Considering the quasi-static approximation, we assume that the sum of moments, sum of forces in *x*-axis and sum of forces in *y*-axis are all equal to zero. This provides us with the governing equations of the model (Eq. 20 to Eq 25).

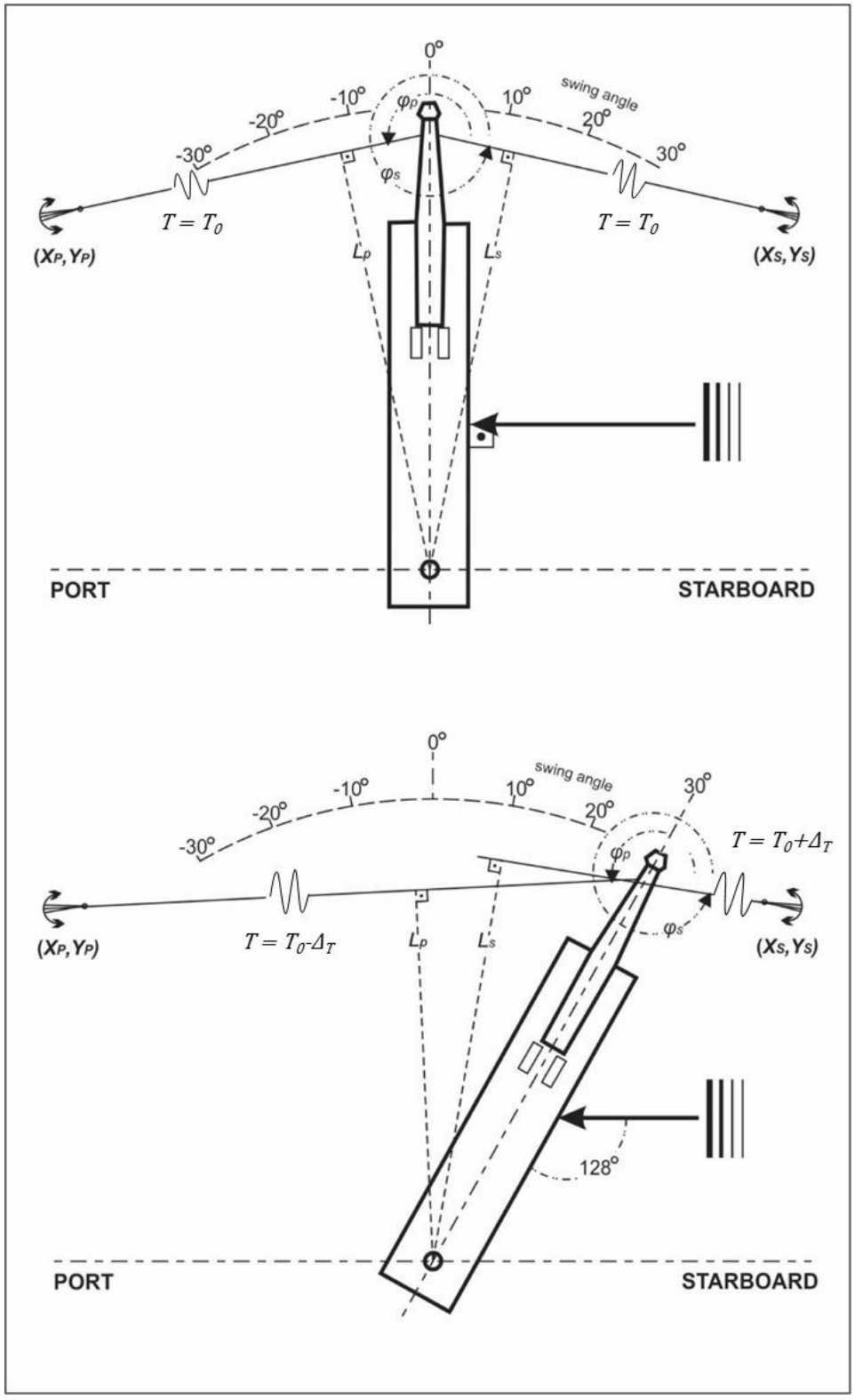


**Figure 25. Generalized model for the swing wire system.**

$$\sum F_x = (T_0 + \Delta t)\cos\varphi_p + (T_0 - \Delta t)\cos\varphi_s + F_{xsp} + F_{xw} = 0 \quad \textbf{[Eq. 20]}$$

$$\sum F_y = (T_0 + \Delta t)\sin\varphi_p + (T_0 - \Delta t)\sin\varphi_s + F_{ysp} + F_{yw} = 0 \quad \textbf{[Eq. 21]}$$

$$\sum M_z = (T_0 + \Delta t)L_p + (T_0 - \Delta t)L_s + M_w L_{CG} = 0 \quad \textbf{[Eq. 22]}$$

The above equations can be solved analytically, resulting on the following solutions:

$$\Delta t = -\left(\frac{M_w L_{CG} + T_0 L_p + T_0 L_s}{L_p - L_s}\right) \quad \textbf{[Eq. 23]}$$

$$F_{xsp} = -\left[(T_0 + \Delta t)\cos\varphi_p + (T_0 - \Delta t)\cos\varphi_s + F_{xw}\right] \quad \textbf{[Eq. 24]}$$

$$F_{ysp} = -\left[(T_0 + \Delta t)\sin\varphi_p + (T_0 - \Delta t)\sin\varphi_s + F_{yw}\right] \quad \textbf{[Eq. 25]}$$

Where:

- $L_s$ = Distance between spud (or pivoting point) to the starboard wire normal;
- $L_p$ = Distance between spud (or pivoting point) to the portside wire normal;
- $F_{xw}$ = Total drift force on the *x* direction on the center of gravity;
- $F_{yw}$ = Total drift force on the *y* direction on the center of gravity;
- $M_w$ = Total drift moment on the center of gravity;
- $L_{CG}$ = Distance from spud position to the center of gravity;
- $F_{xsp}$ = Total reaction force on the *x* direction on the spud;
- $F_{ysp}$ = Total reaction force on the *y* direction on the spud;

The value of pre-tension is calculated by the program in order to avoid negative values for swing wire tension and winch power. That is why pre-tension is not an input on the software. Considering the spring body system as an approximation, we can assume that the model is capable on representing a system with small angles formed between the anchors and the hull, as well as small swing angles. Given this assumption, a careful analysis must be performed on the results for angles greater than 10 degrees, mainly if it can or cannot be considered as consistent. In order to obtain the required winch power for a given cable tension, the cable tension value is multiplied by the angular velocity of the dredge, the latter related to the total time required to perform the swing. Once the system of equations used on the model is described, the results for currents, winds and wave influence on the winch power will be presented separately, in order to provide an insight of the influence of each environmental agent on the required winch power.

### 4.4.1 Wave influence on required winch power

Waves were simulated for 181 different directions (from 0º to 360º, every 2º), 39 peak period values (from 2 to 40 seconds) and 4 different significant wave heights (0.5, 1, 1.5 and 2 meters), providing a total of 28,236 cases. Each case is represented by a full 60º swing, from port to starboard. The maximum value of the analyzed for the swing is extracted from each case, since it will be the representative value for downtime analysis. The results analyzed for the winch model are: swing cable tension, reaction force on the spud and required winch power. The distribution of those variables during a swing for a pure bow wave is presented in Figure 26. The anchors were positioned in order to provide an angle between the ladder and the swing cables that is always smaller than 90º. This way, when at first position, the cable angle in relation to the ladder is 49º, while the cable length between the ladder connection point and the anchor is 82 meters. This condition was used for all analysis described later on this research, except when pointed differently. For the present analysis, no soil reaction forces created by the ladder are considered. It is also important to place that, as a first analysis, it is considered that only the mean drift forces modify the tension of the wires and the first order motions are compensated in the process.

The external forces and moments caused by waves are coherent with the expected results during a full swing for a bow wave. In this case, the maximum spud reaction force in *x* and *y* are 14 and 9 kN, respectively. Maximum values for both port and starboard cable tension during swing is 9.5 kN, and minimum of 0.5 kN, this last representing the pre-tension value. In the end, maximum required winch power is 3 kW for both boards.

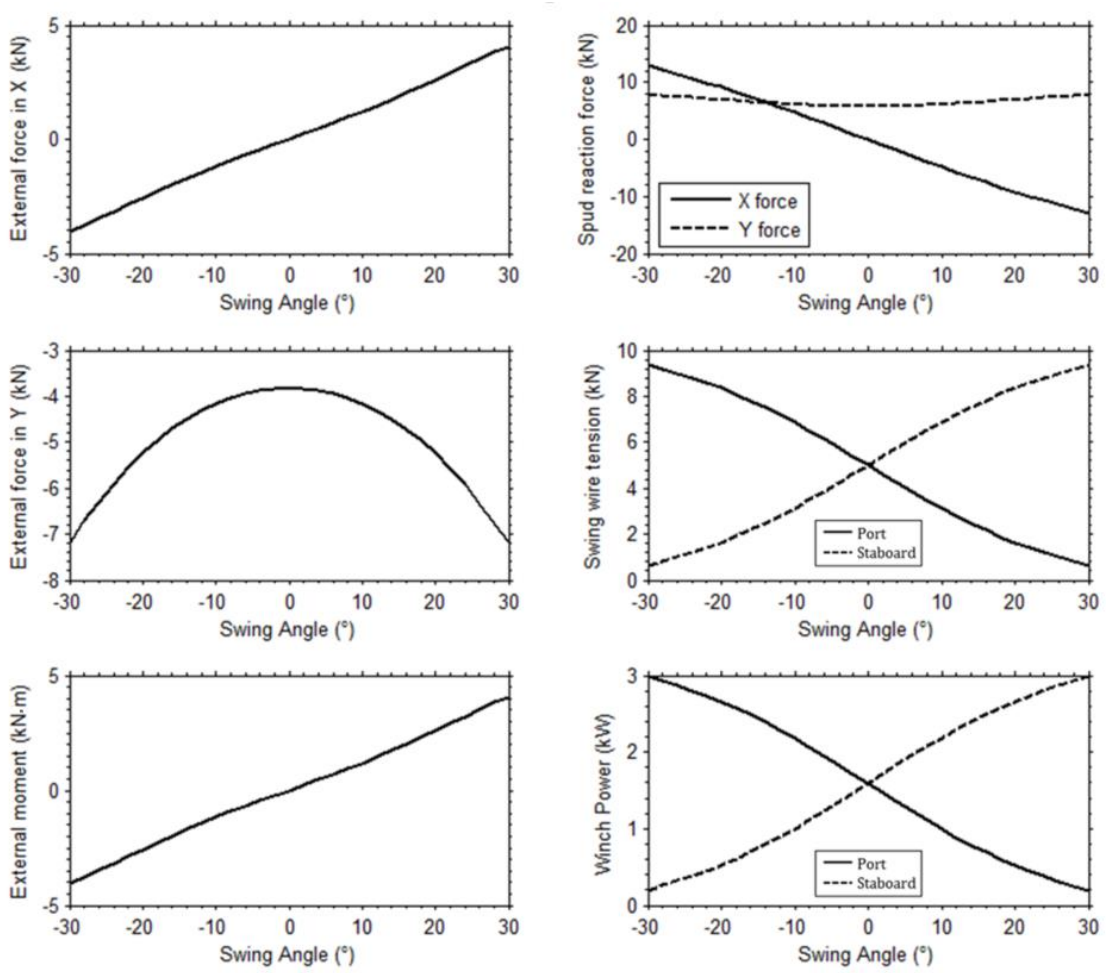


**Figure 26. External forces and moments on the dredge caused by a 0º wave (left) and the swing winches model results (right) during a full swing.**

Results for maximum values during swing for the intermediate results of the swing winches model (cable tension and spud reaction force) are presented on Figure 27. The first two graphics presents the portside cable tension as a function of wave direction, showing that greater tensions are generated for 270º waves. Waves with periods of 7 seconds are most critical for operations (32 kN for a 270º wave), while longer periods are less critical. This is explained by

the fact that this model considers only drift forces on its formulation, for which smaller periods results in greater drift forces and moments.

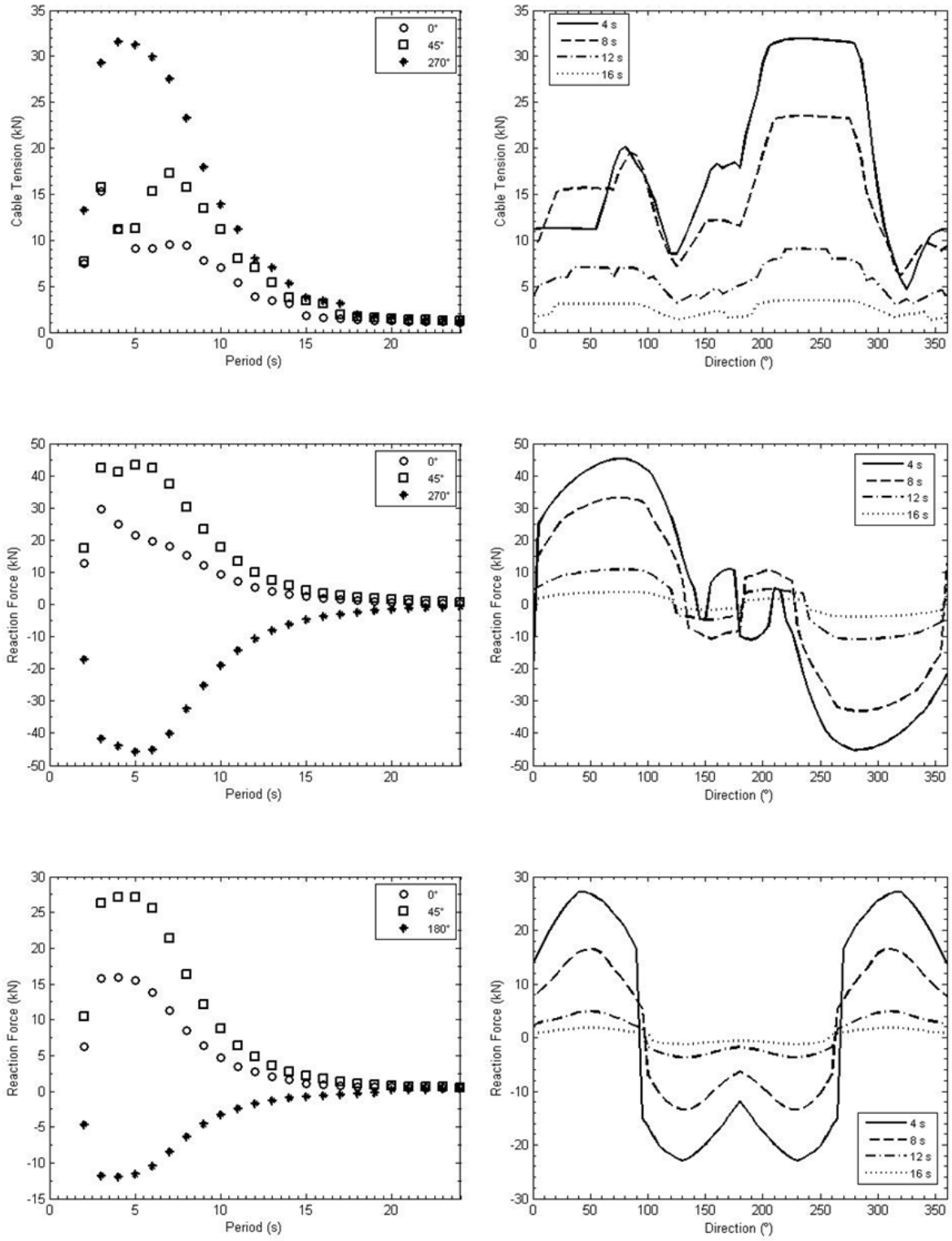


**Figure 27. Portside cable tension (first above), spud reaction forces in x (middle) and y (below) in relation to wave period and direction ($H_s$ = 1m).**

When analyzing the mean reaction forces on the spud, generated by waves, it is noticeable the same relation found for cable tension: smaller periods generates greater forces, with a 40 kN order for forces on the *x* axis (east-west) for a 5 seconds period wave. Since the force is related to direction, the symmetrical inversion from positive to negative can be observed when analyzing the influence of wave direction on spud reaction force. Regarding the influence of wave direction on forces on the *y* axis (north-south), the same symmetrical behavior can be found, while the order of magnitude rises to a maximum of 27 kN.

Considering a 5 minute swing time, the required power for the winches can be calculated. Considering that the winch power is directly related to the cable tension, the relations between period and direction to winch power is expected to be similar to those of cable tension. The results for the series of cases simulated can be observed on Figure 28. A resultant cable tension of 32 kN requires a 10 kW power for the swing winches, considering a wave with $H_s$ = 1 m.

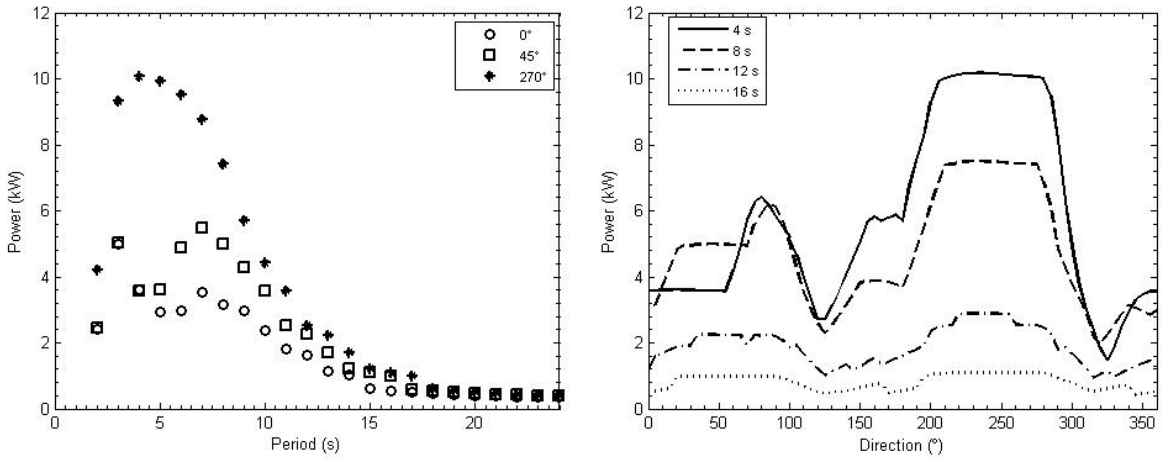


**Figure 28. Required portside winch power as a function of wave period and direction ($H_s$ = 1 m).**

### 4.4.2 Current influence on required winch power

Currents differs from waves once it contains only two variables to be analyzed (magnitude and direction) instead of three (height, period and direction). This condition changes the analysis of the maximum results during swing, changing the comparison of results to current magnitude. Considering this aspect, a number of 181 current directions were simulated for magnitudes of 0.1 to 4 knots, every 0.1 knot, resulting in 7.240 current cases. Only current drift coefficients were utilized in the calculations. The results are presented in Figure 29, and shows that spud reaction forces and cable tensions present a quadratic increase in relation to current magnitude. A value of 100 kN of cable tension was obtained for a 1 knot current, condition that can occur frequently on shelf seas and meso-tidal regime estuaries. Spud reaction values of 100 and 50 kN in *x* and *y* respectively were found for a 1 knot current. The same symmetrical pattern of spud reaction force regarding process direction was found in waves was generated for currents.

The winch power results were similar in pattern to the cable tension results (Figure 30). Currents demands more of the winches to perform a swing than waves for regular conditions found in the Brazilian coast. For example, in order to require a 30 kW power, the dredge must be subjected to a 2 meter wave or a 1 knot current, being the last more frequent than the first on the operation environment.

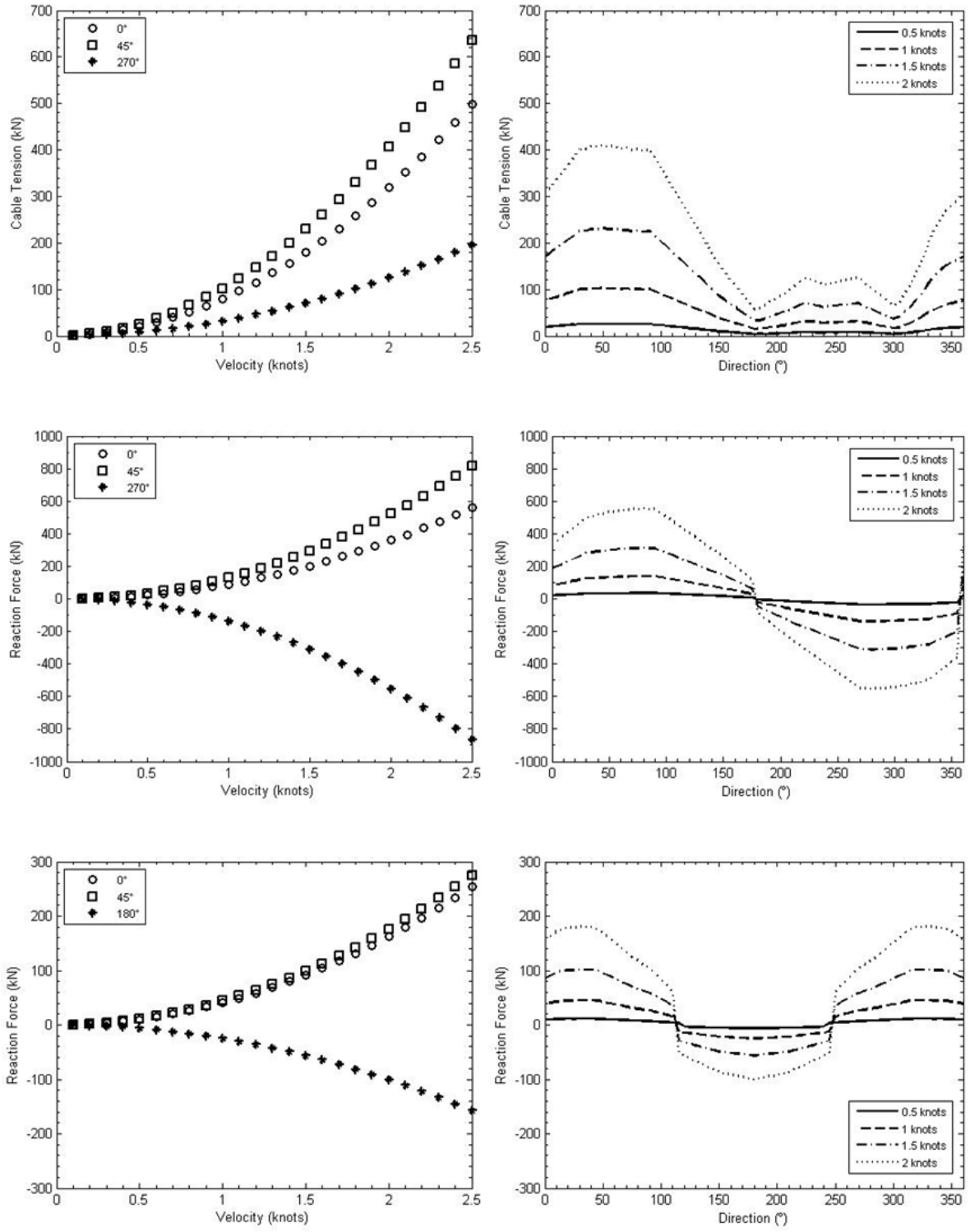


**Figure 29. Portside cable tension (first above), spud reaction forces in x (middle) and y (below) in relation to current magnitude and direction.**

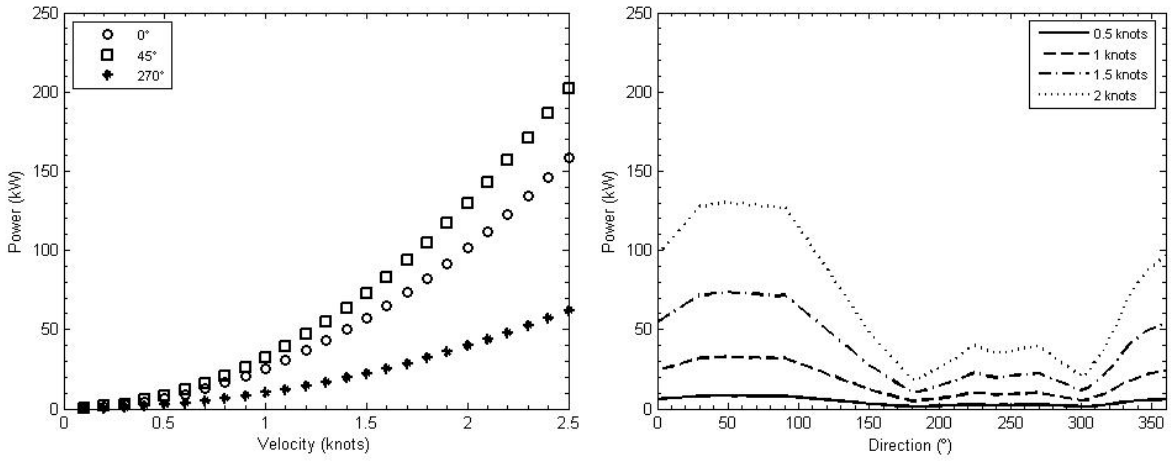


**Figure 30. Required portside winch power as a function of current magnitude and direction.**

### 4.4.3 Wind influence on required winch power

The last environmental agent acting on the winch power model to be analyzed is the wind. As performed for waves and currents, wind cases were simulated for 181 different direction and 41 different magnitudes (0 to 80 knots, every 2 knots), totalizing 7.421 cases. The behavior of the other model generated results (cable tension and spud reaction force) in respect to wind magnitude and direction can be visualized on Figure 31. The response pattern of cable tension and spud reaction forces are very similar to those generated by currents: curves presents a quadratic growth with the increase on wind velocity, and inversion of magnitude value is found due to process direction. The difference in relation to currents is the magnitude of the process necessary to generate the same forces and tensions: in order to generate a 100 kN cable tension, a 1 knot current or a 30 knot wind is required.

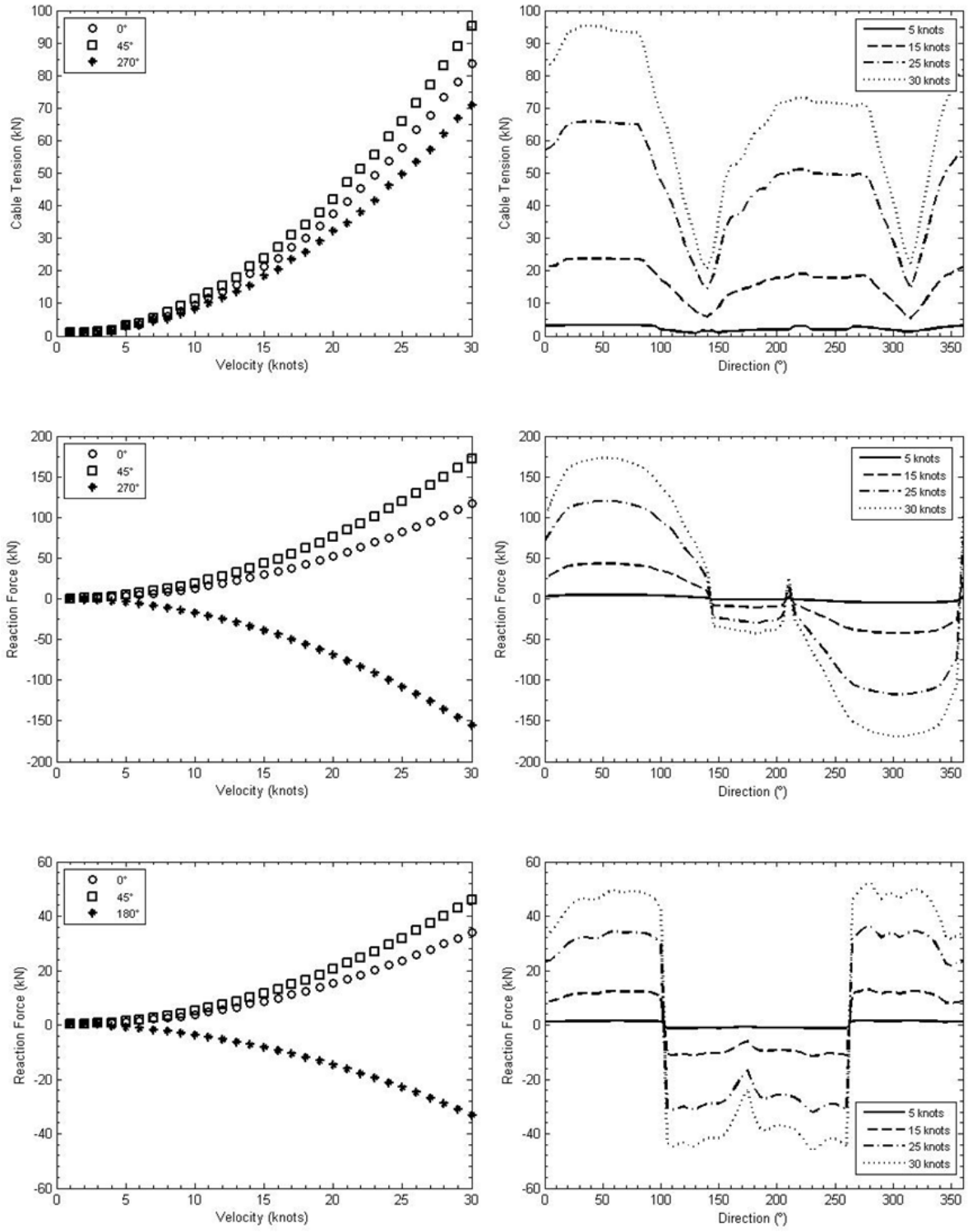


**Figure 31. Portside cable tension (first above), spud reaction forces in x (middle) and y (below) in relation to wind magnitude and direction.**

The same diference of magnitude needed to generate the same variable response is observed on the winch required power. A 30 knot wind will require a 30 kW winch power, the same as a 2 meter wave or a 1 knot current.

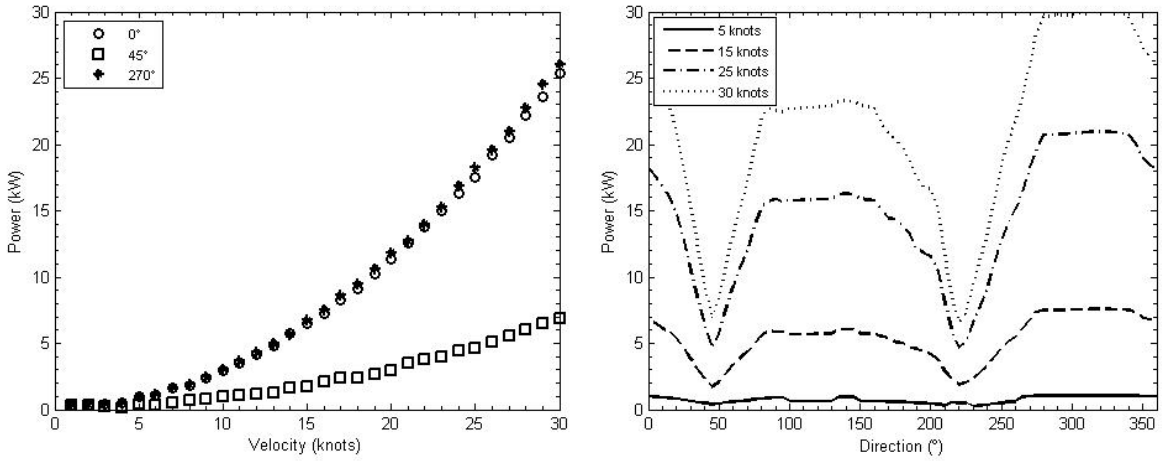


**Figure 32. Required portside winch power as a function of wind magnitude and direction.**

The static forces generated by waves are not as significant as the one generated by currents and winds, so it is expected that the required power for the swing winches when the dredge is subjected to currents and winds will be significantly larger.

Swing cable winches are generally the most powerful winches on a CSD, since other winches are related to parallel activities, such as spud retraction and ladder hoisting. Even when submitted to high waves, such as 2 meters, the required power in order to guarantee the operation is relatively low when considered the total installed power of the Taurus II dredge (24,610 kW), but significative when considered the installed winch power (between 150 and 200 kW). Commentaries regarding the total and remaining installed power for the swing winches, as well as the downtime limit criteria, will be provided further. Other important agent acting on the swing wire tension is the reaction force that the ladder and cutterhead system generates during dredging. Consequently, the influence of it on the required winch power is important during operations. These were not considered in this analysis given the complexity of this relation.

## 4.5 Cutterhead velocity at bottom

Since the forces generated by the interaction between the cutting system (cutterhead and ladder) and the soil is complex, the closest relation between the dredge and the soil that can be defined as a downtime criteria was considered to be the horizontal velocity of the cutterhead at the bottom. The vertical dislocation of the dredge provides a horizontal dislocation of the cutter end, assuming the hinge connection between ladder and hull. At the same time, while dredging, the cutterhead is "buried" on its cutting layer (which for large seagoing cutter suction dredgers can BE as thick as 1 meter). Those two aspects combined suggest that there must be a limit for the horizontal velocity of the cutterhead that allow the system to cut and aspire normally and not to compromise the integrity of the ladder system As it will be discussed later, the type of soil can be considered critical in this limit analysis . In order to calculate the cutting velocity, the variables defined on Figure 33 are applied on a series of calculations.

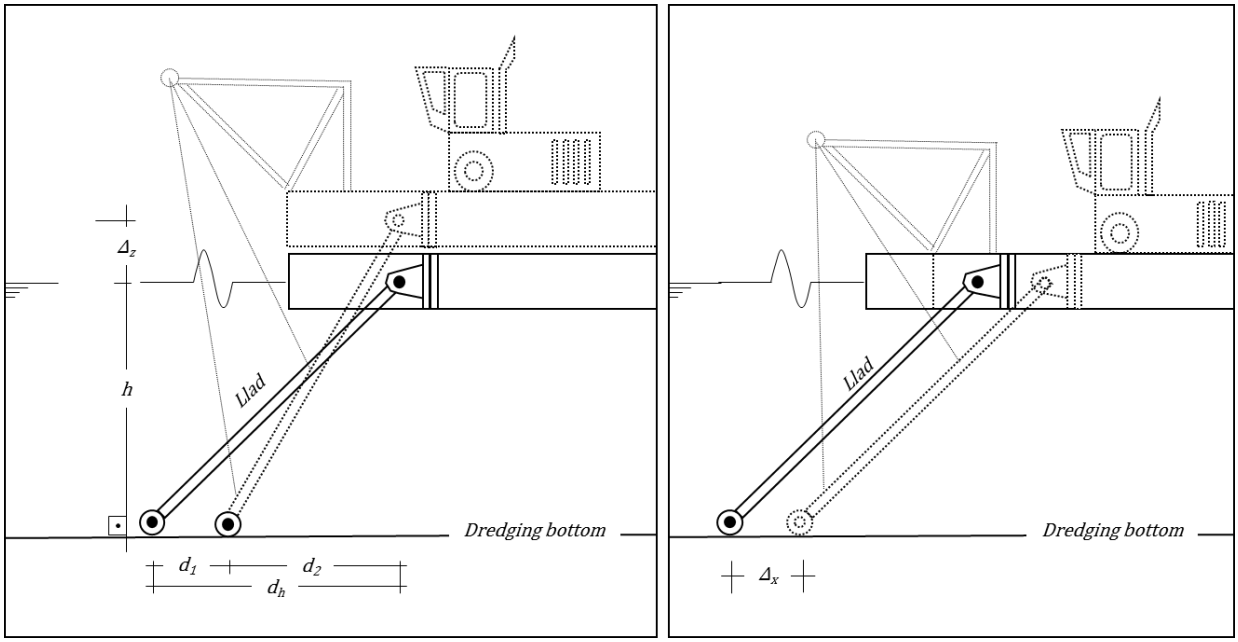


**Figure 33. System definition of variables used for determining cutterhead velocity.**

The first variable to be defined is the vertical dislocation ($\Delta_z$) on the hinge connection point. This variable is obtained by the application of the response amplitude operators to the

simplified Euler's matrix of rotation, as presented by LEWANDOWSKI (2004). First, the origin is displaced to the hinge point using the following matrix:

$$\begin{bmatrix} Dx \\ Dy \\ Dz \end{bmatrix} = \begin{bmatrix} 0 & -\xi_6 & \xi_4 \\ \xi_6 & 0 & -\xi_5 \\ -\xi_4 & \xi_5 & 0 \end{bmatrix} \begin{bmatrix} Xn \\ Yn \\ Zn \end{bmatrix} \quad \textbf{[Eq. 25]}$$

Where:

- $\xi_{4,5,6}$ are the rotation motions pitch, roll and yaw of the hull, obtained by the RAO;
- Xn, Yn and Zn the distances in x, y and z from the CG to the ladder hinge point;
- Dx, Dy and Dz the absolute dislocations in surge, sway and yaw generated from rotation motions.

In order to obtain the relative motion, Dz must be added to heave motion ($\xi_3$), as demonstrated on Eq. 26. The same can be considered for surge motion Dx.

$$\Delta_z(\omega) = D_z(\omega) + \xi_3(\omega) \quad \textbf{[Eq. 26]}$$

$$\Delta_x(\omega) = D_X(\omega) + \xi_1(\omega) \quad \textbf{[Eq. 27]}$$

Further calculations are performed by simple trigonometric relations leading to Eq. 28 for the horizontal distance traveled by the cutterhead at the bottom due to the vertical displacement of the hinge connection point. This distance is added to the maximum surge dislocation in order to obtain the total dislocation of the cutterhead at the bottom ($d_1$). The sum operation is performed on complex mode in order to contemplate the motions phase relation until this equation.

$$d_1(\omega) = \sqrt{{L_{lad}}^2 - h^2} - \sqrt{{L_{lad}}^2 - (h + \Delta_{Zmax}(\omega))^2} + |\Delta_{Xmax}(\omega)| \quad \textbf{[Eq. 28]}$$

The horizontal distance is traveled during the time of half wave period, since the variable to be considered is wave amplitude. By that, we can apply Eq. 29 to obtain the horizontal velocity of the cutterhead $v_{cut}$.

$$v_{cut}(\omega) = \frac{d_1(\omega)}{\pi} \qquad \textbf{[Eq. 29]}$$

Then, dimension is added to the cutterhead velocity by crossing it with the desired wave spectrum (Eq. 30) to obtain the maximum cutterhead velocity $v_{max}$.

$$v_{MAX} = 1.8\sqrt{\int_0^{\omega} S(\omega) v_{cut}(\omega) d\omega} \qquad \textbf{[Eq. 30]}$$

These formulations were applied on the Taurus II dredger response amplitude operators. Maximum cutterhead velocity results during swing are presented on Figure 34. For a 1 meter significant wave height, the maximum velocity obtained is 0.85 m/s on the cutterhead. Largest wave periods generates more intense velocities on the cutterhead, while transverse waves generates slightly bigger velocities than longitudinal waves.

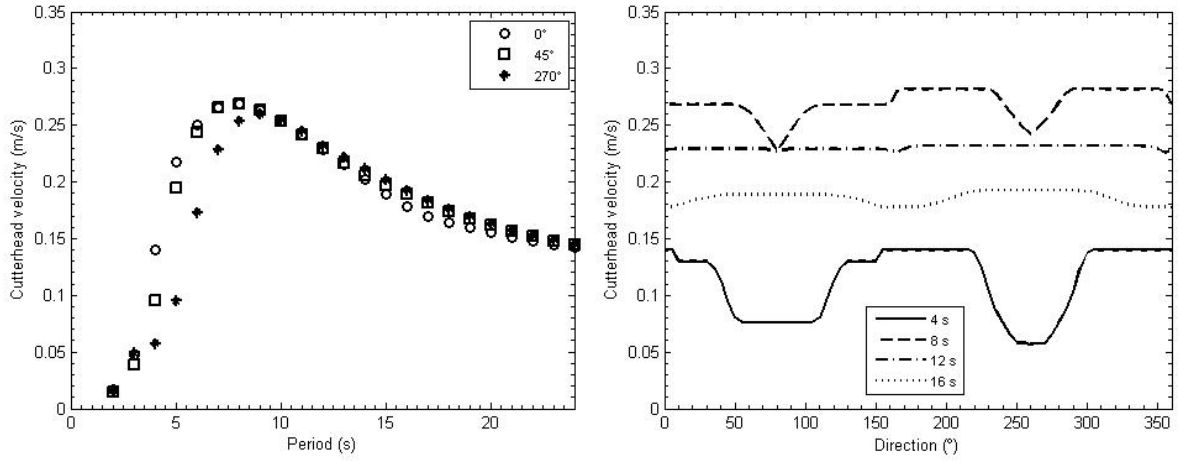


**Figure 34. Cutterhead velocity at bottom ($H_s$ = 1m).**

## 4.6 Spud resistance

In this first version of the code, the last criteria that is considered to influence on dredging downtime is the spud capability of resisting the movements and forces imposed by the hull, those generated by waves, currents and winds. The first assumption is that the spud and hull connection is free to dislocate vertically (Figure 35). This way, only horizontal motions and forces are considered in the model. The second assumption is that the spud can be represented as a cantilever beam model, when it is fixed to the soil and the forces and motions are applied on the connection point of the spud. Given this assumptions, the variable that will be used to analyze the downtime limit is the maximum bending stress ($\sigma$). Once the spud will be subject to both periodic and static motions, the sum between static ($\sigma_s$) and dynamic ($\sigma_d$) stresses will represent the total bending stress on spud.

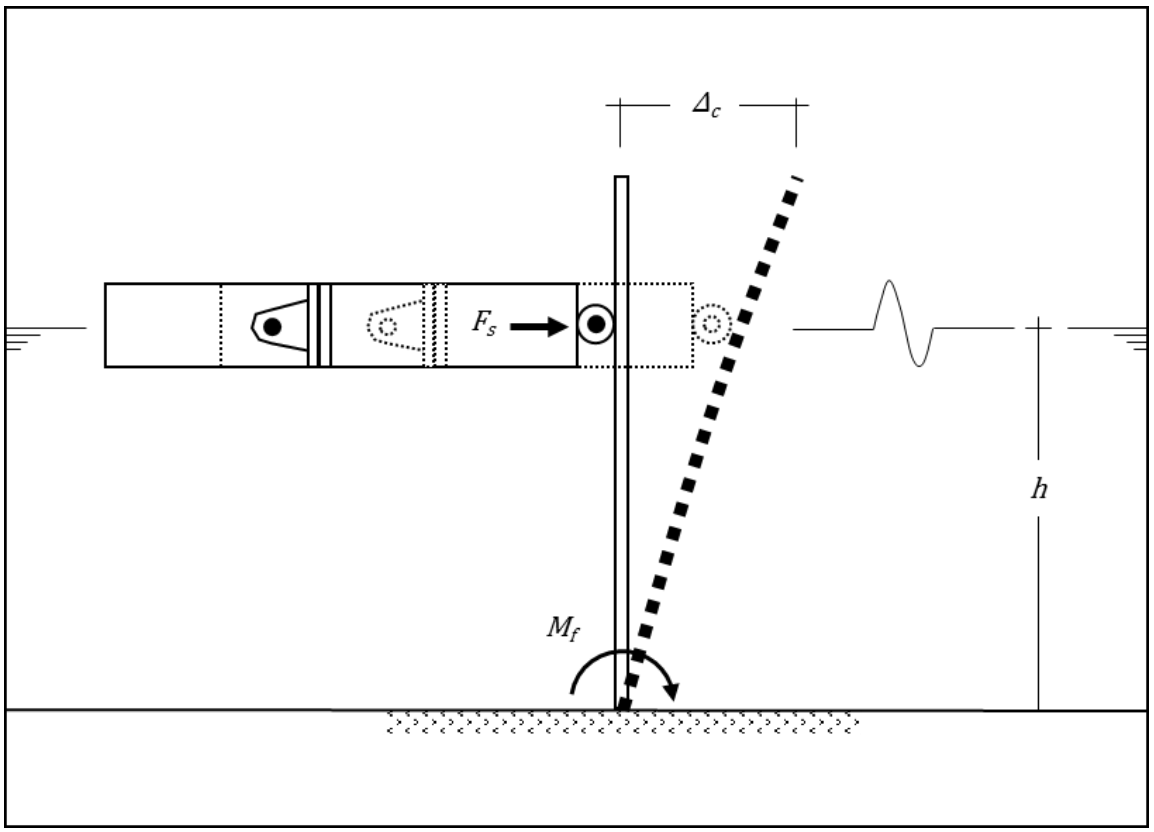


**Figure 35. System definition of variables used to determine spud resistance.**

The resulting force $F_s$, or the influence of static forces on spud, is determined as the composition of wind, waves and current drift forces on *x* and *y*, and define the static stress. The calculation of the static stress is performed by determining the static bending moment ($M_s$) on the connection of the spud to the floor, the distance between the connection point with the hull and the bottom ($h$), the spud radius ($r$) and its stiffness coefficient ($I_{xx}$). The bending moment is the representation of the soil reaction forces, considering no significant deformation of the last.

$$\sigma_s = \frac{M_s r}{I_{xx}} \quad \textbf{[Eq. 31]}$$

When:

$$M_s = F_{sp} h \quad \textbf{[Eq. 32]}$$

$$I_{xx} = \frac{\pi}{4}(r_1^4 - r_2^4) \quad \textbf{[Eq. 33]}$$

Where $r_1$ and $r_2$ are the total spud radius and the spud wall thickness, respectively. The imposed horizontal dislocation on the spud connection is calculated by composing $\Delta_{Xmax}$ and $\Delta_{Ymax}$, which are obtained by the same procedure to define the vertical motion $\Delta_{Zmax}$ presented on Eq. 25 to Eq. 27 and below:

$$\Delta_y(\omega) = D_Y(\omega) + \xi_2(\omega) \quad \textbf{[Eq. 34]}$$

$$\Delta_{Ymax} = 1.8\sqrt{\int_0^{\omega} S(\omega)\Delta_y(\omega)d\omega} \quad \textbf{[Eq. 35]}$$

The motion is then composed to return the total motion.

$$\Delta_{max} = \sqrt{\Delta_X(\omega)^2 + \Delta_Y(\omega)^2} \quad \textbf{[Eq. 36]}$$

The dynamic tension can then be calculated from the total dislocation from the equation considering the cantilever beam:

$$\sigma_d = \frac{\Delta_{max} E r}{h^2} \quad \textbf{[Eq. 37]}$$

Where *E* is the elasticity module of the spud material. For steel, the value for E is 207 GPa. Total bending stress is obtained by adding the static and dynamic components, regardless of the difference between wave and other process direction during a specific swing step. This provides a more conservative approach to the analysis, as the force computed this way is greatest that could possibly be generated. The operational limit is obtained when the total bending stress is smaller than the admissible yield tension, which can be considered as 50% to 70% of the maximum tensile strength of the material and is a user defined input on the model.

KEUNING & JOURNEE (1987) state that the small stiffness ratio of the spud pole would allow neglecting the dynamic stress on the spud, what is not observed in the results. The Taurus II dredger response amplitude operators and its current, wind and wave drift forces were applied on the equations presented above. Figure 36 presents the results for wave generated static stress.

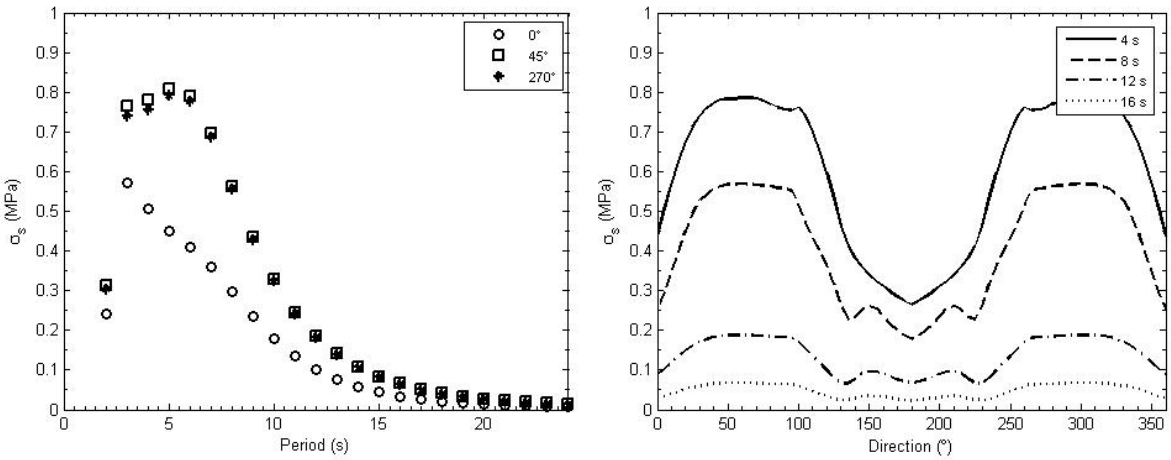


**Figure 36. Wave generated static bending stress ($H_s$ = 1m)**

The stresses generated by waves, when period related, presents high values distributed from 3 to 7 seconds, once it considers the wave drift force and not the wave generated motions. Current and wind generated static stresses are presented on Figure 37 and Figure 38 respectively.

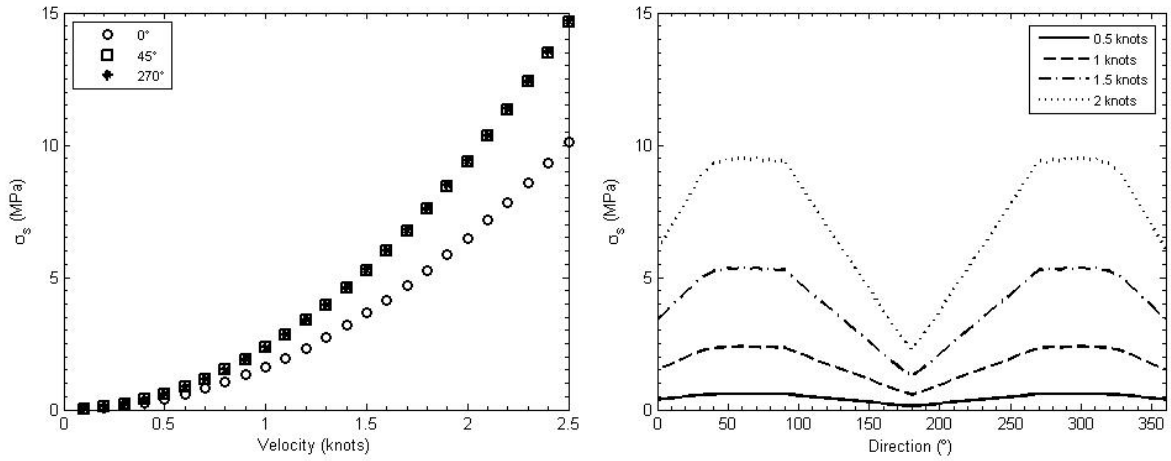


**Figure 37. Current generated static bending stress as a function of current magnitude and direction.**

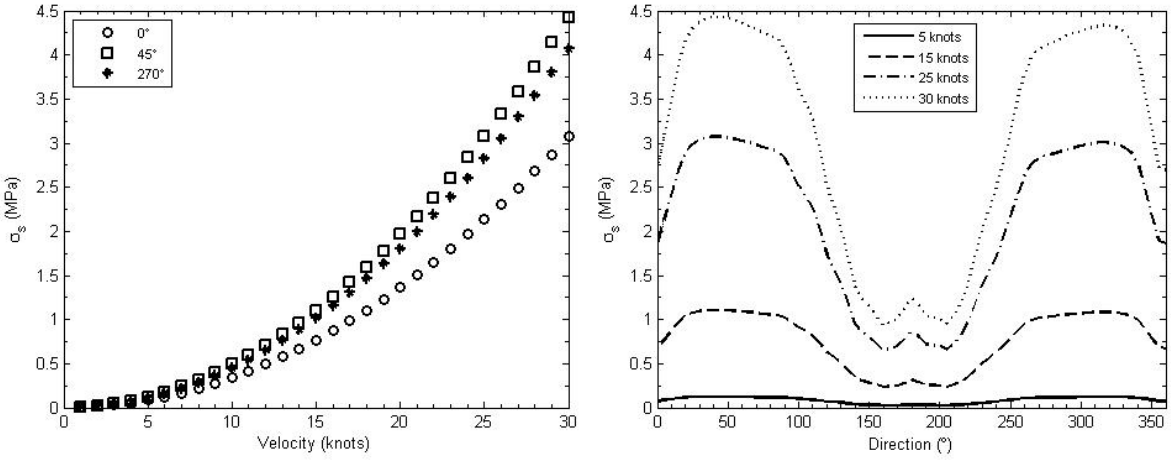


**Figure 38. Wind generated static bending stress as a function of current magnitude and direction.**

Model responses for wind and current generated static stress are similar: Tension increase is proportional to magnitude increase, while transversal winds and currents generates

larger tension values than longitudinal incidence processes. It is possible to notice that currents generates a larger tension than winds for normal conditions of the Brazilian coast. This parameter, when compared in magnitude to dynamic bending stress can be neglected, considering the last as significantly larger. Results for dynamic stress calculation for various periods and directions for a $H_s$ = 1 meter wave can be seen in Figure 39.

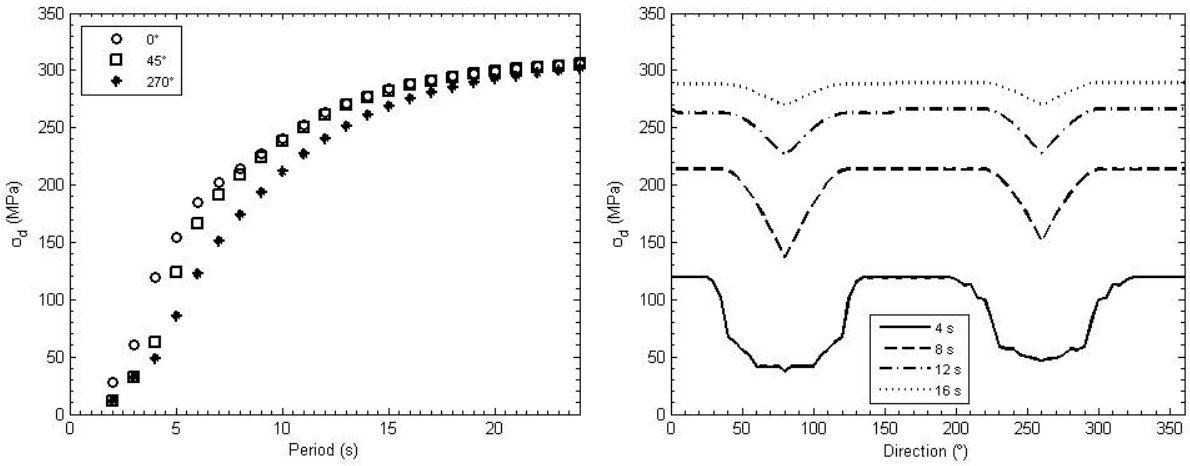


**Figure 39. Wave generated dynamic bending stress ($H_s$ = 1m).**

The large dislocations of the spud pole on the coupling point with the hull explains this difference between magnitudes of static and dynamic bending stress. Drift generated or static forces are not as significant when compared to the imposed dynamics in the spud because of the significantly higher bending moment generated by the second. Presented the trends on critical parameters for dredging operations (spud dynamic stress, horizontal velocity of cutterhead and required winch power) and its variation in relation with periods, magnitudes and direction, the next step is to analyze the limits of each criteria in order to provide the initial base for a downtime analysis. It is important to state that the forces that result from the interaction of the ladder and cutterhead with the soil are not considered. Alhtough the spud stress model is simplified, the results points that operations using the spud pole require waves of low Hs, typically below 1 meter, as it will be assessed further.

# Chapter 5

# Criteria Analysis and Case Study Application

## 5.1 Criteria analysis

As seen in the general results of the spud resistance, winch power and cutterhead dislocation calculations, the period, wave height, magnitudes and directions of waves, winds and currents influence directly in the values of key downtime variables. The next step is to observe those results and determine what are the characteristic values for each relevant downtime parameter and for the different environmental agents, and which system simulated is the most critical for total downtime rates and for which condition. It is important to notice that all cases consider a swing angle of 30º for each board and that the dredger is orientated to north (cutter), using the nautical convention (0º north and 90º east).

The dynamic tension on the spud and the ladder dislocation are the two criteria in which values increase proportional with wave period, due to its strong relation with the translation

motions of the hull. The winch power relation to period is similar in format and frequency dependency with the wave spectrum.

In order to determine the limit of required winch power for the Taurus II dredger, database available online provided the range to be considered for installed winch power (Table 3). A coefficient of 20% from the remaining power was applied for this condition, resulting on 174 kW. Considering this the nominal power, a security factor of 0.7 is applied to obtain a 121.8 kW effective winch power. This value is coherent when compared to winch powers presented by MIEDEMA (2000), and can be said to be between 120 and 200 kW.

**Table 3. Installed power distribution on Taurus II Dredge (SOURCE BOSKALIS)**

| Function | Power (kW) | % of remaining power |
|---|---|---|
| Cutter | *4000* | - |
| Suction pump | *3300* | - |
| Inboard pump | *6760* | - |
| Outboard booster pump | *6000* | - |
| Propulsion | *3680* | - |
| Total instaled power | *24610* | - |
| Remaining available power | *870* | - |
| Instruments and machinery | *261* | ***30%*** |
| Ladder hoisting winch | *261* | ***30%*** |
| Spud retraction | *261* | ***30%*** |
| Swing winches | *174* | ***20%*** |

This value is applied to the results of the winch model calculation to provide the visualization of which sea and forcing states results on values greater than 121.8 kW. In order to obtain the influence of wave height on the required winch power, different wave heights were simulated. Results can be observed in Figure 40, and shows that increase of wave height has a direct relation with the increase of required winch power. While a 1 meter 5 seconds wave requires a power of 10 kW, a 3 meter wave needs approximately 100 kW winch power in order to perform the swing. The port winch will be required for more power for 200º to 300º incident waves, while starboard winch will be more required for 50º to 150º incident waves. Considering the maximum winch power of 121.8 kW, this criterion would not be limiting for a 3 meter wave.

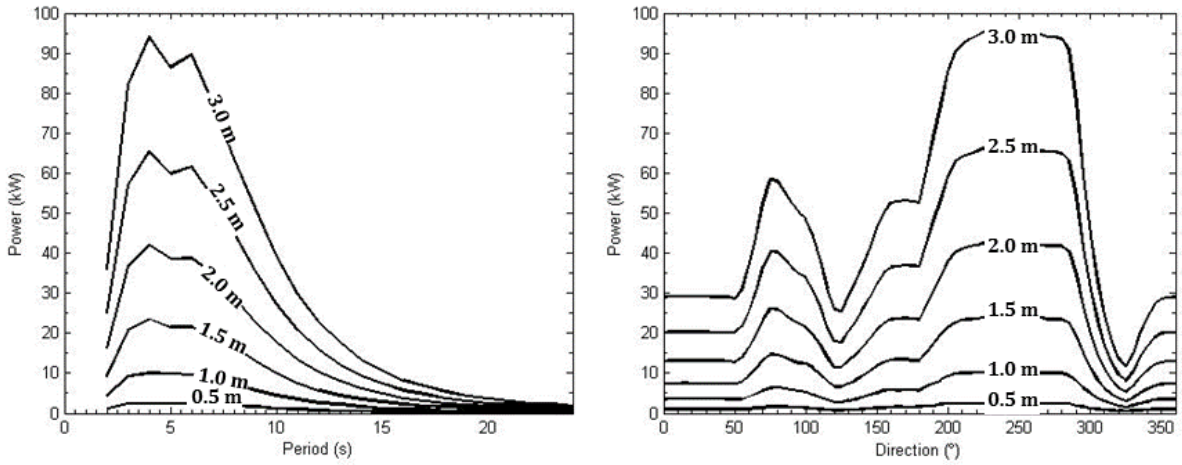


**Figure 40. Variation of portside required winch power regarding wave height. Left graphic is represented by values extracted from a 270º wave.**

The results for currents demonstrates that, in order to a downtime due to winch power capacity be characterized, a current magnitude larger than 2 knots must be present, incident from 22.5º to 90º, in the case of the port winch, or 270 º to 337.5 º in the case of the starboard winch. Results for the required winch power in relation to the maximum accepted winch power to characterize downtime (121.8 kW) for various current magnitudes and directions is presented on Table 4. Nevertheless, current magnitudes of 1.8 to 2.2 knots will generate, in some direction cases, a relative winch power of 0.96, which can be considered very close to the maximum effective power and, depending on the criteria of the operator, could characterize a downtime situation. In terms of this research, the relative winch power to be considered as a reason for downtime must be larger than 1.

The required winch power generated by wind forces and moments is considerably lower than that generated by currents, as exposed on item 8.3. When considered the relative required power regarding the maximum effective power of the winch, the largest wind magnitude simulated (2.2 knots) wasn't able to achive it (Table 5), leading to the conclusion that in order to a winch generated donwitme due to winds be characterized, an extreme wind magnitude must be observed. An extreme wind condition is always acompained by considerably high localy generated waves, those that will characterize downtime condition due to other criteria such as spud resistance, as it will be assessed later.

**Table 4. Maximum relative required winch power during swing due to current magnitude and direction, considering a limit power of 121.8 kW, for port and starboard winches.**

| Current magnitude (knots) | N | NNE | NE | ENE | E | ESE | SE | SSE | S | SSW | SW | WSW | W | WNW | NW | NNW |
|---|---|---|---|---|---|---|---|---|---|---|---|---|---|---|---|---|
| **0 - 0.2** | 0.004 | 0.004 | 0.004 | 0.004 | 0.004 | 0.004 | 0.003 | 0.003 | 0.003 | 0.003 | 0.003 | 0.004 | 0.004 | 0.004 | 0.004 | 0.004 |
| **0.2 - 0.4** | 0.019 | 0.024 | 0.025 | 0.025 | 0.025 | 0.019 | 0.014 | 0.009 | 0.004 | 0.009 | 0.014 | 0.019 | 0.025 | 0.025 | 0.025 | 0.024 |
| **0.4 - 0.6** | 0.051 | 0.062 | 0.067 | 0.067 | 0.067 | 0.051 | 0.036 | 0.021 | 0.010 | 0.021 | 0.036 | 0.051 | 0.067 | 0.067 | 0.067 | 0.062 |
| **0.6 - 0.8** | 0.098 | 0.123 | 0.130 | 0.130 | 0.129 | 0.099 | 0.071 | 0.041 | 0.020 | 0.041 | 0.071 | 0.099 | 0.129 | 0.130 | 0.130 | 0.123 |
| **0.8 - 1** | 0.161 | 0.201 | 0.217 | 0.214 | 0.213 | 0.165 | 0.114 | 0.068 | 0.031 | 0.068 | 0.114 | 0.165 | 0.213 | 0.214 | 0.217 | 0.201 |
| **1 - 1.2** | 0.240 | 0.298 | 0.323 | 0.322 | 0.318 | 0.244 | 0.171 | 0.103 | 0.046 | 0.103 | 0.171 | 0.244 | 0.318 | 0.322 | 0.323 | 0.298 |
| **1.2 - 1.4** | 0.334 | 0.417 | 0.449 | 0.448 | 0.443 | 0.340 | 0.238 | 0.141 | 0.066 | 0.141 | 0.238 | 0.340 | 0.443 | 0.448 | 0.449 | 0.417 |
| **1.4 - 1.6** | 0.444 | 0.553 | 0.599 | 0.595 | 0.590 | 0.453 | 0.317 | 0.188 | 0.087 | 0.188 | 0.317 | 0.453 | 0.590 | 0.595 | 0.599 | 0.553 |
| **1.6 - 1.8** | 0.573 | 0.710 | 0.768 | 0.763 | 0.757 | 0.580 | 0.406 | 0.243 | 0.109 | 0.243 | 0.406 | 0.580 | 0.757 | 0.763 | 0.768 | 0.710 |
| **1.8 - 2** | 0.715 | 0.888 | 0.960 | 0.955 | 0.945 | 0.726 | 0.506 | 0.302 | 0.136 | 0.302 | 0.506 | 0.726 | 0.945 | 0.955 | 0.960 | 0.888 |
| **2 - 2.2** | 0.872 | **1.085** | **1.171** | **1.165** | **1.154** | 0.887 | 0.616 | 0.369 | 0.166 | 0.369 | 0.616 | 0.887 | **1.154** | **1.165** | **1.171** | **1.085** |

**Table 5. Maximum relative required winch power during swing due to wind magnitude and direction, considering a limit power of 121.8 kW, for port and starboard winches.**

| Wind magnitude (knots) | N | NNE | NE | ENE | E | ESE | SE | SSE | S | SSW | SW | WSW | W | WNW | NW | NNW |
|---|---|---|---|---|---|---|---|---|---|---|---|---|---|---|---|---|
| **0 - 2** | 0.003 | 0.003 | 0.003 | 0.003 | 0.003 | 0.003 | 0.003 | 0.003 | 0.003 | 0.003 | 0.003 | 0.003 | 0.003 | 0.003 | 0.003 | 0.003 |
| **2 - 4** | 0.004 | 0.004 | 0.004 | 0.004 | 0.004 | 0.004 | 0.004 | 0.004 | 0.003 | 0.004 | 0.004 | 0.004 | 0.004 | 0.004 | 0.004 | 0.004 |
| **4 - 6** | 0.008 | 0.009 | 0.009 | 0.009 | 0.008 | 0.005 | 0.008 | 0.005 | 0.005 | 0.005 | 0.008 | 0.005 | 0.008 | 0.009 | 0.009 | 0.009 |
| **6 - 8** | 0.014 | 0.014 | 0.015 | 0.014 | 0.014 | 0.010 | 0.010 | 0.010 | 0.010 | 0.010 | 0.010 | 0.010 | 0.014 | 0.014 | 0.015 | 0.014 |
| **8 - 10** | 0.020 | 0.024 | 0.024 | 0.024 | 0.020 | 0.019 | 0.019 | 0.019 | 0.015 | 0.019 | 0.019 | 0.019 | 0.020 | 0.024 | 0.024 | 0.024 |
| **10 - 12** | 0.030 | 0.035 | 0.035 | 0.035 | 0.030 | 0.026 | 0.026 | 0.026 | 0.024 | 0.026 | 0.026 | 0.026 | 0.030 | 0.035 | 0.035 | 0.035 |
| **12 - 14** | 0.041 | 0.046 | 0.047 | 0.046 | 0.041 | 0.036 | 0.036 | 0.036 | 0.031 | 0.036 | 0.036 | 0.036 | 0.041 | 0.046 | 0.047 | 0.046 |
| **14 - 16** | 0.055 | 0.062 | 0.062 | 0.062 | 0.055 | 0.047 | 0.050 | 0.047 | 0.041 | 0.047 | 0.050 | 0.047 | 0.055 | 0.062 | 0.062 | 0.062 |
| **16 - 18** | 0.071 | 0.078 | 0.081 | 0.078 | 0.071 | 0.061 | 0.062 | 0.061 | 0.052 | 0.061 | 0.062 | 0.061 | 0.071 | 0.078 | 0.081 | 0.078 |
| **18 - 20** | 0.087 | 0.098 | 0.099 | 0.098 | 0.087 | 0.076 | 0.077 | 0.076 | 0.066 | 0.076 | 0.077 | 0.076 | 0.087 | 0.098 | 0.099 | 0.098 |
| **20 - 22** | 0.104 | 0.120 | 0.123 | 0.120 | 0.104 | 0.092 | 0.093 | 0.092 | 0.082 | 0.092 | 0.093 | 0.092 | 0.104 | 0.120 | 0.123 | 0.120 |
| **22 - 24** | 0.125 | 0.144 | 0.146 | 0.144 | 0.125 | 0.109 | 0.113 | 0.109 | 0.097 | 0.109 | 0.113 | 0.109 | 0.125 | 0.144 | 0.146 | 0.144 |
| **24 - 26** | 0.150 | 0.170 | 0.172 | 0.170 | 0.150 | 0.130 | 0.133 | 0.130 | 0.114 | 0.130 | 0.133 | 0.130 | 0.150 | 0.170 | 0.172 | 0.170 |

The determination of the maximum longitudinal velocity of the cutterhead while cutting is complex. Three aspects are important to understand this complexity: the difference between the direction of dislocation of the cutterhead (longitudinal and transversal), the type of soil and the cutting and suction capacity of the apparatus. Although the tangential cutting velocity is generally large (> 60 m/s) when compared to the swing velocity (< 0.5 m/s), the ability in removing and suctioning the material is not always proportional. The capacity of the cutterhead teeth of actually cutting the soil is relative to the nature of the soil and the teeth geometry and size (MIEDEMA, 1992-2). A very compact sediment or rock is harder to breach, and the dredging production in terms of volume tends to decrease when compared with water saturated sands or fluid muds. Since the mathematical representation of the cutting process is not an object of this research, the determination of the maximum longitudinal velocity of the cutterhead at the bottom will be obtained by hypothetical scenarios and ratios of the swing velocity.

First, it must be considered that the cutterhead is designed to provide efficiency by cutting laterally (swaying motions), in the same direction of the swing, and not in surge motions. For that reason, the geometry of the cutterhead and its cutting blades is such that facilitates the cutting of successive breaches along the swing line, and not while dislocating longitudinally. Nevertheless, cutting and pumping while surging is possible, as a breach the size of the cutterhead is created while cutting. If the cutter were able to create this breach longitudinally with the same velocity of the longitudinal dislocation, the soil would not create a resistance to this motion, since there would not be any soil on the next point. This process is guaranteed when an overcut condition is observed: the fraction of time that the cutterhead stays in a same position is sufficient to cut and suction more than the volume of the buried section of the cutterhead. The condition to occur overcutting depends the type of sediment, geometry of the cutting blades, dislocation velocity and spinning velocity of the cutterhead.

If the condition observed is the undercutting, that when the fraction of time that the cutterhead stays in a same position is not sufficient to cut and suction more than the volume of the buried section of the cutterhead, two situations can occur depending on the type of sediment. The first is when the cutting blades slides on the bottom surface, given it is not capable of digging sections of it, and instead of cutting and pumping it will polish the surface. This is observed when using non-adequate blade conformation on very compacted clays, for example.

In this case, the swing velocity is extremely slow, and the thickness of the cutting layer is very small. A drastic decrease of production is observed under this condition, but will not limit the longitudinal dislocation, since the cutterhead will skate on the bottom and practically no soil is located at the front of the cutterhead.

The second condition is observed when efficiently cutting hard soils: the dredging is performed with minimum swaying velocity, like the first condition, but instead of sliding on the surface the cutterhead actually cuts and suction the soil fraction proportional to volume occupied by the cutterhead. In this case, the longitudinal dislocation velocity should be a small fraction of the swing velocity, since the resistance presented by the soil in front of the cutterhead is large and will transfer the forces to the ladder and eventually to the hull and spud. This represents the ladder push forces, which are defined by the user as an input and are not calculated. When the dredged material is loose and soft, the third condition occur, when the swing motion will force the cutterhead to occupy the volume of sediment on the next breach point, and the material present on it will be dislocated upward. This fraction will enter the suction pump, facilitated by the rotating motion of the cutterhead. This condition is observed by VLASBLOOM (2003) for different types of soil. However it must be considered that there is a limit for this volume occupation, proportional to the capability of the material to be deformed. In order to understand this process, the following example is given: it is easier to drag a spoon on fluid mud than it is in sand. In this case, the longitudinal velocity must be a fraction or equal to the swing velocity, depending on the type of material that is being dredged.

Considering these hypothesis, a qualitative suggestion is performed in order to provide critical velocities that would characterize a downtime condition. The software allow the user to define this maximum velocity. The maximum longitudinal velocity considered for each type of soil is indicated as a fraction of the swaying or swing velocity $v_s$, is presented in Table 6.

**Table 6. Maximum longitudinal velocity in relation to types of soil and swing velocity.**

| Type of soil | Maximum longitudinal velocity |
|---|---|
| *Rock* | *0.1* $v_s$ |
| *Compact sand/clay* | *0.4* $v_s$ |
| *Loose sand* | *1* $v_s$ |
| *Mud* | *>1* $v_s$ |

In the simulated scenario, the swing velocity is 20º per minute, since it takes the dredger 3 minutes for completing a full 60º swing. Considering the Taurus II geometry, this would result in a swing or swaying velocity of 0.57 m/s. Considering the cut of sand, the maximum velocity of longitudinal dislocation must be equal or smaller than 0.57 m/s. The model results for longitudinal velocity as a function of wave height and period is presented below.

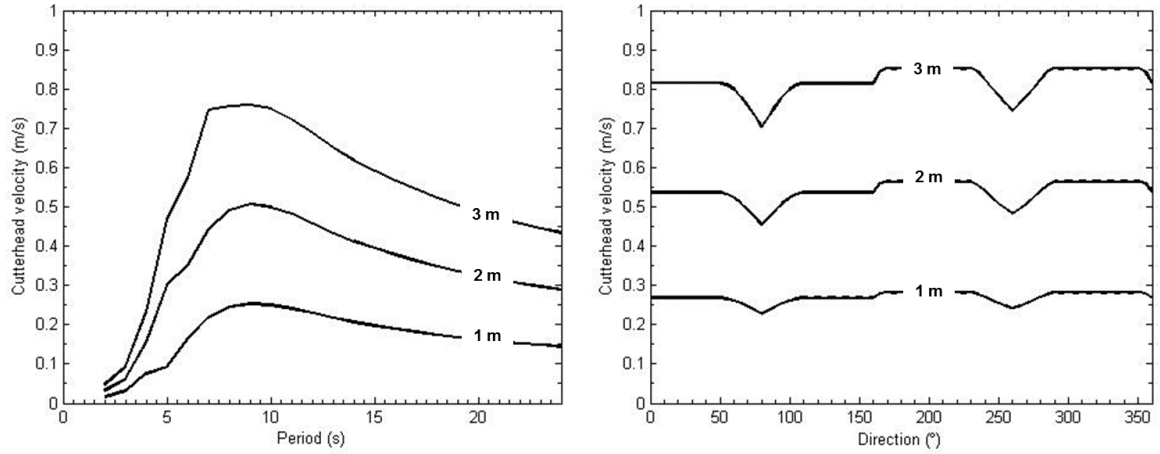


**Figure 41. Longitudinal cutterhead velocity as a function of wave height, period and direction. For period curves, a 90° wave direction was used, while a 8 seconds period wave was considered for representing the variation in direction.**

For the conditions presented on the figure above, significant wave heights smaller than 2 meters would not limit the operation for any period, since the longitudinal velocity of the cutterhead at the bottom is equal or smaller than the swing velocity. For higher waves, the wave period determines the downtime line: for a 3 meter wave, periods between 6 and 16 seconds would create a downtime condition.

The limit for the spud resistance that would characterize a downtime condition is the yield strength of the steel that the spud is built, after applied a security coefficient is applied. In this case, the alloy considered is the ASTM A131 steel, typically used on the construction of ships and naval applications. The maximum yield strength considered for this steel is 390 MPa

(ASTM, 2014). Applying a safety factor of 0.7, the yield strength limit ($\sigma_{lim}$) in this case is 273 Mpa.

Considering the two types of bending stresses simulated, only the static tension is related to the stiffness of the spud pole. For that reason, two different spud thicknesses were simulated to analyze the influence on this parameter on the final stress. Relative bending stress ($\sigma/\sigma_{lim}$) results for 30 and 20 mm spud wall thickness is presented for current and wind generated tensions on Figure 42 and Figure 43 respectively.

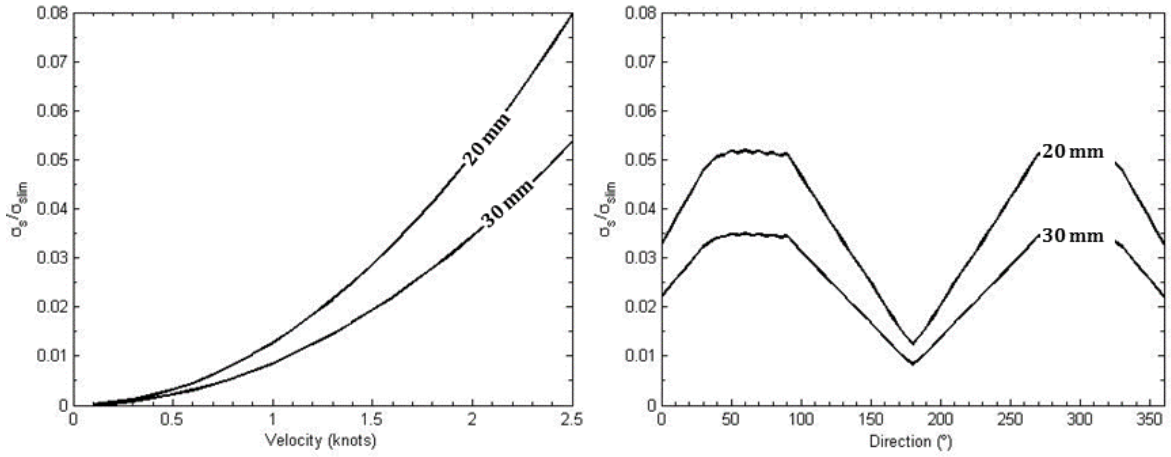


**Figure 42. Relative static bending stress generated by currents. The left hand graphic regards a 270° incidence, while right hand graphics regards a 1.5 knot current.**

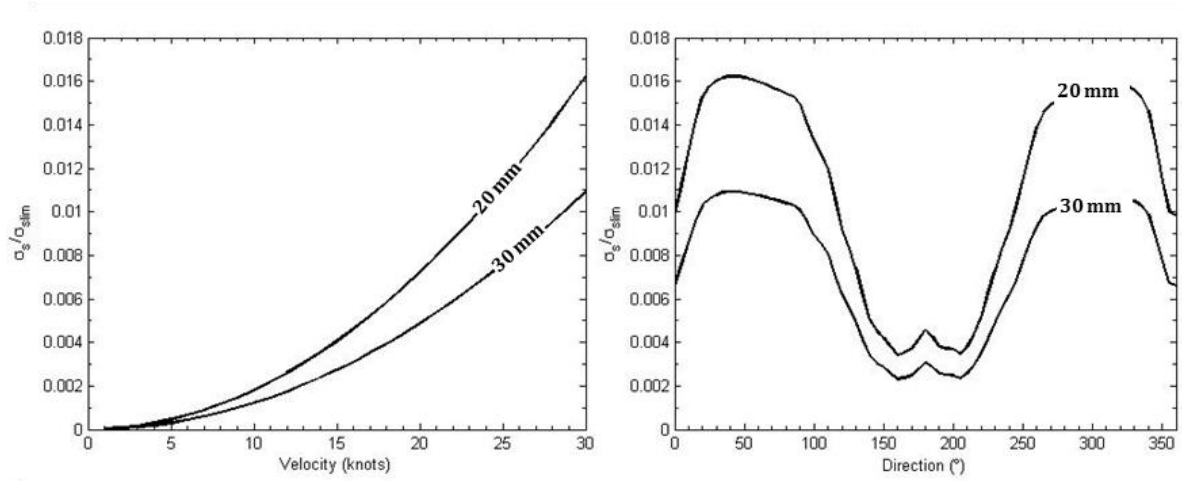


**Figure 43. Relative static bending stress generated by winds. The left hand graphic regards a 270° incidence, while right hand graphics regards a 25 knot wind.**

Regardless of the spud thickness, results shows that current and wind generated static tensions are small enough to be neglected on the process of analyzing downtime conditions. The same can be posted for wave generated static tensions, which are smaller than those generated by current and wind. Results for dynamic relative dynamic tensions are presented on Figure 44.

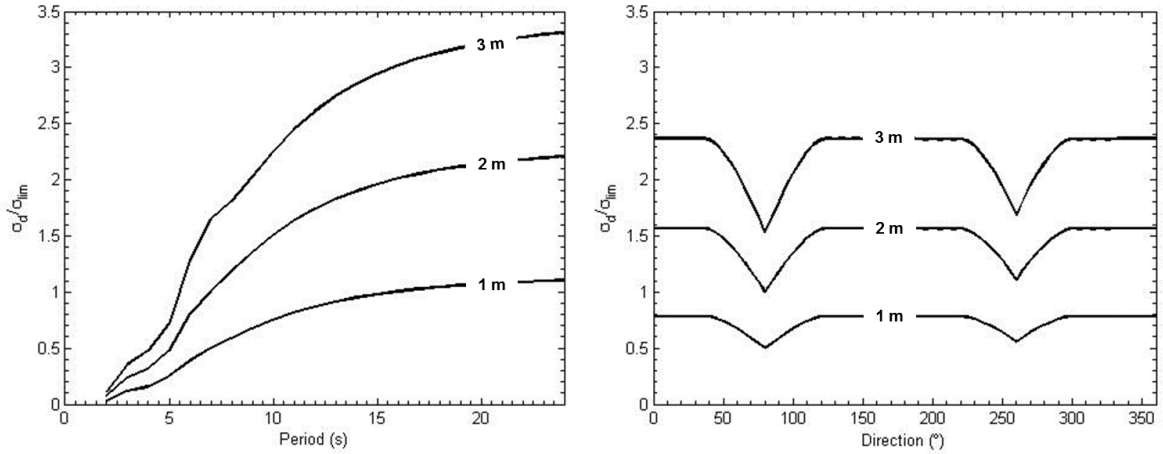


**Figure 44. Relative dynamic bending stress generated by waves for various wave heights. The left hand graphic regards a 45° wave incidence, while right hand graphics regards an 8 seconds period wave.**

Results shows that the wave height is a key element in limiting operation regarding the yield strength of the spud pole. Waves smaller than 1 meter do not generate a downtime condition, while larger wave heights tends to generates relative bending stresses that exceed that one defined by safety. Presented the criteria and values to determine a downtime condition (or downtime lines), the model will be applied for a real scenario in order to evaluate its correspondence to reality.

## 5.2 Case study application

The evaluation of the efficiency of a system of equations that explains the behavior of an environmental or mechanical process is performed by comparing its results with real life situations. This process is known as a model validation, and can be carried out through simply comparing functions and signals for simulated and observed variables, or, in this case, by comparing the total downtime period during an operation. This second approach is based in quality, and not quantity, and due to lack of data regarding the exact downtime periods of the Taurus II dredger during an operation, it was the only option for this research. The operation available for evaluation is the dredging of the beach and surf zone of what today is a port located on the Brazilian coast. Unfortunately no meteorological or oceanographic data was available for that port, so a hypothetical time series of wind, wave and current parameters was developed based on the climate of the southeastern Brazilian coast. This is not the optimum scenario to be analyzed, once it practically eliminates the possibility of using the spud due to relatively large wave dynamic. However this is the only case study available and can be useful as a preliminary test for the code, since it allow the application of simultaneous wave, wind and current data on the models developed. This port was conceived by dredging inland to create an artificial channel. The fact that the location was an open and high dynamic beach based the decision of using a robust CSD to perform the breaking of the beach line, the zone were the wave and current dynamics are most critical on the coastal area. The surf break and the rip currents provides a harsh operational environment for any vessel.

Since no time series is available for the actual dredging period, one alternative to analyze downtime periods of the operation is to calculate, through the use of joint correlation diagrams, the percentage of time that the dredger could or not operate during a period similar to that in which it operated. For example, if a determined wave condition that generates a relative dynamic stress on spud greater than 1 has a frequency of occurrence of 25%, it is considered that at least 25% of the time the dredge will not operate. The sum of the percentages of times that the dredge will not operate due to any of the criteria considered is the total downtime for the operation. However, joint correlation diagrams analyze each process (wind, waves and currents) separately, while these processes occur simultaneously in nature. In order

to obtain the correlation between these processes, a complex multivariate analysis can be performed to create typical scenarios. However, a different approach was developed. As suggested by VAN DER WAL & DE BOER (2004) and GRUNDLEHNER ET AL. (2001), an alternative downtime analysis can be performed by creating simultaneous scenarios of winds, currents and waves that represents the period of operation. Given this, the time series created for waves, winds and currents were used as input to the calculations of the CSD systems.

In order to create a time series, the wave series for the region that the Taurus II dredger operated (northern Rio de Janeiro Coast) was obatined from the WAVEWATCH III global wave generation model for the months of September of 2011, when the dredging operation took place. The time series was extracted from an offshore point and do not consider coastal modification processes of waves (refraction and bottom friction). However, this can be considered satisfactory given the lack of measured data, and numerical propagation of wave data is not the scope of this research. Wind data was obtained from the NOAA/NCEP reanalysis model for the point nearest to the operation area. The currents time series was determined by observed patterns on the Brazilian coast: due to tidal dynamics, the current direction is preferentially parallel to the coastline, with magnitudes that varies from 0.1 to 1.5 knots. A random function to generated data regarding this two conditions was developed in order to create a time series, considering a bi-directional, semidiurnal flow.

Using this time series, the sum of forces generated by waves, winds and currents are used to determine the required winch power and static stress on the spud, while the wave motions can be used to calculate the longitudinal velocity of the cutterhead and the dynamic stress of the spud pole. Time series for these criteria can be generated and the amount of hours for which the values of these variables exceeds the limits determined previously in relation to the total amount of hours in the time series results in the final downtime period of the operation. First, the dredge orientation in relation to the north have to be considered in order to evaluate the influence of the direction on each process. Due to refraction processes, waves will tend to come parallel to the coast. This condition defines the best dredge working orientation to be perpendicular to the coastline, since stern waves will generate less motion and forces than a lateral wave. Considering this remark, the considered dredger working orientation is 260º in relation to north, since the cutter will be positioned in direction to the coast in order to be able to dredge the shallower areas. The time series used for the simulations represents simultaneous

wind magnitude and direction, current magnitude and direction, significative wave height, period and direction. The created time series for these parameters are presented on Figure 45, Figure 46 and Figure 47.

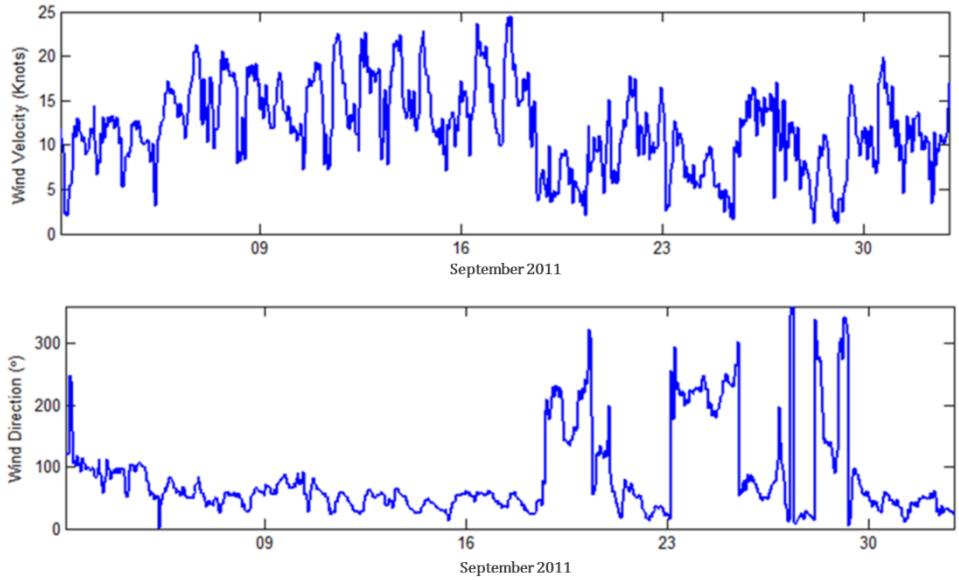


**Figure 45. Wind velocity and direction time series used for the analysis.**

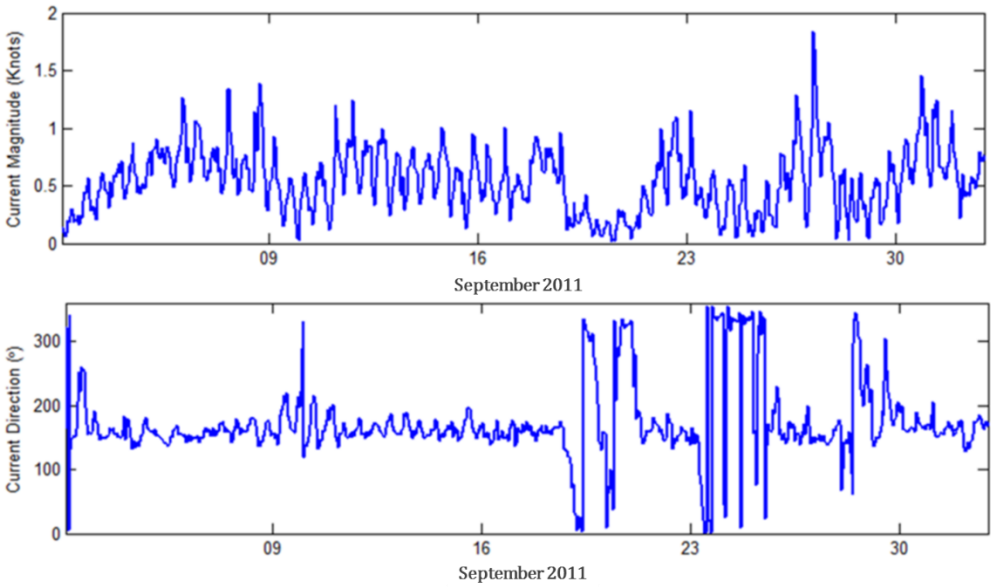


**Figure 46. Current velocity and direction time series used for the analysis.**

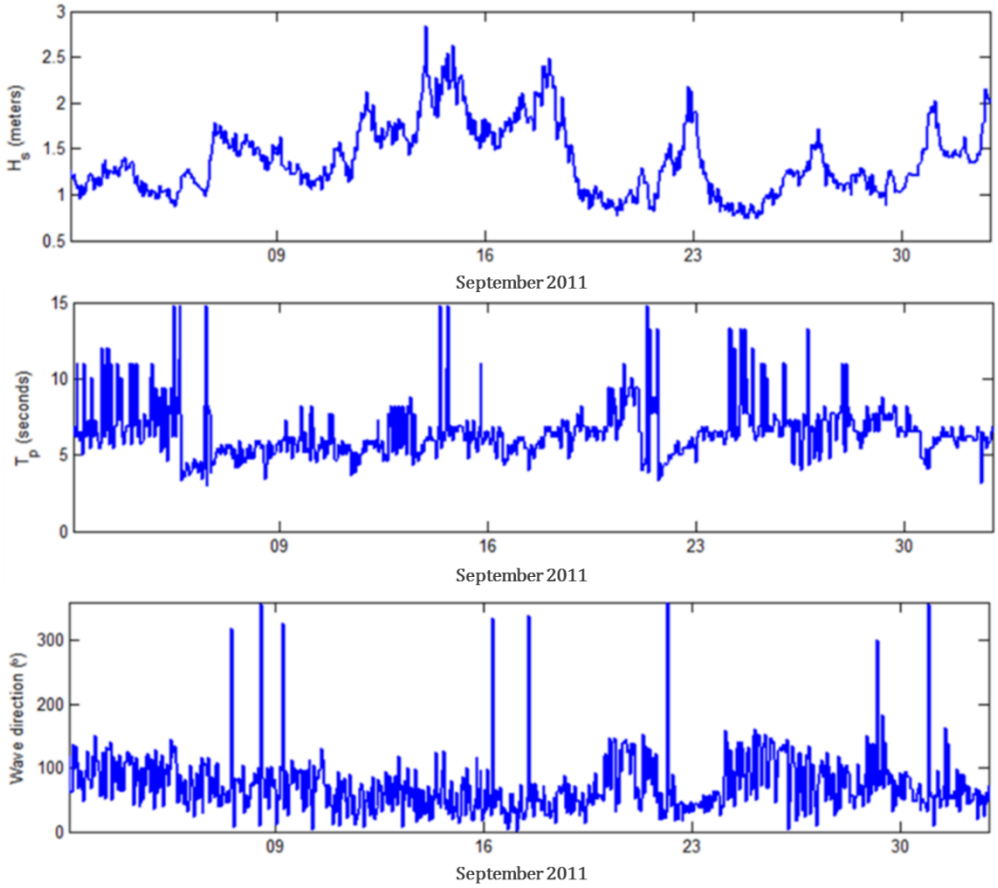


**Figure 47. Significant wave height, wave period and direction time series used for the analysis.**

Minimun significative wave height simulated is 0.76 meters, while maximum wave heights encountered for the time series is 2.84 meters. Minimum wind magnitude encountered is 0.62 knots, while maximum is 12.58 knots. For currents, the minimum magnitude simulated was 0.007 knots, while maximum values of magnitude is 0.94 knots.

Considering the limitations in terms of dredger orientation (given the coast orientation), two scenarios for maximum swing angle were simulated: 30° and 10° for each board, taking 5 and 1.6 minutes to perform a full swing, respectively. Results for required port and starboard winch power generated by the hypothetical time series are presented on Figure 48.

The main pattern observed is that 10° swing angle results are smaller than the 30° results. This can be explained for the fact that the dredger will be more subjected to lateral

waves and currents when performing a 30° swing than the 10° swing. Next, results for the simulated cutterhead velocity and dynamic stress are presented on Figure 49 and Figure 50.

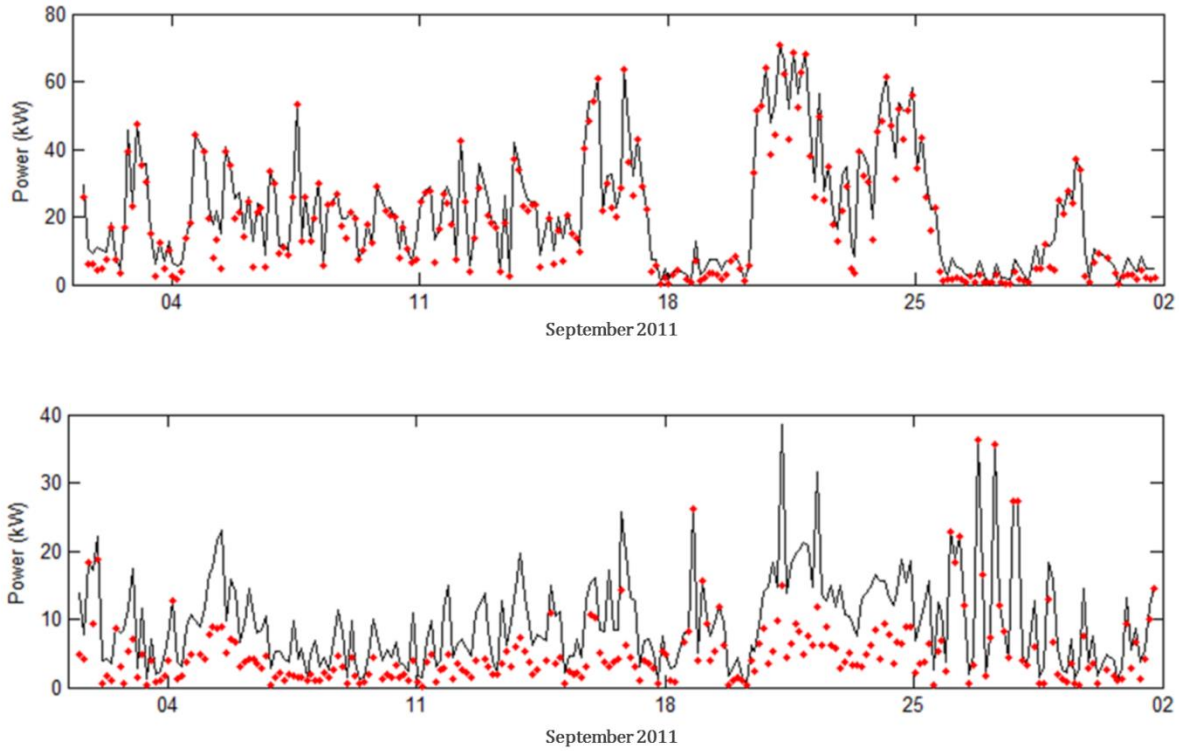


**Figure 48. Maximum Port (above) and starboard (below) required winch power in kW during swing for the hypothetical time series. Black line represents simulations with 30° swing angle, while red dots represents simulations with 10° swing angle.**

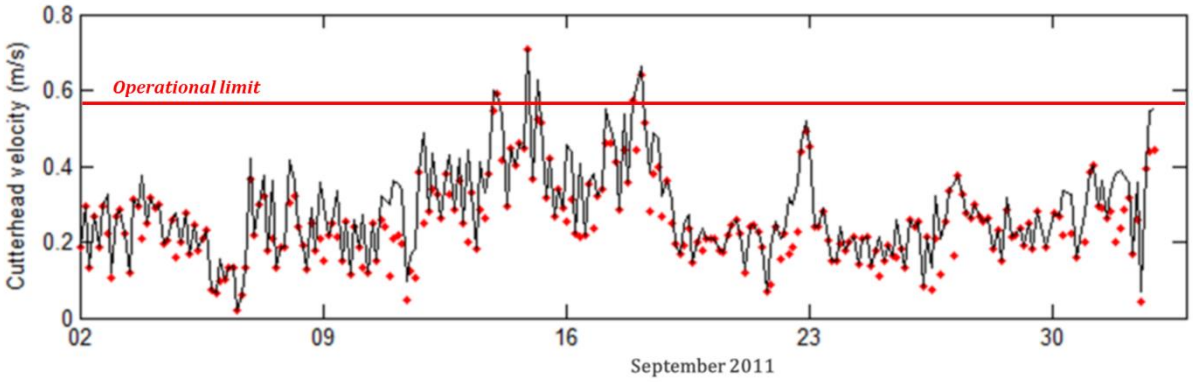


**Figure 49. Maximum Cutterhead velocity during swing for the simulated time series. Black line represents simulations with 30° swing angle, while red dots represents simulations with 10° swing angle.**

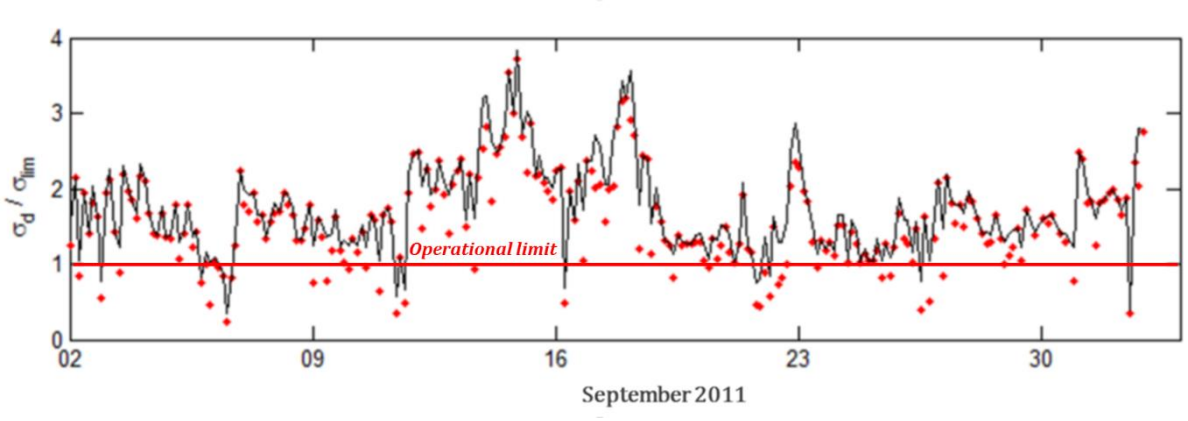


**Figure 50. Maximum dynamic stress of the spud pole during swing for the simulated time series. Black line represents simulations with 30° swing angle, while red dots represents simulations with 10° swing angle.**

Four main statistical parameters were obtained from the results of the simulations: maximum value, minimum value, median and mean. These results are presented on Table 7 and Table 8, for a 30° and 10° swing angle, respectively. It can be seen, from the time series results and its statistics, that the 10º swing angle results on smaller values for the parameters, given the condition described previously.

**Table 7. Main statistical parameters for the simulations results considering a 30° swing angle.**

| Parameter | Required port winch power (*kW*) | Required starboard winch power (*kW*) | Cutterhead velocity (*m/s*) | Relative dynamic tension ($\sigma_s$/ $\sigma_{lim}$) |
|---|---|---|---|---|
| *Minimum* | *0.38* | *0.48* | *0.021* | *0.34* |
| *Maximum* | *70.60* | *38.46* | *0.70* | *3.83* |
| *Median* | *18.96* | *8.44* | *0.26* | *1.53* |
| *Mean* | *21.78* | *9.76* | *0.28* | *1.57* |

**Table 8. Main statistical parameters for the simulations results considering a 10° swing angle.**

| Parameter | Required port winch power (*kW*) | Required starboard winch power (*kW*) | Cutterhead velocity (*m/s*) | Relative dynamic tension ($\sigma_s$/ $\sigma_{lim}$) |
|---|---|---|---|---|
| *Minimum* | *0.18* | *0.16* | *0.03* | *0.22* |
| *Maximum* | *75.72* | *38.61* | *0.70* | *3.71* |
| *Median* | *16.76* | *3.79* | *0.25* | *1.53* |
| *Mean* | *19.72* | *5.30* | *0.27* | *1.57* |

Results for required winch power, regardless of winch board and swing angle, is smaller than the limit of 121 kW for both months simulated. Cutterhead velocity at bottom varies from 0.02 to 0.70 m/s, with most values for both months simulated being 0.26 m/s. Relative dynamic stresses have a minimum value of 0.22, and a maximum of 3.83. This way, the fact that the winch power were never required to its limit and that the majority of events weren't able to generate longitudinal cutterhead velocities greater than the lateral velocity, the the main downtime generating condition is the dynamic stress on the spud pole. The amount of time that each variable exceeded its limits, or are above the downtime line, were extracted in order to obtain the total downtime caused by each system. Results are presented on Table 9.

**Table 9. Downtime percentage for September 2007 and September 2008, for each system simulated.**

| Swing angle (°) | Required port winch power ($kW$) | Required starboard winch power ($kW$) | Cutterhead velocity ($m/s$) | Relative dynamic tension ($\sigma_s/\sigma_{lim}$) |
|---|---|---|---|---|
| *10* | *0%* | *0%* | *2.87%* | *85.66%* |
| *30* | *0%* | *0%* | *2.87%* | *94.67%* |

Results for downtime are similar when performing a 10º and 30º maximum swing angle. Dynamic bending stress on the spud pole determines the main stop criteria, since values for the simulated time series are larger than the yield tension limit on 85% and 94% of the time. The opposite condition is the required winch power: no environmental condition was able to characterize downtime for this criterion during the periods analyzed. For cutterhead velocity, the maximum swing angle influence on the results is not significant, once downtime percentages for each condition varied approximately 3% due to this criterion. These results shows the sensibility of the system to the motion imposed by the hull on the spud pole. Although no observed downtime data was available, one important information from the dredging operator qualitatively endorses the results obtained: the operation was found extremely limiting while using the spud anchoring solution. For that reason, a christmas tree anchoring arrangement was used to substitute the spud system. This system, composed by three anchors positioned at the bow (opposite cutting extremity) provides fixation for the bow section, still allowing a rotation motion of the dredger. It was stated by the operator that after the application of this methodology, dredging productivity improved considerably. Downtime decreased after

the dredger was able to create a sand bar behind the dredging area by pumping the dredged material directly to the surf zone behind it by the use of a rainbow pump. This sandbar sheltered the operation area from waves, making possible an operation with spud poles.

# Chapter 6

# Conclusions and Final Remarks

## 6.1 Conclusions

After reviewing the literature indication of the dredger systems that most affected the weather downtime rates of a dredging operation, three models were developed: a swing winches required power model, a longitudinal cutterhead velocity model and a spud resistance model. Although accelerations on the bridge and deck were pointed by some authors as a key element on downtime estimation for a dredging operation, it was not taken into account in this research. The reason for this decision was that the wave height necessary to generate a downtime condition was not as high as the one needed to create a uncomfortable situation for the crew, considering the the only solution for the anchoring system is the spud pole. Given the complexity of the interaction between the dredger and the soil during cutting, the cutterhead velocity at the bottom was chosen due to formulae developed to calculate its dislocation during time to represent this process.

The influence of environmental agents on the imposed forces, moments and motion of the hull were determined by the application of coefficients found in literature and of a numerical

model of the vessel in waves. Motions are only accounted for waves, and considerations on roll viscous damping were important to determine the magnitude of the absolute motion of a certain point on the dredger.

The swing winches model was based on system of equilibrium equation of static forces and moments in order to obtain the intermediate variables to determine the inputs for calculating the total required winch power. Current presents itself as the process that influenced on the winch power requirement the most. However, when applied to the case study, this system of the dredger was not decisive on its downtime, since the magnitude of currents on the operation area were not as intense as those be found in other locations such as macro-tidal estuaries and rivers. On environments such as those, this system have the potential to be the most critical for operation downtime, as waves are not as present on these places as they are in open ocean.

The longitudinal cutterhead velocity results presented a high sensibility to wave induced motions on the dredger. Although it is not the most suitable variable to represent the interaction between the dredger and the soil, the fact that it can be calculated by a frequency domain system of equations guarantees the model efficiency. This way, as a suggestion for future researches, the relation between the cutterhead velocity at the bottom and the forces resulting from the interaction of the dredger and the soil should be analyzed. This velocity could provide, together with the system mass and inertia, the reaction forces of the cutting process on the spud and hinge point of the ladder, variables that could increase, for example, the static stress of the spud pole.

This dissertation indicates that the key system that generates weather downtime on Cutter suction dredgers is the spud pole. The imposed motion of the hull on the spud pole, or forced dislocation, generates considerable bending moments on the connection point between the spud and the soil, which are significantly higher than the static bending stress. For an energetic, wave dominated coast such as the analyzed port region, the operation of the cutter suction dredger is compromised by this factor, as noticed in statements of a real operation. Although some authors suggested that the stiffness ratio of the spud pole created a condition in which no dynamic components should be accounted for the determination of bending stress, the combination of static loads, cutterhead velocity at the bottom and required winch power downtime rate would not match the observations in reality. The only information regarding field observations of the dredging downtime is that the use of the spud pole made the operation

almost impossible. This correspond to the results obtained from the models. However, the lack of specific data regarding the cause of operation downtime and the operation stop dates due to waves reduces the quality of the validation analysis. In the end, the models developed could be considered efficient to be used as a project analysis tool, in order to choose operation parameters such as the best dredge alignment for the operation and the best swing anchor position, as well as determine the expected downtime rates.

## 6.2 Suggestion for future work

Suggestion for the development of the subject for further researches are

- The validation of the relation between wave imposed motions on the dynamic stresses, by creating field measurements and tests were significant wave height measures are simultaneous with spud deflection measurements;
- Study the interaction between the ladder and cutterhead with the soil by searching models that allow a linear analysis as a function of relevant parameters;
- Analyze the spud stress model, which is very simplified and analyze an eventual soil interaction influence on its results;
- Include other downtime generating aspects obtained by information from operational or dredge design crew;
- Perform verification tests and validation on alternative operations ;
- Develop the formulation for the Christmas tree anchoring system;
- Provide the code the ability to calculate the optimum dredger heading as a relation to the direction of incidence of the external processes, considering the limitation imposed from the dredging range given the channel or dredging area alignment;
- Develop a user friendly interface and generate an executable software to take away the necessity of using the Matlab environment.

# REFERENCES

ALFREDINI, P.; ARASAKI, E. **Obras e Gestão de Portos e Costas**. 2. Ed. São Paulo: Blucher. 2010. 804 p.

ASTM A131 / A131M-14, **Standard Specification for Structural Steel for Ships**. ASTM International, West Conshohocken, PA, 2014.

BRAY, R. N.; BATES, A. D.; LAND, J. M. **Dredging**. 2. Ed. London: Butterworth-Heinemann. 2006. 448 p.

CHAKRABARTI, S. (2001). Empirical Calculation of Roll Damping for Ships and Barges. In: **Ocean Engineering. V. 28**. pp 915-932.

DHAVALIKAR, S. S.; NEGI, A. (2009). Estimation of Roll Damping for Transportation Barges. In: **Proceedings of the ASME 28thInternational Conference on Ocean, Offshore and Arctic Engineering**. Honolulu. 8p.

DOBROCHINSKI, J. P. H. **A Coastal Forecasting System for Vitoria Bay (Southeast Brazil) based on Delft3D Fews**. Internship Technical Report: TU Delft. 2013. 45 p.

EISMA, D. **Dredging in Coastal Waters**. 1. Ed. London: CRC Press. 2003. 224 p.

GRUNDLEHNER, G. J.; VAN DER WAL, R. J.; DE BOER, G. J. (2003). Downtime Analysis Methods for Offshore Dredging Operations. In: **CEDA Dredging Days 2003**. 14 p.

HAJIARAB, M.; GRAHAM, J. M. R.; DOWNIE, M. (2010). Prediction of Roll Damping in the Frequency Domain Using the Discrete Vortex Method. In: **Proceedings of the ASME 29th International Conference on Ocean, Offshore and Arctic Engineering**. Shanghai. 3p.

HERBICH, J. B. **Handbook of Dredging Engineering**. 1. Ed. New York: McGraw-Hill. 2000. 992 p.

HOLTHUIJSEN, L. H.; BOOIJ, T. H. C.; HERBERS, C. (1989). A prediction model for stationary, short-crested waves in shallow water with ambient currents. In: **Coastal Engineering, Vol. 13**. p. 23-54.

KEUNING, P. J.; JOURNEE, J. M. J. (1983). Calculation Method for the Behaviour of a Cutter Suction Dredge Operating in Irregular Waves. In: **10th World Dredging Congress**. 20 p.

LEWANDOWSKI, E. M. **The Dynamic of Marine Craft: Maneuvering and Seakeeping**. 1. Ed. World Scientific. 2004. 300 p.

LEWIS, E. V. **Principles of Naval Architecture, Vol 1: Stability and Strength**. 2. Ed. Society of Naval Architects. 1988. 310 p.

MAGNUSON, A.H. (2010). Analysis of Transport barge nonlinear roll motions in a seaway using an equivalent linearization procedure. In:**Proceedings of the ASME 29th International Conference on Ocean, Offshore and Arctic Engineering**. Shanghai. 8p.

MIEDEMA, S.A. (1983). Basic design of a swell compensated cutter suction dredge with axial and radial compensation on the cutterhead. **CO/82/134, Delft University of Technology**. 64 p.

MIEDEMA, S. A. (1992-1). New Developments of cutting theory with respect to dredging the cutting of clay. In. **Symposium "Zicht op Baggerprocessen**". 32 p.

MIEDEMA, S. A. (1992-2). The Cutting Forces in Saturated Sand of a Seagoing Cutter Suction Dredger. **In. WODCON XIII**. 29 p.

MIEDEMA, S. A. (1999). Consideration on Limits of Dredging Processes. In**. 19th Annual Meeting & Technical Conference of the Western Dredging Association**. 29 p.

MIEDEMA, S. A. (2000). The Modeling of The Swing Winches of a Cutter Dredge in Relation with Simulators. In. **Texas A&M 32nd Annual Dredging Seminar**. 32 p.

NEWMAN, J. N. **Marine Hydrodynamics**. Chestnut Hill: MIT Press. 1. ed. 1977. 402 p.

OWENS, R.; PALO, P. (1982). Wind Induced Steady Loads on Ships. Naval Civil engineering Laboratory, Port Hueme California: **Technical Note**. 61 p.

OVERHAGEN, J. L. V.; BOOR, M.; KIK, A.; KRAMERS, C. H. M. (2004). On the Conceptual Design of Large Cutter Suction Dredgers: Considerations for Making Choices. In: **WODCON XVII**. 16 p.

PARENTE, C. E. **Uma Nova Técnica Espectral para Análise Direcional de Ondas**. Rio de Janeiro: UFRJ. 1999. 200 p. Thesis (Doctorate).

SUGUIO K; NOGUEIRA ACR. 1999. Revisão crítica dos conhecimentos geológicos sobre a Formação (ou Grupo?) Barreiras do Neógeno e o seu possível significado como testemunho de alguns eventos geológicos mundiais. **Geociências**, São Paulo 18: 461-479.

VAN DER WAL, R. J.; DE BOER, G. (2004). Donwtime Analysis Techniques for Complex Offshore and Dredging Operations. In: **OMAE 2004**. 9 p.

VLASBLOOM, W. J. Designing DredgTing Equipment. In: **Dredging Engineering Lecture Notes, TU Delft.** 2005. 79 p.

VLASBLOOM, W. J. The Breaching Process. In: **Dredging Engineering Lecture Notes, TU Delft -** COLLEGE WB3413 DREDGING PROCESSES. 2003. 79 p.

WAMIT. **User Manual**: Version 7.0. 2012. 372 p.

WICHERS, J. E. W.; CLAESSENS, E. J. (2000). Prediction downtime of dredges operating in the open sea. In: **Texas A&M 32nd Annual Dredging Seminar**. 15 p.

WICHERS, J.E.W. (1980) On the Forces on a Cutter Suction Dredger in Waves. In: **WODCON IX**, Vancouver.12 p.

WICHERS, J.E.W. (1981) Hydrodynamic Behavior Of Cutter Suction Dredges in Waves. In: **World Dredging and Marine Construction, November 1981**. 17 p.WICHERS, J.E.W. (1987) **Handbook of Coastal and Ocean Engineering**, Volume 3, Chapter 7. “The behavior of dredging equipment